Filtering out the Ash: Mitigating Volcanic Ash Ingestion for Generator Sets

---

A thesis

submitted in partial fulfilment of the requirements for the degree

of

Master of Science in Hazard and Disaster Management

at the

University of Canterbury

by

Daniel John Hill

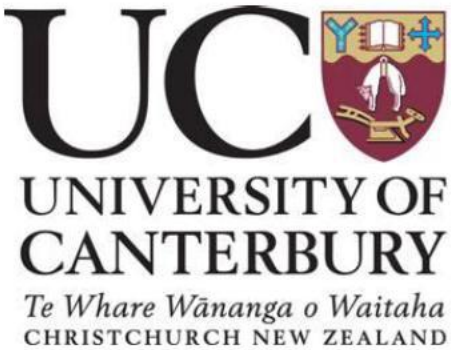

University of Canterbury

2014

Frontispiece

November 2012 eruption from Te Maari Crater, Mt Tongariro,

New Zealand (Schaumkel, 2012)

Abstract

Volcanic eruptions produce a range of hazards which can impact society. The most widespread of these hazards is volcanic ash fall which can impact a range of critical infrastructure. Power systems are particularly vulnerable to ash fall hazards and the resulting impacts may lead to power supply disruption. This can lead to cascading disruption of dependent systems, such as hospitals, water and wastewater treatment plants, telecommunications and emergency services. Typically, large emergency power generator sets are used to provide emergency power supply for essential services during electrical power outages. There has been little study of what impact ash fall exposure will have on generator performance. International experience suggests large generators can experience rapid performance reduction when exposed to high concentrations of suspended or falling ash due to obstruction of air filters and radiators, causing overheating of the engine and shut down of the generator system. However, it is not clear at what ash fall thresholds generators are likely to be disrupted.

This research uses custom designed empirical laboratory experiments to investigate the performance of large generators subjected to a range of volcanic ash fall types and intensities, simulating both proximal and distal ash fall exposure from a range of eruptive styles. It also investigates the application of temporary external filters to minimise the ingestion of volcanic ash into generator housings. The results are used to inform recommendations on the likely impacts of ash to generators and the most effective type of mitigation, which maximises filtration whilst maintaining generator performance.

Control tests recorded high particle concentrations (~0.006 mg/m^3) which indicate substantial ash contamination is possible. Multiple factors were considered to determine the best mitigation measure including the lowest particle concentration, highest air speed and the ease with which the measure could be fitted. The study found material filtration to be the most effective measure; however as the quality of filtration increased, the air speed was reduced and thus so was the volume of air available to the generator engine. Therefore, the type of filtration required is dependent the ash fall intensity. The study also found that a deflection hood is an effective mitigation measure; maintaining airspeed while reducing particle concentrations within the generator. This research informs risk management strategies for critical infrastructure organisations to reduce the risk of generator disruption during volcanic ash falls.

Acknowledgments

I would first like to thanks my supervisors, Dr. Samuel Hampton and Dr. Thomas Wilson, your guidance, patience and support have been invaluable.

I would also like to thank the Auckland Engineering Lifelines Group and the University of Canterbury's Summer Scholarship Scheme for the financial support which made this project possible.

A big thank you to the department's administrators and technical staff (Pat Roberts. Janet Warburton, Janet Brehaut, Dr. Kerry Swanson, Rob Speirs, Chris Grimshaw, Sacha Baldwin-Cunningham, John Southward, Cathy Higgins and Matt Cockcroft) for all your assistance and help throughout the research project.

Thanks to Dr. Anekant Wandres for building the giant, sieve. It is awesome and increase production far more than I could have expected.

Thanks to Peter McGuigan of the Civil Engineering Department who allowed me use the department's laser particle analyser and to Shaun Williams for training me in its use.

Thanks to Anja Moebis for additional help with laser particle analysing.

Thanks to Vaughn McKenzie of Orion Networks and Steve Palmer of Facilities Management for the opportunity to tour real large format generators.

To my classmates from the CoUGAR research group, the collaborative environment you have all encouraged has greatly added to my post graduate experience.

Grant, Shane and James thanks for putting up with all my geology talk at home, the discussion and feedback has proven extremely useful. In particular thanks to Grant for help with proof reading and all the other advice for writing a thesis.

Lastly to Mum and Dad, Thanks for your support an encouragement over all my years at University, it is very much appreciated.

Table of Contents

List of Figures

List of Tables

Abbreviations / Glossary

CDEM – Civil Defence and Emergency Management

Critical infrastructure – Built infrastructure which is critical to the effective operation of society. Includes services such as hospitals, water and wastewater treatment plants, and emergency services. .

Flashover - The unintended electric discharge over or around an insulator (Wardman et al., 2012b).

GENSET – Any combination of internal combustion engine and generator for the purpose of electrical power generation.

Hazard – Hazard refers the occurrence of a natural process which may adversely impact society.

Lifeline – A service, on which people rely, may provide essential services such as hospitals, water and wastewater treatment plants, and emergency services. .

Risk – The combination of Hazard and Vulnerability. A reduction in one component will lead to an overall reduction in risk

Risk assessment – Process to determining risk outlined in ISO 31000 comprised of risk identification, assessment and treatment.

Risk management – Identification, assessment, and prioritization of risks.

Volcanic Ash – The subset of material produce by volcanic eruptions which is less than 2mm in diameter. Fine ash is < 0.063mm; coarse ash is between 0.063 & 2mm.

Vulnerability – The exposure of society to a damaging natural process.

Chapter 1 Introduction

Volcanic eruptions are perhaps the most dramatic expression of the power of our planet. Eruptions produce a range of hazards which can impact society. Since 1600 AD, an estimated 278,880 people have been killed by volcanic hazards (Auker et al., 2013). The majority of deaths were caused by direct volcanic hazards such as lahars, pyroclastic density currents and ballistics (Tilling, 2003). Volcanic ash is seldom associated with casualties and is typically viewed as a lower severity impact, causing disruption to society rather than deaths; however the widespread nature of ash can adversely impact public health and critical infrastructure over a wide geographical area (Wilson et al., 2012b). The impacts of volcanic hazards, including volcanic ash, can be reduced through appropriate volcanic risk management, land-use planning and implementation of mitigation measures as part of a risk management framework.

The widespread distribution of volcanic ash can lead to a range of societal impacts. One of the most common impacts is disruption of power systems, which may lead to cascading disruption for dependent systems such as hospitals, water and wastewater treatment plants, and emergency services. Typically, large emergency power generator sets are used to provide emergency power supply for essential services. However, there has been little study of what impact ash fall exposure will have on generator performance. International experience suggests these large generators can be rapidly disrupted when exposed to high concentrations of suspended or falling ash due to obstruction of air filters and radiators, causing overheating of the engine and shut down of the generator system. However, it is unclear what intensities of ash fall or what mitigation measures might provide useful risk management guidance for generator set operations.

This research aims to identify the risks to large format generators from ash fall, evaluate methods of reducing its impact and provide recommendations on the best mitigation method.

1.1 Conceptual Framework

The International Standards Organisation (ISO) has produced a standardised framework for risk reduction, focused on the identification, analysis, evaluation and treatment of risk (ISO 31000). The standard can be applied to volcanic risk management in order to reduce the

vulnerability of society to volcanic hazards (**Figure 1.1**). It is used as the conceptual framework for this thesis.

The fundamental equation of risk is

Hazard x Vulnerability = Risk (ISO, 2009)

Hazard refers the occurrence of a process which may adversely impact society. Hazard incorporates both the magnitude of natural process and the probability of occurrence (ISO, 2009). Vulnerability refers to the ability of society and the built environment to withstand the occurrence of the natural process which gives rise to the hazard (ISO, 2009). Reducing vulnerability can involve modification of the hazard, though this is rarely possible with volcanic hazards (Blong, 1996). Other mitigation measures include land use planning (risk avoidance), treatment of individual infrastructure components and increased infrastructural redundancy.

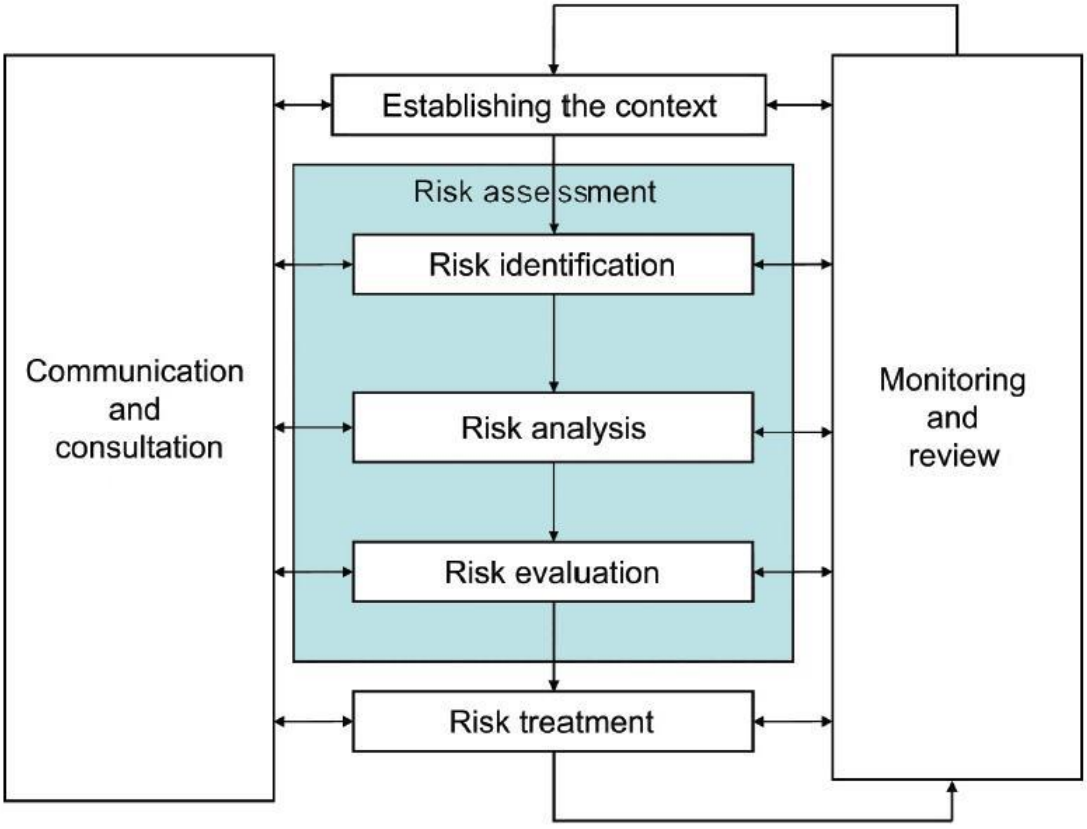

Figure 1.1: ISO 31000:2009 - Risk management framework (ISO, 2009)

In risk management, establishing the context involves identifying the objectives and scope of the study (ISO, 2009). Defining the scope may involve activities such as defining the type of impacts which are to be reviewed, establishing the spatial extent of the study area and identifying the range of vulnerable components to be tested (ISO, 2009).

Risk identification involves three parts. Firstly, all sources of risk must be identified along with their consequences and areas of impact (Oehmen et al., 2010). The second part involves reviewing the vulnerability of the built environment and identifying the communities and critical infrastructure which may be impacted and how they may be impacted. Lastly historical events are reviewed through physical investigation and literature review. The purpose of the risk identification step is to identify all factors which require analysis in the following step (ISO, 2009).

Risk analysis and evaluation develops a deeper understanding of the risks identified in the previous step, in order to compare and prioritise the most significant risks (ISO, 2009). In the context of volcanic risk, this involves the assessment of the magnitude and frequency of the process and the vulnerability of exposed populations and infrastructure. Evaluation is typically carried out using deterministic or probabilistic approach.

Risk treatment involves measures which reduce the impact of the hazards on populations and the built environment (ISO, 2009). The nature of volcanic eruptions makes the management of its processes difficult or impossible; therefore reduction of the vulnerability is required. This may be addressed through measures such as land use planning, protection of specific infrastructure components or increased redundancy (ISO, 2009).

1.2 Application of ISO 31000 to this Study

The study follows the risk management framework outlined in ISO 3100. The thesis is structured around this framework. This section: firstly 'establishes the context' of the risk management study; and secondly how remainder to the risk management process is applied in the thesis is presented.

1.2.1 Establishing the Context

Volcanic risk management is becoming increasingly important as the Earth's population increases. Larger populations residing in close proximity to volcanos will lead to an increase of society's exposure to volcanic hazards and therefore an increase in the overall risk.

Volcanic risk management has been used successfully in the last 50 years to save lives and reduce damage to property through timely warnings and evacuation, improved monitoring and mapping, improved infrastructure and effective land use planning (Auker et al., 2013). While most volcanic hazards can be effectively mitigated through land use planning and evacuations, these measures are less effective or appropriate for mitigating volcanic ash impacts (Hansell et al., 2006). Volcanic ash risk management has instead focused on hazard and risk awareness; warnings; and preparedness activities (Blong, 2000), such as development and implementation of temporary mitigation actions. The latter requires a comprehensive understanding of the likely impacts of volcanic hazards and identification of suitable mitigation actions.

Due to the widespread nature of volcanic ash dispersal and the wide range of possible physical and chemical properties, impacts are difficult to mitigate through simple solutions. The most feasible mitigation measures may involve treatment of impacts at an individual infrastructure component scale. However, there has been limited systematic impact collection for volcanic ash impacts to critical infrastructure systems (Jenkins et al., 2014), especially when compared to other hazards, such as earthquake or hurricane. The lack of quality quantitative data makes evidenced-based risk analysis for component based mitigation difficult. However, controlled, laboratory based experimentation has been used recently to aid the identification of vulnerable components and failure modes, thus allowing the development of mitigation measure best suited to individual components (e.g. research on the impact of ash on high voltage lines (Wardman et al., 2012a) and investigation of the effect of ash and gasses on personal computers (Wilson et al., 2012a)).

A critical infrastructure sector particularly vulnerable to ash fall impacts is electricity networks. Electricity is vital to society in order to maintain an expected standard of living. Power failure can lead to cascading failures within the built infrastructure due to critical infrastructure's dependence on electrical power. For example, power failure may restrict the functionality of a water treatment plant; the lack of water may then restrict the services a hospital can provide. High voltage electrical lines are particularly vulnerable to ash impacts due to the conductive nature of wet ash, which can lead to insulator flashover. Flashover is the unintended electric discharge over or around an insulator (Wardman et al., 2012b). Wardman et al. (2012b) conducted laboratory experiments and concluded small amounts (~3 mm) of wet volcanic ash are sufficient to cause flashover of high voltage lines. In the event of electrical supply failure, lifeline providers are likely to use pre-existing generators to

supplement their power requirement in order to continue provision of critical services, until supply can be restored (Beavers, 2003).

This study aims to identify the failure modes of ash affected generators in order to ensure the highest level of functionality in the event of volcanic ash fall. The study focuses on Auckland as a case study to provide constraints for experiments. Auckland was chosen as it is New Zealand's largest city and is at risk of ash fall from both proximal and distal sources. The broad range of ash types which may impact Auckland enables the findings of this study to be applied in a range of vulnerable locations.

The city of Auckland is New Zealand's largest city and the 2013 census show 32% of New Zealanders reside within the Auckland region (Carey and Bursik, 2000). The region contributes ~36% of New Zealand's gross domestic product (GDP) (Wilson and Houghton, 2000). The city is located within a monogenetic basaltic field, (Allen and Smith, 1994) where there is a risk of direct ash fall which may affect critical infrastructure, in particular electrical lines/supply. There are also a number of distal volcanoes in the North Island which have the potential to deposit ash in the Auckland region (Magill et al., 2006). In the event of ash fall in Auckland, backup generators may be used to restore power dependent critical infrastructure. Generators operating in an ashy environment may be at risk of failure, potentially severely restricting their performance and that of any dependent systems. In addition, the Auckland region has limited electrical supply generation and 70% of Auckland's and Northland's electricity demand is generated south of the region (Transpower, 2013) which is also vulnerable to ash fall hazards from the Taupo Volcanic Zone and Taranaki volcano. Therefore, in the event of ash induced disruption of electricity supply into Auckland, the region is likely to experience disruption of electrical supply, requiring the use of generators to restore lifeline services.

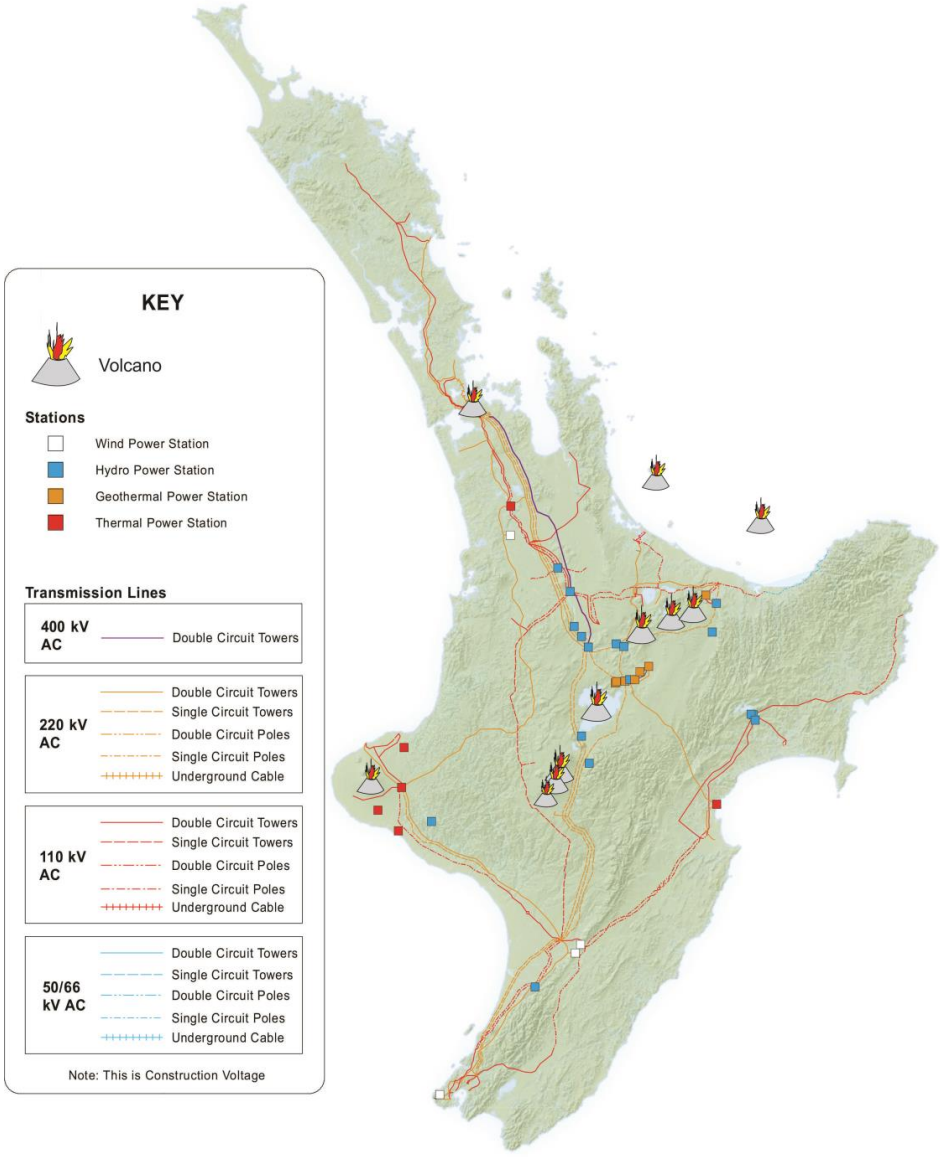

Figure 1.2: Map indicating the transmission lines and the distribution of volcanic ash sources within the North Island, New Zealand. Modified from (Transpower, 2013).

This study reviews literature describing the potential ash fall risk to the Auckland region and identifies the likely fall rates and grain sizes which may impact Auckland. This is essential to determine as the grain size and fall rates are key controls on the failure of a generator and experimental setup. The study uses these variables and common generator failure modes to tests the performance of six potential mitigation measures to determine the most effective method of reducing ash ingestion without inducing failure though use of the measure itself.

1.2.2 Application of Risk Identification, Assessment and Treatment in this Study

Risk identification was undertaken by reviewing literature regarding the formation, properties and dispersal of volcanic ash in the natural environment (Chapter 2). This review also

covered the operation of generators in both dusty and ash filled environments. A case study supported the review by identifying specific failure modes for generators experiencing ash ingestion. Risk analysis was supported by the case study and developed through initial laboratory testing and site visits to generator installations (Chapter 3). Risk reduction was undertaken by trialling various mitigation methods in laboratory experiments to determine the most effective mitigation measures (Chapter 4). The results were then discussed and mitigation measure identified (Chapter 5). Finally the knowledge gained through the risk reduction process was communicated to stakeholders through conclusions and recommendations (Chapter 6), to assist generator operators to mitigate the ash fall hazard.

1.3 Aim and Objectives

The goal of this research is to identify the risks to large format generators from ash fall, evaluate methods of reducing its impact and provide recommendations on the best mitigation method.

The research objectives are:

- Determine the ash characteristics (e.g. grain size, density, composition, abrasiveness) which will damage or disrupt diesel generator operation
- Review the ash fall hazard for the Auckland region including the potential ash fall rates and grain size distributions
- Determine failure modes for exposed critical generator components and comparing the variability of failure modes to varying ash characteristics
- Investigate the effectiveness of appropriate mitigation and preparedness actions to protect generators and related equipment
- Provide guidelines on the use of temporary filters, including the type of filter and the frequency with which they should be changed

Chapter 2 Literature Review

2.1 Introduction

A literature review was conducted to address the thesis research questions by: assessing the ash fall hazard of the Auckland region, including reviewing how ash is produced and dispersed, and what volcanic sources might produce ash affecting Auckland; identifying the likely impacts to power supplies from volcanic ash fall and reviewing the types of generators used as backup power supplies, including their functionality. Its purpose is to review available knowledge, identify knowledge gaps and inform the design of the testing methodology (Chapter 3).

The chapter will:

- Review the properties of volcanic ash, focusing on those which influence power systems
- Determine volcanic ash dispersal and deposition, including remobilisation
- Review of the potential sources and characteristics of the ash fall hazard for the Auckland region
- Review of large format generator types in use as a source of backup power and their functionality
- Explore the likely impacts volcanic ash can have on generator operation, focussing on the case study of Bariloche, Argentina

2.2 Volcanic Ash

Volcanic ash is produced during explosive eruptions is the widest reaching of all the volcanic products. Volcanic ash is defined as material produced by explosive volcanic eruptions that is <2 mm in diameter (Wilson and Stewart, 2013). Ash fall poses a risk to a range of systems. Impacts documented include the damage to: agricultural systems, high voltage power lines, HVAC (heating, ventilation and cooling) units and water treatment plants.

2.2.1 Formation of Volcanic Ash

Volcanic ash is formed during explosive decompression of magma which occurs as magma ascends within the conduit (Heiken and Wohletz, 1985). Fragmentation produces fine grain particles which are released high into the atmosphere by the eruption column. Volcanic ash can form by the following eruption processes:

- **Magmatic eruption:** As magma ascends within the volcanic conduit, from the magma chamber toward the vent, decompression causes dissolved volatiles to exsolve, forming bubbles (Cashman et al., 2000). The primary volatiles are H_2O and CO_2. As the magma continues to decompress, bubbles grow and form a foam layer, further decreasing the density of the magma. When the mixture reaches ~75-83% volume-percent vesicles, explosive fragmentation occurs, producing ash particles (Klug and Cashman, 1996). The explosive transformation from liquid magma to particles and gas, accelerates the mixture up the conduit to form an eruption column (Klug and Cashman, 1996).
- **Phreatomagmatic eruption:** Phreatomagmatic eruptions occur in a similar manner but do not rely on the presence of volatiles within the magma to cause explosive fragmentation. Instead, fragmentation occurs when magma comes in to contact with a water source, such as a ground water, surface water or ice (Morrissey et al., 2000). Ash produced during phreatomagmatic eruptions is generally finer than magmatically derived ash, due to the abundance of water; however water can cause the particles to clump together, creating accretionary lapilli (Morrissey et al., 2000).
- **Phreatic eruption:** A phreatic eruption occurs when water, under pressure, flashes to steam when the pressure is suddenly reduced. The key difference between phreatic and phreatomagmatic eruptions is the lack of juvenile material in the former (Mastin, 1995). Ash is produced when the explosive expansion of the steam converts thermal energy to mechanical force, fragmenting rocks which overlie the hydrothermal system (Browne and Lawless, 2001).
- **Lava dome collapse:** Ash is also formed during lava dome collapse. Cooling of the dome causes the outer layer to become more viscous, preventing degassing of exsolved volatiles (Fink and Anderson, 2000). A combination of internal pressure and external forces, such as gravity, can cause the wall to fail. The dome will then undergo rapid decompression, fragmenting the lava within, to form volcanic ash (Alidibirov and Dingwell, 2000).

2.2.2 Dispersal of Volcanic Ash

The mode of dispersal is controlled by the density of an eruption's jet phase, with respect to the surrounding atmosphere (Rhoades et al., 2002). A jet which is denser than the surrounding atmosphere will move laterally as a pyroclastic density current (PDC), while a jet which is less dense will form a vertical plume, the movement of which is largely controlled by high elevation winds.

2.2.2.1 Volcanic Plumes

Volcanic plumes are composed of a mixture of volcanic particles, gasses and air which is produced primarily by explosive eruptions (Rhoades et al., 2002). The plume is generated when magma fragmentation ejects particles at high velocity into the atmosphere. Energetic plumes are capable of rising to altitudes of up to 50km (Rhoades et al., 2002). The key control on the height of a volcanic plume is its level of buoyancy. The plume will continue to rise until the density equalises with the surrounding atmosphere. The density of the plume is controlled by the magma composition (particle density), amount of volatiles released (gas supply) and vent shape (affects discharge rate). These factors will also affect the longevity of a volcanic plume (Sigurdsson et al., 1999).

The plume is composed of three primary regions: the jet phase, convective phase and the umbrella region (**Figure 2.1**). In the jet phase, the upward movement of particles is controlled by the explosive forces of the eruption (Rhoades et al., 2002). When the plume reaches the maximum height achievable (using the initial vertical movement of the particles) convection takes over. In this phase the plume is less dense than the surrounding atmosphere, causing the particles entrained within the plume to rise under buoyant convection (Rhoades et al., 2002). Transition to the umbrella region occurs at the level of neutral buoyancy, where the density of the plume and the surrounding atmosphere equalise. At this point the plume will begin to spread out into the umbrella region. The movement of the plume at this height is primarily controlled by the wind direction (Rhoades et al., 2002). Large plumes can reach atmospheric trade winds, potentially transporting particles thousands of kilometres from source (Rhoades et al., 2002).

Ash fallout can occur at any point in the column but requires particles to reach the edge of the plume (Parfitt and Wilson, 2009). The greater the height a particle reaches, the further it is

likely to be transported perpendicular to the wind direction. The stronger the wind, the greater the distance the particle will travel downwind before depositing (Parfitt and Wilson, 2009). Using the wind direction and speed at different heights, combined with the particle size and the eruption mass, it is possible to calculate how high a particle will reach in a plume and therefore using the wind and terminal velocity calculations, where it is likely to land (Parfitt and Wilson, 2009). Ash fallout occurs in three distinct phases (Rose et al., 2001). Coarse particles fall out within the first one to two hours, close to the source. In the second phase, smaller particles aggregate due to electrostatic attraction (Schumacher and Schmincke, 1995). The particles then become large enough to fallout. This phase occurs during the first 24 hours, leaving only very fine particles suspended. The third phase occurs in the days to weeks following an eruption, when fine particles slowly fallout under their own weight, as the buoyancy of the plume decreases. The particles can be transported thousands of kilometres, from source to deposition. The combined effect of the three phases causes the exponential thinning relationship of ash fallout with increasing distance from vent (Pyle, 1989).

2.2.2.2 Pyroclastic Density Currents

Co-ignimbrite plumes can form during pyroclastic density currents, due to the buoyant rise of particles and gasses above the flow (Valentine and Fisher, 2000). As the flow travels, a separate low density layer forms above the main flow. The layer is composed of fine grain material and hot gasses which entrain the surrounding air to form a plume (Valentine and Fisher, 2000). The plume is then modified by local winds and deposits ash away from the flow. Ash from a co-ignimbrite plume is typically finer than ash from magmatic or phreatomagmatic plumes, due to the secondary abrasion which occurs within the flow (Valentine and Fisher, 2000).

2.2.2.3 Remobilisation

Dispersal by remobilisation occurs when wind transports ash from its initial deposition location. While ash deposited in this manner is likely to be thinner than primary ash fall, local thickening can exacerbate the problem in some localities (Sparks et al., 1983). Remobilisation will also occur long after the initial eruption, posing a long term hazard (Wilson et al., 2011). Less energy is required to remobilise smaller ash grains therefore remobilised ash deposits tend to have a higher proportion of fine grain particles (Fowler and Lopushinsky, 1986). In addition to remobilisation by natural means, ash may be re-suspended in an urban environment by the movement of vehicles and other machinery.

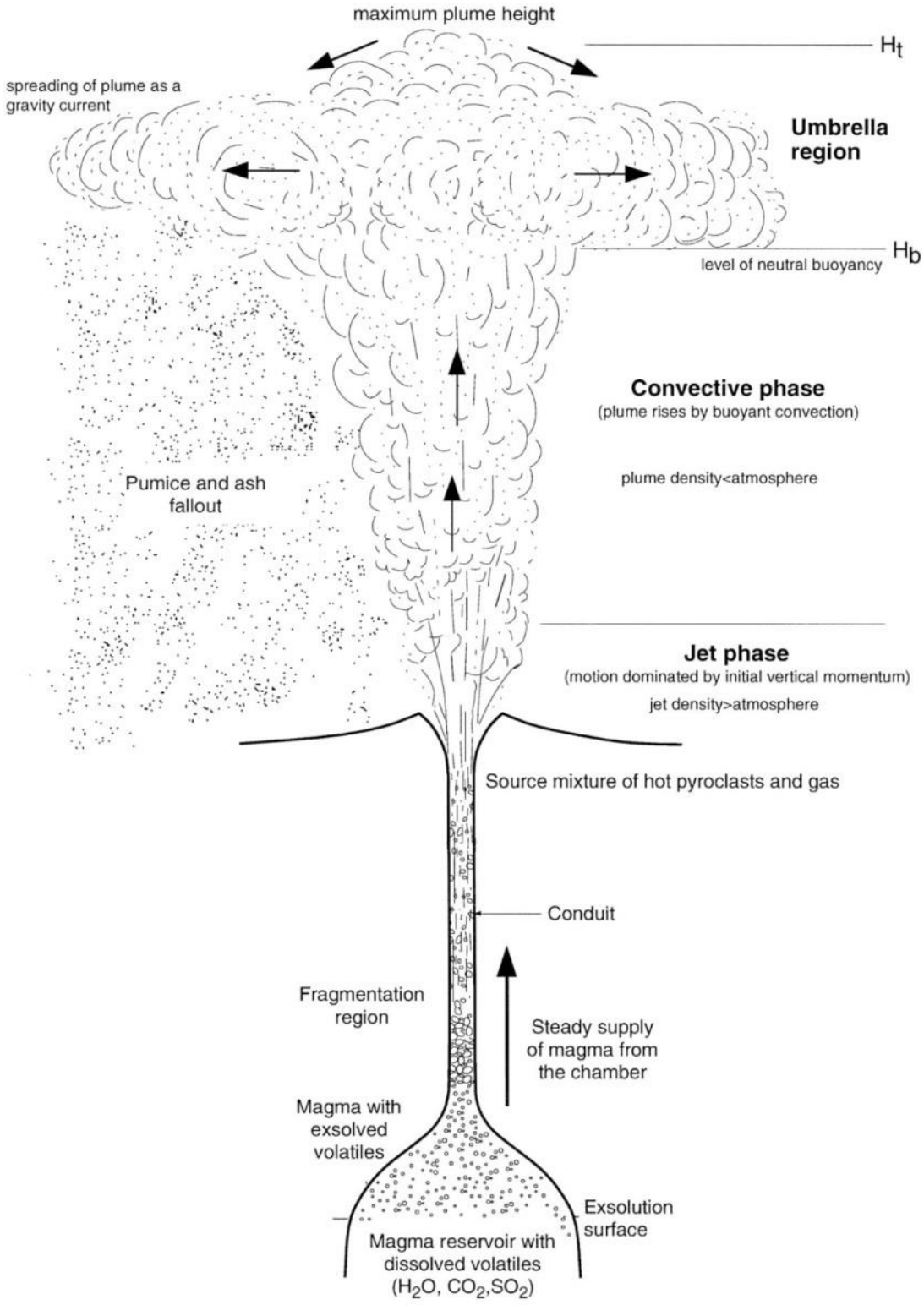

Figure 2.1: Formations of a volcanic eruption plume through degassing of silicic magma. As magma degasses it forms a mixture of gasses and magma fragments. The pressure of degassing causes material to accelerate upwards, forming the Jet Phase. Heat within the mixture entrains surrounding air, forming the Convective Phase. Above the level of neutral buoyance (Hb) the plume spreads out, forming the Umbrella region (Rhoades et al., 2002).

2.2.3 Properties of Volcanic Ash

The properties of volcanic ash are important influences on the dispersion and impacts of ash fall. The properties can vary greatly, depending on the gas/magma composition and the style of eruption (Rose and Durant, 2009). In addition, the density and grain size of ash control the distance ash can be transported. Large, dense particles will fall out close to the vent, while small, less dense particles may be deposited at great distances (Bonadonna et al., 1998). The following sections detail the properties of volcanic ash including: composition, grain size, abrasiveness, morphology, density, surface chemistry and conductivity.

2.2.3.1 Composition

Volcanic ash is composed of crystal, glass and lithic particles (Rose and Durant, 2009). Crystal particles form as phenocrysts and reflect the composition of the magma. Glass particles are also sourced from the magma but are cooled rapidly, following the eruption to form glass (Rose and Durant, 2009). Lithic particles are derived from the wall rock of the conduit and vent and represent old material which may or may not be volcanic in origin.

2.2.3.2 Grain size

Volcanic ash is defined as particles, produced by explosive decompression; with a diameter <2 mm (Rose and Durant, 2009). Grain size is primarily controlled by the type of eruption. Those which are wet or involve magma with high silica compositions are likely to be finer than low silica, dry eruptions (Rose and Durant, 2009). Grain size is also controlled by distance from the vent. Coarse particles fallout close to source, leaving finer particles to be deposited at greater distances (Rhoades et al., 2002). Fine grain ash is more readily ingested into generators due to its low mass. In addition, the transportation of fine ash long distance increases the possibility of impacting infrastructure. Grain size is of key importance in this study as it is the primary control on the suspension and ingestion of ash into a generator

2.2.3.3 Morphology

Ash forms irregular shaped particles, due to the explosive nature of its formation (**Figure 2.2**). Particle shape is controlled by the eruption type, magma composition, volatile content and transportation history (Heiken, 1972). Particles from magma with high volatile content are likely to be jagged, as the ash is derived from the fragmentation of vesicle walls. Ash which comes into contact with water is likely to have a blocky morphology, due to the stresses within the quenched magma (Heiken, 1972). Particles transported post deposition may become rounded, due to abrasion against other particles. The particles may also

aggregate to form clusters, especially in the presence of water (Heiken, 1994). The angular shape of ash particles contributes to abrasion within generators which can severely reduce the service life of components, increasing downtime.

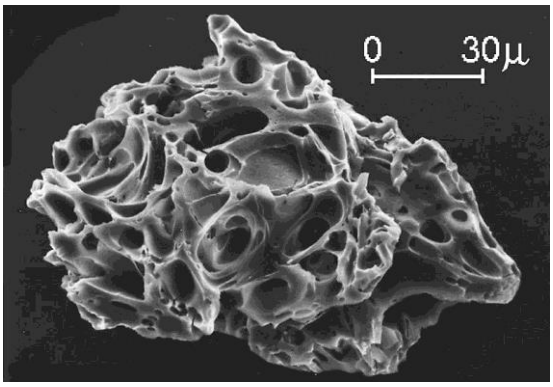

Figure 2.2: A scanning electron micrograph image of a vesiculated ash particle from the 1980 eruption of Mount St. Helens volcano in Washington State (Photograph A.M. Sarna-Wojcicki.).

2.2.3.4 Abrasiveness

Volcanic ash can be abrasive, due to it jagged morphology and hardness (up to 7 on the Mohs hardness scale) (Heiken, 1994). Particle abrasion can accelerate corrosion, caused by soluble salts present on the surface of ash particles as it exposes treated surfaces such as painted metal.

2.2.3.5 Particle Density

Density of volcanic ash particles is controlled by the composition of the source magma. Ash with high silica content will have a lower density than ash formed from low silica magma. The density of volcanic ash can vary from 700 kg/m^3 for pumice to 3,200 kg/m^3 for lithics (Wilson et al., 2012b). Glass shards and crystal densities range from 2,350-2,450 kg/m^3 and 2,700-3,300 kg/m^3 respectively. Density will control the ability of ash to be ingested within generators; less dense particles are more likely to be ingested. The increased percentage of glass in low density ash will also contribute to increased abrasion, due to its hardness.

2.2.3.6 Surface Composition and Conductivity

During the residence time of ash particles within the buoyant plume, soluble acids and salts are deposited on the surface. The most common acids are sulphuric acid (H_2SO_4), hydrochloric acid (HCl) and hydrogen fluoride (HF). Deposited salts include calcium sulphate ($CaSO_4$) and sodium chloride (NaCl) (Witham et al., 2005). When ash is dry, it is highly resistant to electrical conduction (Nellis and Hendrix, 1980). However water causes the salts to dissolve, forming a conductive layer over the ash particle. Wardman et al. (2012a)

note that fine grain ash is more likely to be conductive as it retains moisture more effectively than coarse grain ash. In addition, Wardman et al. (2012a) found that, while all grain sizes had very low resistivity values (e.g. <100Ωm) and therefore high conductivity, compaction preferentially increased the conductivity of coarse grain ash (>1 mm). The primary hazard from the conductivity of volcanic ash is flashover of high voltage electrical lines (Wardman et al., 2012a). During such an outage, the reliable operation of large format generators will be essential for lifeline providers.

2.2.3.7 Fall Rate

The ash fall intensity (fall rate) is essential to effectively test the ash fall hazard to generators. The study of generators requires the rate of ash fall in addition to the total deposited mass to effectively determine the likely mass ingested by the generator, as this is likely the primary control on the mean time to failure. Fall rates are important to understand the rate of ash ingestion and the mean to time failure of a generator. The fall rates used in the experimental phase of this study are further explained in Section 3.3.3, detailing the likely fall rates within Auckland and the rates used during experimentation.

2.3 Ash Fall Hazard for the Auckland Region

One of the thesis aims is to consider the risk of ash fall to large format generators, within the Auckland region. To achieve this, an understanding of the Auckland ash fall hazard is required. The following sections detail the potential sources, likelihood and magnitude of ash fall in the region.

2.3.1 Sources

The Auckland region is at risk of ash fall from two distinct sources. The Auckland Volcanic Field (AVF) is a source of proximal ash fall hazard. Distal ash sources include Mt. Taranaki, the Taupo Volcanic Zone and Tahua volcano (Mayor Island) (**Figure 2.3**).

The AVF contains over 50 predominantly monogenetic basaltic cones. A future eruption is expected to come from a new vent located within the field. This is likely to cause devastation close to the vent (i.e. several kilometres) from blast, pyroclastic density currents and lava flows (Johnston, 1997). Ash falls are likely to be produced, impacting much larger areas of the city, due to its proximity; however ash deposition will be controlled by the duration and height of any eruption column and the wind conditions at the time of the eruption. In addition, large expanses of ocean and a high groundwater table in the AVF mean interaction

between magma and water is likely, increasing the volume of ash produced and decreasing the grain size (Morrissey et al., 2000) (see Section 2.2.1).

Ash fall from distal sources is possible from a range of volcanoes to the south of Auckland (Table 2.1). The frequency and magnitude of distal ash fall hazards in Auckland is dependent on the eruption frequency of these volcanoes, the magnitude of their eruption and the wind conditions at the time of the eruption, as this will control dispersal direction of the ash (Rhoades et al., 2002). Magma composition, typologies and typical volcanic explosivity index (VEI) ranges for distal ash source volcanoes are presented in Table 2.1. VEI was determined by review of referenced papers and the catalogue of eruptions in the LaMEVE database (Crosweller et al., 2012).

Table 2.1: Type and typical magnitude of volcanoes which could impact Auckland

Volcano	Distance to Auckland (km)	Type	Wind toward Auckland (%)[a]	VEI Range
Auckland Volcanic Field	---	Monogenetic basaltic field	---	0-3 (Magill and Blong, 2005)
Mt Taranaki (Egmont)	271	Andesite-dacite stratovolcano (Turner et al., 2009)	4.5	4 - 6 (Turner et al., 2009)
Taupo Volcanic Centre	228	Rhyolitic Caldera (Houghton et al., 1995)	2.5	4 - 7 (Walker, 1981)
Okataina Volcanic Centre	188	Caldera with Rhyolitic and Basaltic Lava Domes (Cole et al., 2010)	2.2	5 - 6 (Cole et al., 2010)
Tuhau Volcano (Mayor Island)	135	Shield Volcano (Houghton et al., 2010)	3.4	4 - 6 (Houghton et al., 2010)
Tongariro Volcanic Centre	272	Andesitic Stratovolcanoes (Cole et al., 1986)	2.8	4 - 6 (Moebis et al., 2011)

a) *The percentage of wind toward Auckland is based on measurement taken 4 times a day over 16 years. Where a measurement showed the wind directed toward Auckland at any height the measurement deemed to be conducive to transporting ash toward Auckland.*

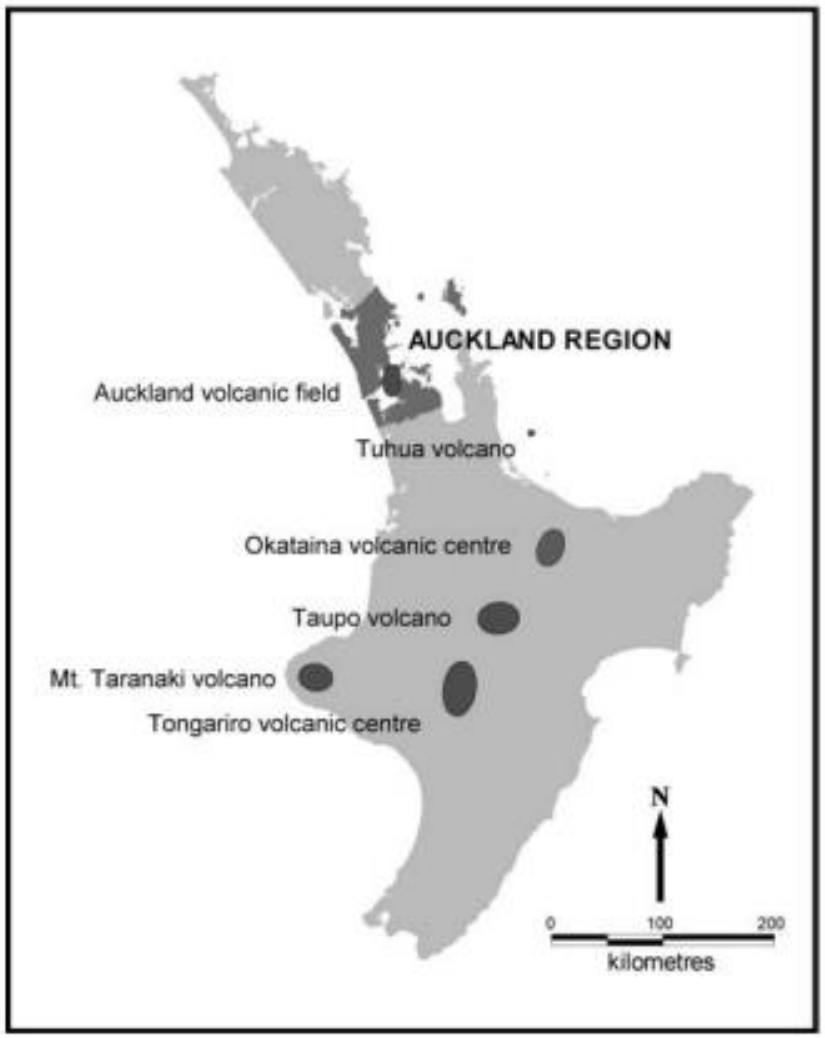

Figure 2.3: Map of New Zealand's North Island indicating sources of volcanic ash which are capable of causing ash fall within the Auckland region.

2.3.2 Likelihood and Magnitude of Ash Fall in Auckland

To understand the hazard posed by the both proximal and distal sources, data detailing the frequency and magnitude of past ash fall from these sources is necessary. Work in the Auckland region has focussed on lake cores to determine the frequency of ash fall events. Drilled primarily in maars, the lake cores contain 106 different tephra layers from proximal and distal sources over the last 80,000 years (Molloy et al., 2009). Mt Taranaki has been identified as the most frequent ash contributor to the region, while Tahua has only two events within the record (Molloy et al., 2009) (**Table 2.2**). While these records provide an indication of the frequency of ash fall in the past, they do not provide a clear forecast for the future, due to periods of high and low eruptive activity from the source volcanoes, over the time period of the record. In addition, the preservation potential of ash deposits within the record means that the total number of ash falls indicated by the cores is likely to be an underestimation of

the true number. Hurst and Smith (2010) note that in the case of AVF ash fall, as little as half of all events may be recorded within the cores. Changes in the climate over the past 80,000 years may also impact dispersal, especially for distal sources, due to changing wind conditions (Hurst and Smith, 2004). Analysis of modern climate records suggests the wind is only conducive to transporting ash towards Auckland from the distal sources identified on ~18 days in any given year (~5%) from all distal volcano sources (G. Wilson 2014, pers. Comm., 18/3).

Due to the uncertainties associated with lake core records, there have been several attempts to develop probabilistic ash fall models which forecast the volume and frequency of ash fall in Auckland, from both proximal and distal volcanic sources. Magill et al. (2006) used the ASHFALL model to develop a catalogue of simulated tephra dispersal patterns. They found AVF eruptions were highly variable with maximum thicknesses ranging from 0.1-150 mm. Magill et al. (2006) also concluded Andesitic eruptions (primarily Mt Taranaki) deposited a mean thickness of 1.7 mm, but were confined to a limited section of the region. Rhyolitic eruptions recorded larger thicknesses ranging from 30 mm in the south to 9 mm in the north. The model had a mean thickness from all sources of 7 mm in the south to 1.5 mm in the north but reported maximum thicknesses of 150 mm for an AVF source, 12 mm from an andesitic source and up to 830 mm from rhyolitic centres (Magill et al., 2006).

Table 2.2: Minimum, median, mean and maximum thickness of tephra layers identified within the Auckland region (Newnham and Lowe, 1991, Newnham et al., 1999, Sandiford et al., 2001 and Shane and Hoverd, 2002) Table from (Magill et al., 2006).

Centre	Number of layers	Minimum (mm)	Median (mm)	Mean (mm)	Maximum (mm)
AVF	16	1	4	20	190
Tongariro	7	1	1	2	2
Egmont	51	1	2	3	20
Tuhua	2	70	70	70	70
Okataina	17	1	3	45	630
Taupo	4	1	6	10	27
TVZ	11	1	3	6	20

Another model produced by Hurst and Smith (2010) estimated the cumulative ash thickness at any given location within the North Island, based on return period. This was based on a magnitude-frequency relationship for all active volcanoes in New Zealand's North Island and wind statistics. This model estimated, over a 500 year return period, the likely cumulative ash

thickness in Auckland is < 1mm, while over 10,000 years the region could expect a cumulative thickness of 16mm.

While probabilistic models provide estimated long term averages, it is difficult to account for large individual events. The Magill et al. (2006) study modelled for maximum thickness to account for such events. One significant event recorded within lake cores is the Rotoehu eruption (64 - 45ka (Newnham et al., 2004)) from Okataina which is estimated to have deposited 630 mm of ash over the Auckland region (Molloy et al., 2009) (**Table 2.2**).

Table 2.3: Frequency of ash fall within the Auckland region over the last 80,000 years. Frequency grouped by source (Molloy et al., 2009).

Source	Approx. return period
Mt Taranaki	1,500 years
Okataina and Taupo	3,800 years
Auckland Volcanic Field	3,500 years
Tongariro Volcanic Centre	11,400 years
Tahua Volcano	40,000 years
Any Source	750 years

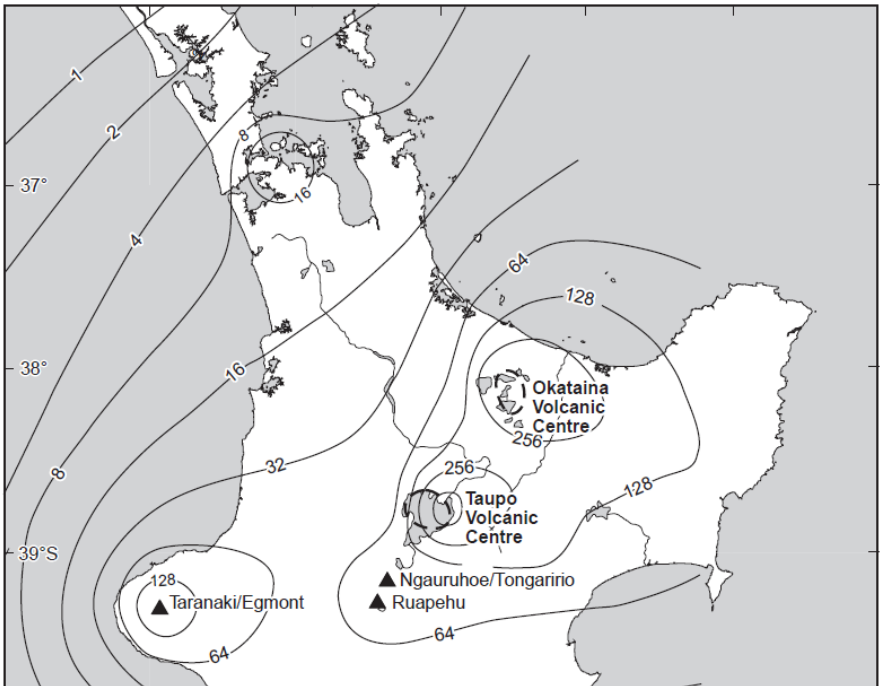

Figure 2.4: Ash isopach map for all North Island volcanic sources, for a 10,000yr return period. Ash depth are in millimetres (Hurst and Smith, 2010).

2.4 Vulnerability of Power Systems

High voltage (HV) transmission lines have been shown to be vulnerable to volcanic ash falls (Wardman et al., 2011). Specific hazards to HV lines identified by Wardman et al. (2012b) include:

- The accumulation of ash on high voltage (>33 kV) insulators can lead to flashover which may cause outages and damage the insulators
- Disruption of generation facilities. For example ash ingestion into hydro-electric turbines can cause accelerated abrasion
- Controlled outages may be necessary to allow for the cleaning of ash
- Abrasion and corrosion of exposed equipment
- Breakage of lines, either directly by ash loading or indirectly by breaking of vegetation over the lines

Distribution networks, while operating at lower voltages (<33 kV), may also be at risk of flashover since smaller insulators are used (Wardman, 2013). The large number of distribution lines also makes prevention of flashover difficult. The majority of New Zealand's generating capacity lies to the south of the Central Plateau (Nair and Zhang, 2009). Two HV lines supplying Auckland carry power through the North Island; the primary line is located 10-15 km east of the Tongariro volcanic centre (Figure 2.5) (Wardman et al., 2012a). Therefore ash fall in Auckland city or on the HV lines supplying the city may lead to outages in the city. In the event of failure within the network, generating sets are likely to be used to ensure continued electricity continuity for critical infrastructure such as hospitals, water and wastewater treatment plants, telecommunications and emergency services (Tang et al., 2006). It is probable that many commercial operators would also utilise large number of generating sets to continue their operations.

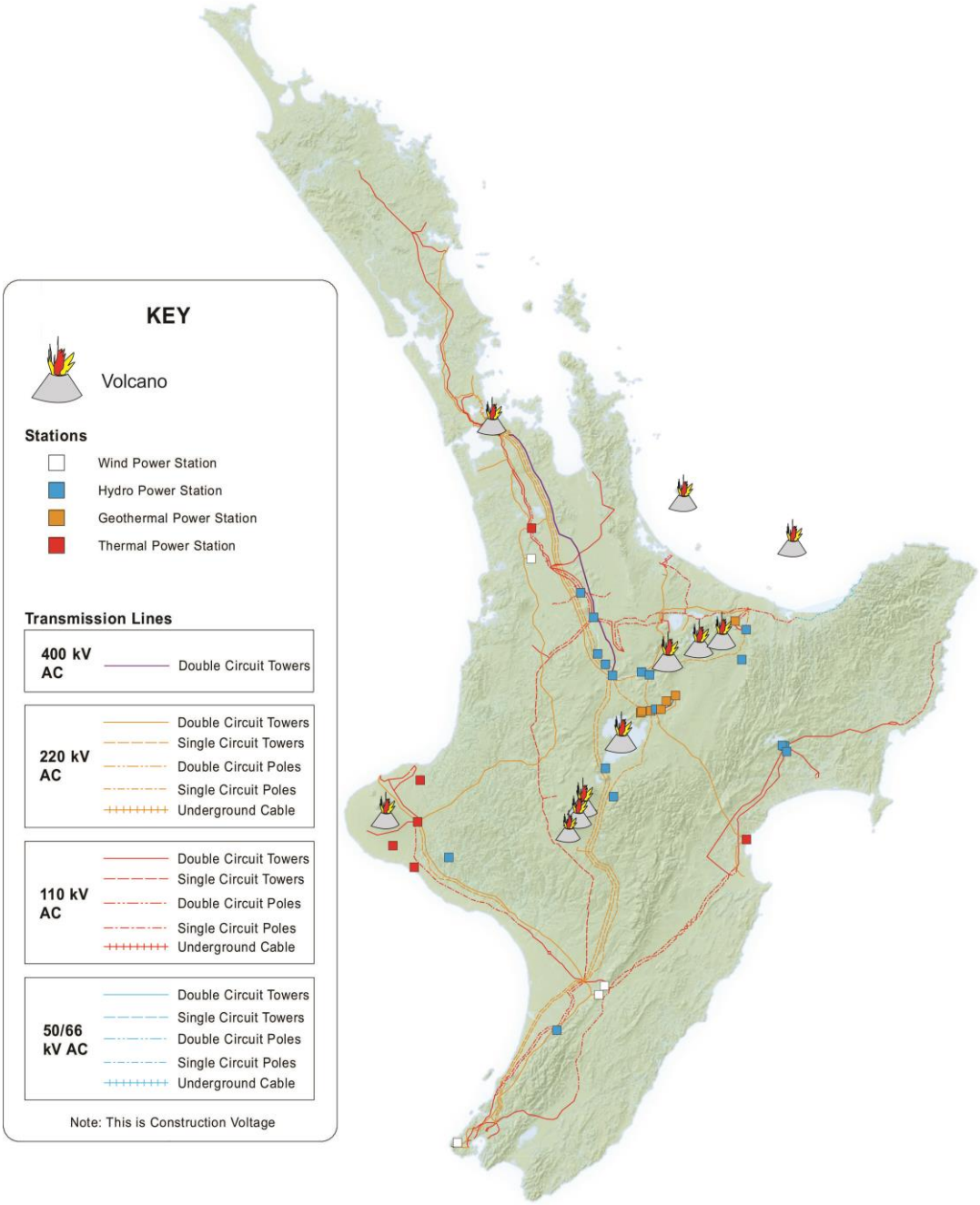

Figure 2.5: Map indicating the transmission lines and the distribution of volcanic ash sources within the North Island, New Zealand. Modified from (Transpower, 2013).

2.4.1 Generating Sets

Generating sets are likely to be used during an ash induced outage to supply backup power (Tang et al., 2006). A generating set (Genset) is defined as any combination of an internal combustion engine and an electric generator (De Almeida et al., 2002). This combination is used to produce anything from a few hundred watts up to a few megawatts (Caterpillar Electric Power, 2014). As the focus of this study is on the power requirements of critical

infrastructure, only Gensets rated over 500kW are considered (approximately the power requirements of 70 homes (Ministry of Economic Development, 2010)). This group of generators will be referred to as large format generators.

The most common rating for large format generators, used as backup supply in New Zealand, is a 550kW prime (V McKenzie 2013, pers. Comm., 12/8). Generators are provided with two ratings: prime and standby (Siu and Lopopolo, 2011). The prime rating relates to electric power the unit can provide on a long term basis, without damaging the machine (De Almeida et al., 2002). The standby rating is the level of power the unit can produce on a short term basis. This is usually defined as one hour in every ten (Siu and Lopopolo, 2011).

Large format generators are typically configured with an air intake at one end which cools the radiator (**Figure 2.6**). The radiator is paired with the internal combustion engine, with the radiator pipe and exhaust connected to the side and top respectively. The engine air intake is usually located at the top of the engine block (**Figure 2.6**). Finally, a sealed generator uses the kinetic energy of the turning shaft, powered by the engine, to produce electricity.

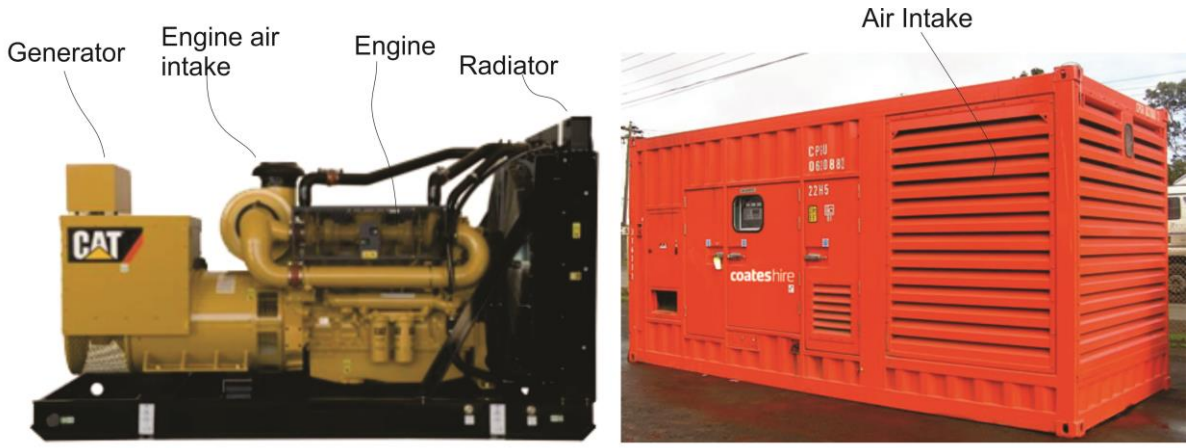

Figure 2.6: Left: Standard diesel generator (Model: Perkins – 1006TAG) annotating key components. Airflow is from left to right (Caterpillar Electric Power, 2014). Right: Typical generator enclosure with large air intake louvers (Coates Hire, 2014).

2.4.1.1 Generator Case Study: Bariloche, Argentina.

A recent volcanic eruption sequence affecting the township of Bariloche, Argentina, provides an ideal case study for the impacts of volcanic ash on large format generators. The town of Bariloche, population 133,500 (2010) (INDEC, 2012), is a major tourist centre in northern Patagonia. Following the 2011 eruption of Puyehue-Cordon Caulle, Bariloche located 92 km southwest of the vent, received up to 45 mm of ash fall in less than 24 hours (Wilson et al., 2013). A particular vulnerability of the town's electricity supply was the single national grid

connection point supplying the town. During the ash fall, deposited ash caused power outages, due to flashover of ash contaminated high voltage insulators and switch yard equipment. The single line meant there was no other means to supply the town from the national grid. The town had previously been supplied by five generators. The facility was retired when the town was connected to the national grid but was kept operational for backup purposes. The facility consists of three existing gas/diesel turbine generators and two diesel internal combustion generators.

During the ash fall crisis, these generators were activated to provide emergency power supply for the town. However, the generators sufferer repeated problems related to ash ingestion. Air intakes for the turbine generators were located approximately 1.5 metres from the edge of a sloping roof which provided some protection from direct ash fall (**Figure 2.7**). The intakes were covered with a coarse wire mesh and a fine wire particle filter. Despite the protection of the roof, sufficient ash was available to cause blockages of both the air intakes and the condensers (**Figure 2.8**). Ash sliding off the roof, in front of the equipment, exacerbated the problem during and after ashfall.

Air intakes for the diesel generators are located on the roof of the complex (**Figure 2.7**) and are directly exposed to the atmosphere. The intakes blocked rapidly during ash fall and required frequent cleaning. Ash obstruction within the condensers resulted in a loss of performance and an inability to maintain sufficient cooling to the generators which automatically shut down as a safety measure. Following each shutdown, the filters had to be taken apart and cleaned with high pressure water.

Due to the significant down time, a decision was made to build a new 20 MW generator farm to the south of the town. The farm consisted of 22 units, each capable of 1 MW (two extra units to allow full load during maintenance). Similar ash ingestion problems were experienced at the new site due to exposure to on-going light ash falls (~1-2 mm at a time) and from wind remobilisation of ash deposits. However the impacts were reduced by design modification which reduced ash ingestion. While ash was still able to enter the generator casings (**Figure 2.9**), hoods fitted over the intakes reduced direct ash fall ingestion. Ash which was still ingested into the casing, and therefore available to the engine air intake, was mitigated through the use of high-density insulation foam which was placed over in air intakes by technicians at the farm. The filters removed some of the coarse ash, reducing the load on the standard filters thereby increasing their service life. Prior to the fitting of the

temporary filters, replacement of the primary filters was required after each substantial ash fall.

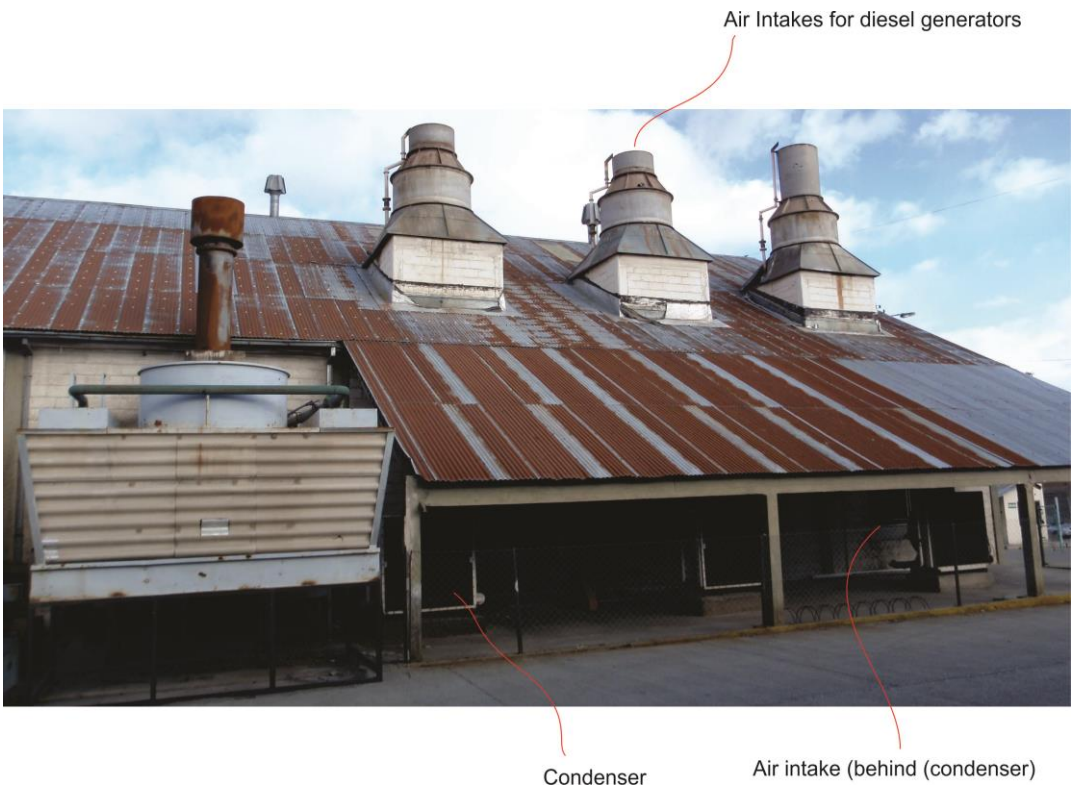

Figure 2.7: Building in Bariloche housing the existing three gas/diesel turbine generators and two diesel internal combustion engine generators. Air intakes are located under roof at bottom of the photograph.

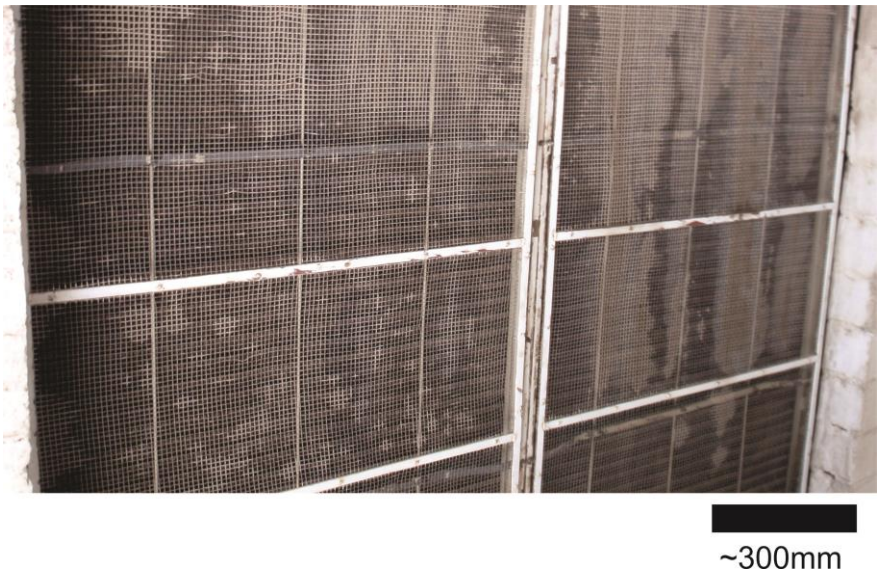

Figure 2.8: Ash deposited on generator air intakes in Bariloche. Intakes required frequent cleaning with high pressure water to maintain airflow.

In addition to ash build up on air intakes and cooling equipment, corrosion was a significant issue over the medium to long-term. Exposed metals such as nuts, bolts and even stairs quickly began corroding. Corrosion is evident in the new generator farm which was six months old at the time the photographs were taken (**Figure 2.9**). Other issues experienced were ash abrasion of fittings such as pipe insulation and blockages of fuel valves leading to overfilling and fuel spills.

Figure 2.9: Left: Ash deposited on the engine block of a generator within the new 20MW generator farm. Deposited ash can potentially be ingested by the engine air filter which may lead to stalling. Centre: Hood fitted over the air intake of a 1 MW generator to reduce ingestion of direct ash fall. Right: Corrosion on fittings within the new generator farm.

2.5 Ash fall Impacts to Air-Handling Systems

It has been well established that volcanic ash fall can disrupt air-handling systems (Blong, 1996, Wilson et al., 2012b). Empirical laboratory research by Barnard (2010) investigated this and found air handling units were vulnerable to blockages from volcanic ash. Empirical data shows a maximum failure threshold of 35 mm of wet ash or 50 mm of dry ash for the common split type systems (part of unit mounted inside, part outside). The primary failure mode was obstruction of air flow to the condenser, causing overheating and failure of the condenser by tripping the pressure safety switch which shut down the unit (**Figure 2.10**). Ash covering the condenser fins also acted as an insulator, reducing the condenser's performance. The condenser can be reset once it has cooled but repeated shutdowns may cause long term damage. Barnard (2010) found that the test unit was unable to maintain its pre-test

performance, even after extensive cleaning, indicating overpressure had damaged the condenser.

Barnard (2010) trialled temporary filtration by fitting EU3 medium filters designed to remove 80% of particles at 10 µm but only 45% at 1 µm. Testing showed that the filter was effective in reducing the ash ingested into the condenser but it reduced air flow and rapidly blocked, necessitating frequent cleaning.

Figure 2.10: Heating, Ventilation and Cooling (HVAC) condenser after ~32 mm of wet ash was applied over ~ 4.5 hours (Barnard, 2010).

2.6 Analogous Contaminants

A range of other airborne particulate contaminants were considered, including fine sands from dust storms and coal dust from mining operations.

Potentially any dusty environment poses a risk to generators through blocking of air intake filters. In particular dust storms contain a large amount of airborne particles and were investigated as an analogue; however this was discounted as the typical particle concentrations of dust clouds (0.231 mg/m^3) was significantly lower than volcanic ash fall (up to 9 g/m^3) (Emeis et al., 2011).

Another potential analogue investigated was coal dust. Operators of large format generator in the Stockton Coal Mine, New Zealand have found that coal dust rapidly contaminates generators working in the mine environment and can cause overheating by restricting the airflow (D. Creelman 2013, pers. Comm., 28/3). The use of coal dust as an analogue was also discounted as the median grain size was significantly smaller than volcanic ash (~48 µm) (Cashdollar, 1996).

2.7 Failure Modes

The case study of Bariloche, Argentina, identifies possible failure modes for generators exposed to volcanic ash fall. In the short term (hours to days) the primary failure modes were stalling and overheating, due to ingested ash which blocked the condensers and engine air intakes. In the long term (months to years) failure is likely to occur, due to corrosion and abrasion of the generator's internal parts. Complete mitigation of all the failure modes requires all ash to be excluded from the generator casing. While that may not be possible, the best method of reducing the frequency of failure is to reduce the quantity of ingested ash. This can be achieved by fitting temporary filtration over the air intakes such that airflow is not significantly impacted.

2.8 Summary

Auckland is at risk from a number of volcanic sources. If power is cut to critical infrastructure, large format generators are likely to be used to supply backup power. However, large format generators are vulnerable to ingestion of volcanic ash which can clog air filters, abrade and corrode internal parts and restrict airflow, leading to overheating and thus shut-down. The next chapter will outline the design of an experimental test apparatus to test the application of a number of mitigation measures.

Chapter 3 Methodology

3.1 Introduction

This chapter presents the methodological design for the empirical investigation of volcanic ash ingestion for large generator sets and exploration of possible temporary-filtration strategies. This includes:

- Selection and preparation of ash for use in the testing, including specific parameters such as grain size, and fall rate
- design of an apparatus which replicates (at a smaller scale) the process of suspended ash being ingested into a generator set
- selection and preparation of temporary ash reduction measures (filtration and other techniques)
- data collection tools for monitoring ash ingestion and ash reduction measures performance

The methodology is informed by the reviewed literature from Chapter 2.

3.2 Testing Facilities

Testing was undertaken in the Volcanic Ash Testing Laboratory (VAT Lab; www.vatlab.org) at the Department of Geological Sciences, University of Canterbury. The laboratory is designed to facilitate the testing of critical infrastructure components in a controlled environment. The facility maintains a stable temperature and humidity, reducing the effects of environmental variability on the testing.

3.3 Defining Ash Types and Fall Rates to be utilised within Testing

Essential to this study is the identification of likely grain size and fall rate values, from the volcanoes which may impact Auckland (Chapter 2). To ensure the testing applied realistic ash grain sizes and fall rates, a review of available data sets was undertaken on well documented eruptions (**Table 3.1**). To analyse recorded data sets, two groupings were selected to establish trends: 1) Grouping by both eruptive style and petrology and 2) grouping by volcanic explosivity index (VEI), ranging from 0-8, as defined by Newhall and Self

(1982). After considering both methods VEI was chosen as the preferred method due to insufficient data to appropriately populate groupings based on eruptive style and petrology (see Section 2.2.1).

3.3.1 Distance Controls on Ash Fall Intensity and Grain Size

Data was obtained from eight eruptions chosen because published material was available detailing grain size and/or fall rate had been recorded with a sample location, consisting of 64 individual sampling sites (Table 3.1). Where samples provided a named location, but no specific distance, Google Earth was used to determine the distance. Where the location was uncertain the data was not used. The results of the analysis inform the ash fall and intensity and grain sizes which are reasonable for use with testing.

Table 3.1: Summary of fall rate and grain size data.

Volcano	Year	Grain Size Samples	Fall Rate Samples	VEI	Data Quality	Reference
Montserrat	1997	5	0	3	Measured	(Bonadonna et al., 2011)
Hudson	1991	4	0	3	Measured	(Scasso et al., 1994)
Pinatubo	1991	21	0	6	Measured	(Kienle and Swanson, 1980)
Eyjafjallajökull	2010	17	14	4	Measured / eye witness reports	(Bonadonna et al., 2011)
Mt. St. Helens	1980	6	0	5	Measured	(Sarna-Wojcicki et al., 1981)
Redoubt	2009	0	7	3	Eye Witness reports	(Scott and McGimsey, 1994)
Mt. Augustine	1976	0	7	3	Eye Witness reports	(Wilcox and Coats, 1959)
Mount Spurr	1953	0	7	4	Eye Witness reports	(Kienle and Swanson, 1985)

3.3.2 Grain Size

Grain size data was recorded at 52 of the 64 locations and is presented in **Figure 3.1**. The presented data has been coded dependant on the VEI of the eruption from which it was ejected. Grain size data was difficult to obtain, as the samples required either a distribution or median grain size, along with a sample location. Some studies did not give median grain size or grain size distributions or did not state the exact location of the sample area, making it unsuitable for this purpose.

The grouping of data (**Figure 3.1**) across VEI indices, at similar distances, implies the correlation between grain size and distance is stronger than that of VEI and grain size. It should be noted however, that the large magnitude and large ash volumes associated with silicic eruptions, increases the likelihood of studies reporting grain size and fall rate data, potentially skewing results.

In the application of this data set for Auckland, the distance of Auckland from each volcanic source has been identified (Figure 3.3). From this, a distal event will likely deposit ash predominantly between 2 – 6 phi (20 - 250µm). Proximal eruptions occupy a wide range of possible grain sizes from -1.5 to 5 phi (30 – 2,000µm). In the Auckland region grain size will likely be controlled by eruption style and the influence of water interaction, with finer grain sizes being produced when magma interacts with water (Section 2.3).

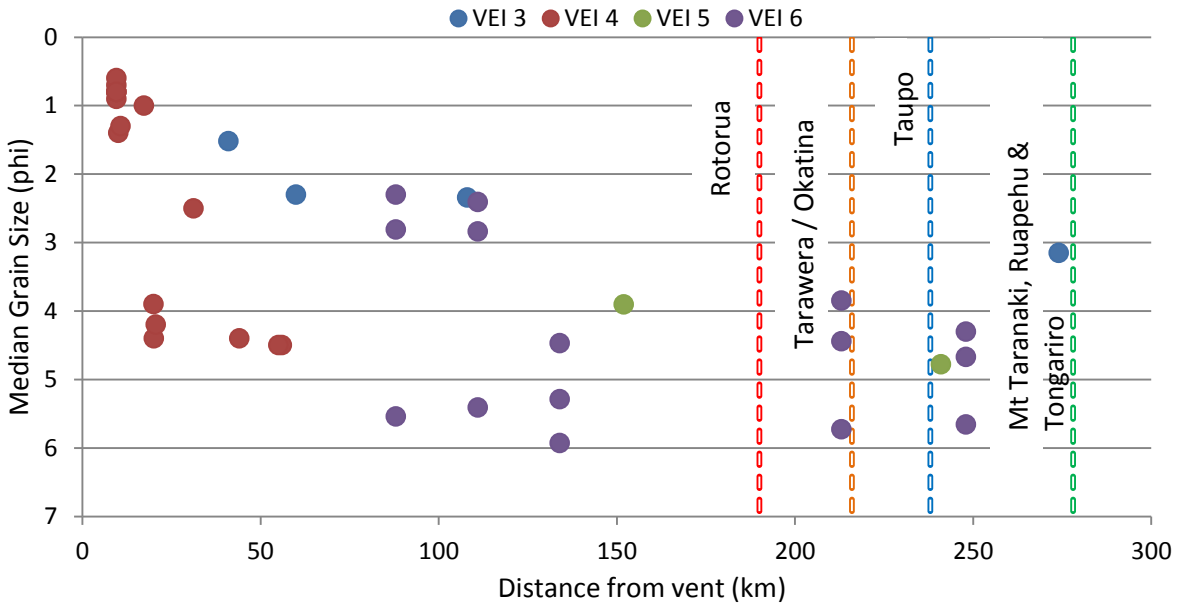

Figure 3.1: Collated database of volcanic eruptions of varying VEI magnitudes and their median grain size deposited at distances from the eruptive vent. Also indicated is the distance from known NZ ash producing volcanoes to Auckland (section 2.3.1).

3.3.3 Fall Rate

Fall rates, or the rate at which ash will be introduced into the testing environment is crucial to understand the time period over which a generator may fail. In reviewing fall rate data sets, details of four eruptions were found to be of consistent and reliable data, Eyjafjallajökull (2010) (Bonadonna et al., 2011), Redoubt (2009) (Scott and McGimsey, 1994), Mt. Augustine (1976) (Wilcox and Coats, 1959) and Mt. Spurr (1953) (Kienle and Swanson, 1985). This resulted in 27 locations (total among all studies) being presented (**Figure 3.2**). It is important to note that the ranges of eruption magnitude is limited, containing only eruptions between 3-4. The lack of data makes any kind of evaluation by VEI problematic as the data only covers two indices. However, **Figure 3.2** does suggested that ash fall rate decreases with distance from the erupting vent. A similar presentation of the geographical distance of Auckland, from eruptive sources, is also shown to aid ash fall rate parameter selection for the experimentation.

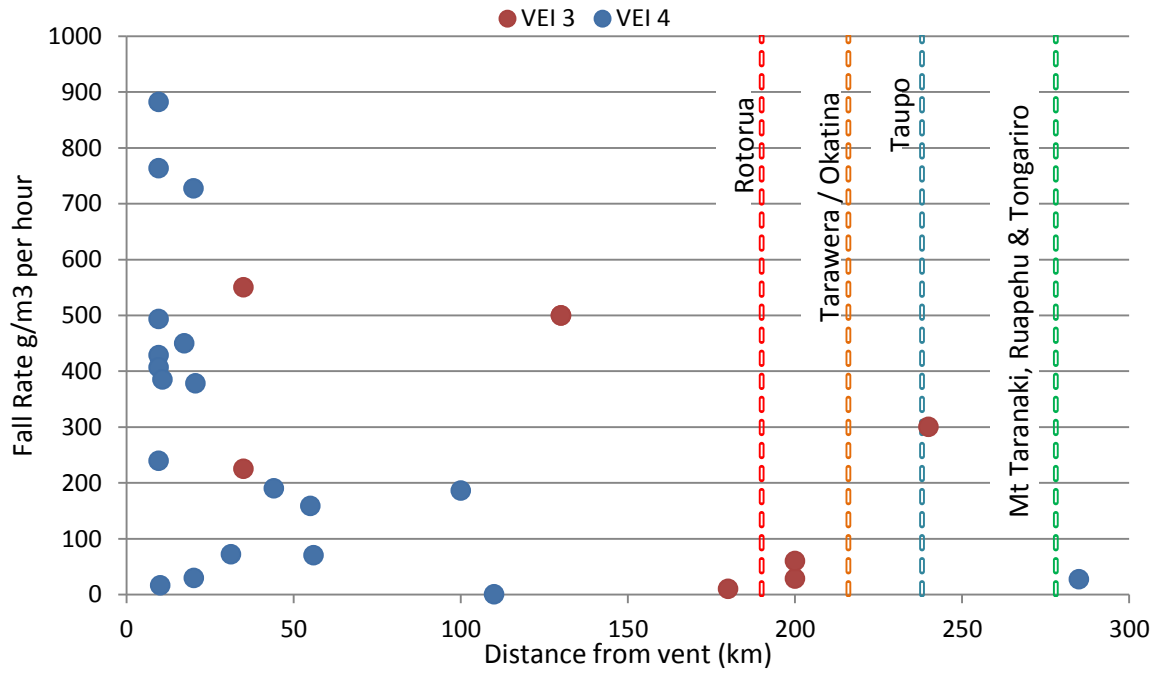

Figure 3.2: Relationship between ash fall rate and distance from vent as a function of magnitude, showing distances from NZ ash producing volcanoes to Auckland.

3.3.4 Summary of Ash Fall in Auckland

In reviewing this data (Figures 3.3. and 3.4) the ash fall grain size and ash fall rates were estimated for the Auckland region (**Table 3.2**). Grain sizes and fall rates within these ranges will be used within testing regimes. Expert judgment was used to select fall rates and grain size for testing. The fall rate selected for the primary testing was 340 g/m^2/hr. This rate was

applied to the entire primary testing regime to allow the data to be compared. In addition two further tests were undertaken at higher fall rates to determine the impact of a proximal, high intensity, ashfall. The median grain size selected were ~200 µm to allow the limited ash sets to fit within the ranges set by the eruption styles and the proximity to source.

Table 3.2: Grain size range and fall rates to be used in testing

	Proximal		Distal	
	Likely range	Selected for tests	Likely range	Selected for tests
Grain Size	30 - 2,000 µm	Sieved to <1,000 µm	20 – 250 µm	Sieved to <500 µm
Fall Rate	340 – 2,000 $g/m^2/hr.$	~340 $g/m^2/hr.$ up to 2,000 $g/m^2/hr.$	0 – 400 $g/m^2/hr.$	~340 $g/m^2/hr.$

3.3.5 Volcanic Ash

The testing methodology involves the introduction of volcanic ash into a testing chamber at rates similar to what could be expected in reality (see Sections 3.3.4). This required large volume of ash for the experiments. Large volumes of fresh volcanic ash is difficult to obtain, as at the time of testing, no volcanos within New Zealand have recently erupted, and importing ash from overseas is problematic due to New Zealand's strict biosecurity laws. Additionally, fine grained volcanic ash often weathers rapidly, precluding mining in-situ ash deposits for use in laboratory testing (Wilson et al., 2012a). Therefore the most practical method of providing large quantities of volcanic ash is through the production of a 'pseudo ash' from course, non-weathered pyroclasts and lavas.

Pseudo ash was developed in the Volcanic Ash Testing Laboratory (VAT Lab) at the University of Canterbury by Barnard (2010) and later refined by Wardman et al. (2012a) and (Wilson et al., 2012a) These have primarily been crystalline basaltic 'pseudo ashes'; however Auckland is at risk from ash compositions which range from basalt to andesite to rhyolite, and may be crystalline through to highly vesiculated. Therefore this research included two further ash types, in addition to the crystalline basaltic 'pseudo ash'. These are outlined in the following section. From herein this study refers to the three 'pseudo ashes' as Ash A, Ash B and Ash C as explained in Table 3.3.

Table 3.3: Ash types used for testing.

Source Rock:	Eruption / Ash Fall in Auckland	Ash Name
Basaltic Lava	Distal Basaltic/Andesitic or proximal wet AVF eruption	Ash A
Basaltic Scoria	Proximal dry basaltic AVF eruption	Ash B
Rhyolite Pumice	Distal TVZ eruption	Ash C

3.3.5.1 'Pseudo Ash' Rock Sources

Three source ashes needed to be produced for introduction to the testing chamber (**Table 3.3**). This required three source materials to be locally sourced (New Zealand), then manufacture and characterise the pseudo ash. This section documents this process.

Source rocks for Ash A were obtained from the Gollans Quarry, owned by the Lyttleton Port Company, located to the east of the container terminal. The material is basaltic lava, part of the Lyttleton Volcanic Group (Scott and McGimsey, 1994). Samples ranged from approximately 200 to 500 mm in diameter and were unweathered to prevent contamination of alteration products such as clay, which may alter the physical properties of the ash produced.

Source rocks for Ash B were obtained from a quarry within strombolian deposits of the Punatekahi cone, located on the northern edge of Lake Taupo. The basaltic scoria has a vesicularity of 40 - 80%, with an average bulk density of 1,600 kg/m^3. The clasts range from 20 - 30 mm in size and are packed with small amounts of fine grained material (Wilcox and Coats, 1959). The rock was freshly crushed and unweathered.

Source rock for Ash C was obtained from a block and ash flow within the Kaharoa Pyroclastics (Scott and McGimsey, 1994), exposed in a quarry on the south side of Mt Tarawera, near Lake Rerewhakaaitu. The pumice grains range from 10 – 710 µm (Scott and McGimsey, 1994). The pumice was carefully selected from within the outcrop to ensure the sample was relatively unweathered. This was achieved by scraping away the initial weathered material.

3.3.5.2 Pseudo Ash Production

Pseudo ash production requires a process of splitting, crushing, pulverising, sieving and dosing as outlined in Wilson (2011). However this varies for each ash type produced in this

study. After processing, all ash was stored in sealed, thick plastic sample bags to exclude contaminats and moisture.

Ash A

Ash A was produced by breaking large sections of rock (~400 mm in diameter) into smaller pieces, using a hydraulic press (Figure 4A). Pieces measuring <50 mm in diameter were then processed using a jaw crusher (Figure 4B). This device employs a stationary plate mounted against a moving plate in a 'v' shape to crush the rocks as they pass through. The crusher produces rock flakes of various sizes, with a maximum of approximately 10 mm in diameter. The flakes are further processed, using a disk pulveriser (Figure 4C), to produce smaller particles. The disk pulveriser uses a stationary disk, aligned with a rotating disk, to crush material. The gap between the plates determines the final grain size distribution produced. Finally the material was processed with an auto sieve, to obtain grains <1 mm in diameter.

Figure 3.3: Apparatus used in the production of pseudo ash. From left; a hydraulic press, a jaw crusher and a disk pulveriser.

Ash B and C

Material for Ash B and C was small enough to process without the use of the hydrulic press or jaw crusher; however as the samples are not from solid rock, moisure levels were higher. Initial crushing of the samples resulted in highly bimodal grain size distribution and a large degree of particle rounding. To resolve the issue, samples were dried in an oven at 110°C for 48 hours, lowering the moisture level.

Dosing with soluble salts

In work by (Broom, 2010), during the initial development of the basaltic pseudo ash (Ash A), a method of dosing the ash was developed to allow the surface chemistry to imitate volcanic

ash. Dosing was not used in this experiment as the primary research aims were focused on the blocking and obstruction of filters, rather than corrosion and conduction. It is possible that by not dosing the samples, some properties, such as aggregation of particles during fall, may have been altered from that of volcanic ash. However, this was considered to be only a minor limitation.

3.3.5.3 Pseudo Ash Characteristics

Grain Size Characteristics

The grain size distributions of the three pseudo-ashes were plotted against distributions from the 1996 Ruapehu eruption, 2008 Chaitén eruption, 2010 eruption of Montserrat, 2006 eruption of Merapi and the 2009 eruption of Redoubt to ensure their grain size distributions were similar to real volcanic ash types which may impact Auckland (**Figure 3.4**). The distributions were analysed by a Horiba LA-950a laser sizer.

Pseudo ash plots within the grain size distributions of the real ash, and also maintains a similar distribution shape (Figure 3.4), indicating it is a reasonable analogue for volcanic ash in terms of grain size. **Table 3.2** estimated reasonable ranges for the median grain size of proximal ash was between 31-4,000 µm, while the distal range was estimated at 31-250 µm. Ash types A, B and C fit within this range, recording median grain sizes of 153 µm, 183 µm and 182 µm respectively.

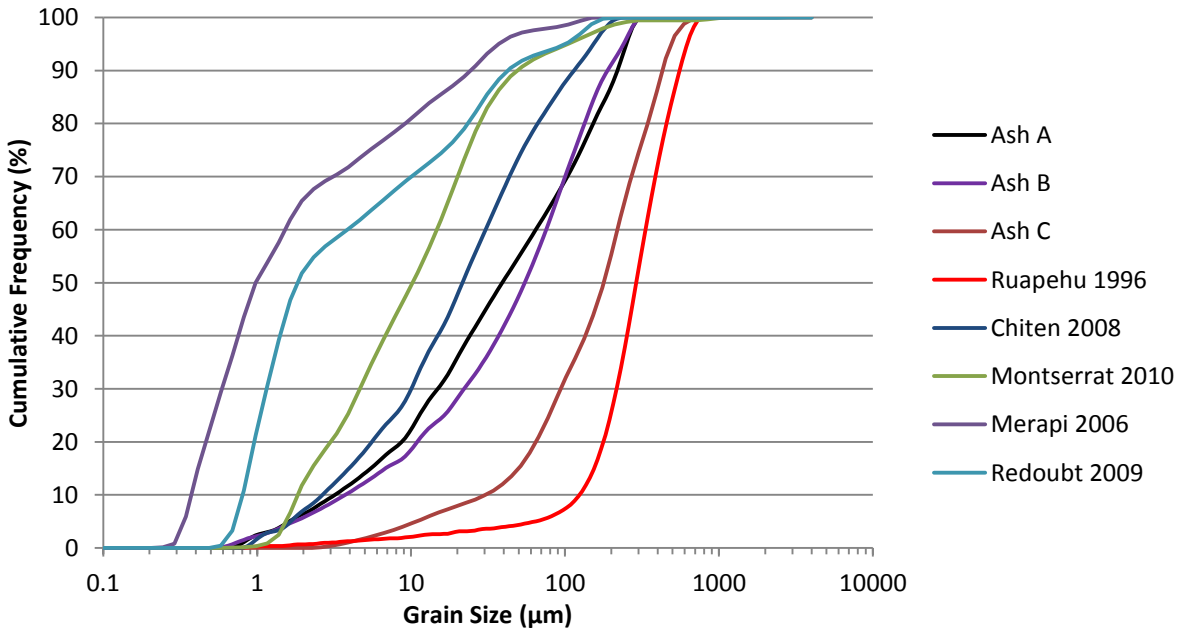

Figure 3.4: Cumulative frequency plot of volcanic ash grain size distributions from Chaitén, Ruapehu, Montserrat, Merapi, Redoubt and three pseudo ash samples (A, B, and C).

Density

A higher density is a potential limitation of pseudo ash, due primarily to its solid rock source. Ash developed under natural circumstance, is produced when the walls of bubbles within magma rupture during explosive decompression (section 2.2.1). The result of this violent reaction is a lightweight, irregular shaped particle, which does not pack efficiently. These characteristics result in low bulk densities.

The bulk density of each ash type was calculated using a glass vessel of a known volume. Ash was sieved into the vessel, replicating natural ash fall. The mass was then recorded and the density calculated (**Table 3.4**). Bulk density of natural ash varies from 500-2,000 kg/m^3 dependant on the level of compaction. While the pseudo ash samples have slightly higher densities they are suitable for use in this experiment.

Table 3.4: Bulk density of the three pseudo ash types.

Ash Type	Ash A	Ash B	Ash C
Density	1,790 kg/m^3	1,568 kg/m^3	1,100 kg/m^3

3.4 Replication of a Generator Setup: Design and Build of an Analogue Generator Apparatus (AGA)

Large format generators are typically installed in either a casing, similar to a shipping container or within a building fitted with appropriate ducts for air supply and exhaust. This study will assume this casing is present, as the confining nature of the case will result in higher suspended particle concentrations than an open room. By taking this approach, this study aims to avoid underestimating ash impacts on large format generators.

Utilisation of a generator was not viable for this study, as a result an analogue testing apparatus (AGA) was constructed in the VATLab to replicate the key vulnerable elements of a large format generator (section 2.7) including the radiator and engine air intakes. The AGA (Figure 3.8) was scaled down to replicate the key dimension of a large format generator. Fans were added to simulate normal airflows produced by a radiator fan. A further housing was constructed to replicate an environment where ash is being introduced; above this housing is a mounted ash shaker. Monitoring devices and stations were fitted and recorded data was used to determine ash reduction measure (ARM) effectiveness, details of which are discussed

in the following sections, and utilised to determine when and if the failure modes would occur (Figure 3.5)

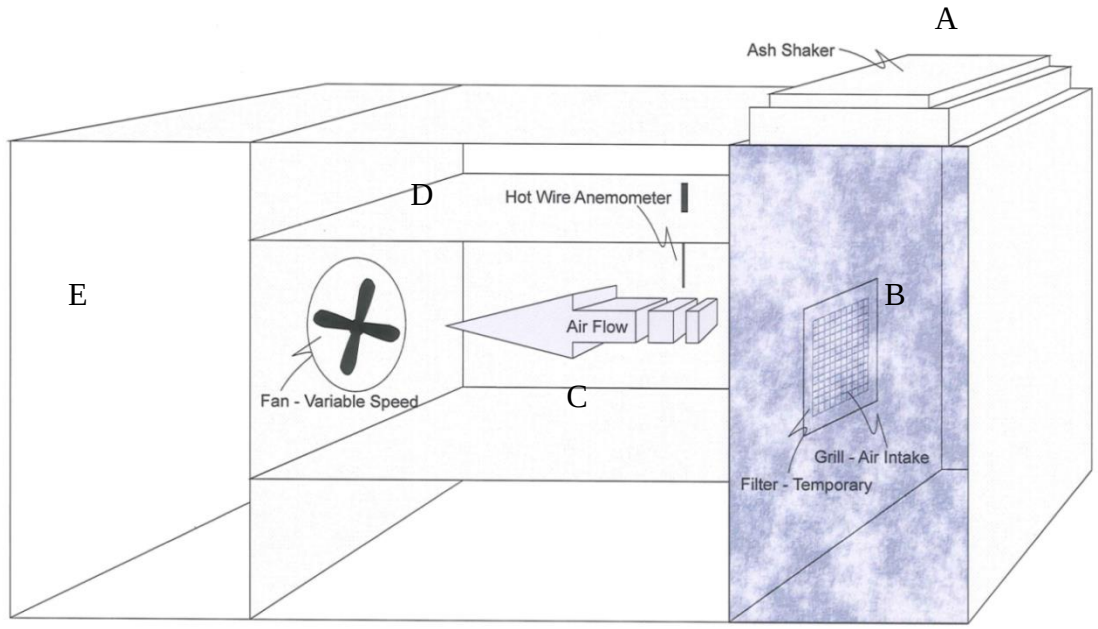

Figure 3.5: Diagram of testing apparatus, showing the AGA at centre. Key details the AGA's design, including an ash shaker at the top right (A and **Figure 3.6**), a drop chamber on the lower right (B), testing chamber in the centre (C), a combustion chamber filter within the testing chamber (D) and a discharge chamber at left (E).

Key components of the AGA testing setup are outlined below;

Drop Chamber

The drop chamber, positioned directly below the ash shaker, is constructed with three solid sides and a door at the front. The base is covered with a plastic liner to ease removal of ash following each test run. The top of the chamber contains an opening measuring 500 x 500 mm to allow ash to enter the chamber. On the left of the chamber another opening, covered by a grill measuring 300 x 200 mm provides the ingress point for ash into the testing chamber. The grill also provides mounting points for the temporary filters and the deflection hood. The height of the chamber was designed to ensure the majority of ash particles dispensed from the shaker reach terminal velocity prior to passing the grill. The equations used to determine the minimum height are discussed in Section 3.3.3. The chamber has a section cut from the wall to allow photographs of the mounted ARM to be taken.

Ash Dispersal

Sitting on top of the drop chamber is the ash dispersal system, an ash shaker constructed from wood with a stainless steel mesh, forming a box for ash to fall through. At the side of the box a hammer mechanism is used to vibrate the particles though the mesh and into the drop chamber. The shaker is discussed further in Section 3.4.2., in particular calibration of ash fall rates and variations between pseudo ashes.

Height and placement of the shaker unit is defined by the height at which ash particles reach terminal velocity, therefore reflecting a natural ash fall. To achieve terminal velocity, the dispersal system required sufficient height above the intake grill, within the drop chamber. The required minimum height was calculated using the following formulas, derived by Bonadonna et al. (1998).

1. $Vt \approx (3.1g\rho d/\sigma)^{1/2}$
2. $Vt \approx (g\rho d2/18\mu)$
3. $Vt \approx d(4\rho 2\, g2/225\mu\sigma)^{1/3}$

Where Vt is the terminal velocity, g is the acceleration due to gravity (9.81 m/s^{-2}), ρ is the density of the particles, d is particle diameter, σ is the density of air and μ is the dynamic viscosity of the medium.

Equation 1 represents particles >1,000µm in diameter, equation 2 represents particles between 1,000 and 60 µm and equation 3 represents particles <60 µm in diameter (Bonadonna et al., 1998). The boundaries between equations are a function of air pressure; at lower elevations the boundaries move slightly toward smaller grains. It is important to note that terminal velocity calculations are estimates, due in part to the irregular shape of the particles, causing tumbling during their decent (Wilson and Huang, 1979).

To determine which equation to apply, the 90th percentile particle was found from the laser sizing results (

Table 3.5). Using the above equations, a minimum drop chamber height of 130 mm was required to allow most of the particles to reach terminal velocity prior to reaching the grill, with the built AGA having a height above intake of 800 mm the drop chamber's design was sufficient.

Table 3.5: Terminal velocity calculations

Sample	90^{th} percentile max. size	Terminal velocity of largest particle	Height required for *Vt*
Ash A	588.9 µm	1.62 m/s	130 mm
Ash B	658.9 µm	1.42 m/s	102 mm
Ash C	446.2 µm	0.99 m/s	51 mm

Testing Chamber

The testing chamber is a long horizontal box measuring 1,200 x 400 x 400 mm scaled to model the internal dimensions of a generator casing. At the right of the chamber, the grill of the drop chamber allows air to enter. The front of the chamber contains two large windows, allowing observations to be made during a test run. A number of monitoring devices are used in this chamber which are discussed further in Section 3.5.

Fan

At the left, a large fan is mounted to provide airflow through the chamber. The fan measures 300 mm in diameter and is capable of sustaining consistent airspeeds through the grill, details of airspeed required in testing is further covered in section 3.4.1. The speed of the fan is variable allowing for lower airspeeds.

Particle Tracker

The particle tracker can be used as an analogue for the engine air intake as the airflows are similar. The particle tracker measures the level of particle concentration within the testing chamber. The tracker draws air directly from the testing chamber and discharges into the void space above. The use of the particle tracker as a monitoring device will be discussed further in (Section 3.5).

Discharge Chamber

The discharge chamber receives air from the testing chamber, which contains various concentrations of ash depending on the test being run. The chamber is fitted with a door contain an outlet grill. The primary purpose of this chamber is to contain discharged ash, reducing airborne concentrations in the laboratory environment.

3.4.1 Calibration of Air Flow

To gain insight into the required airspeed requirements of generator setups, site visits were conducted. This utilised the same airspeed testing equipment (hotwire anemometer) used in testing. The key calibrating unit utilised in this study was a Cummins DQFAD, located at the University of Canterbury. The 1 MW generator required airspeed of ~7.5 m/s over the intake measuring 2.76 m^2 , drawing the required 1,244 m^3/min of air for cooling (Cummins, 2013). The AGA's fan was fitted with a variable transformer which allowed the voltage delivered to the fan to be modified, speeding up or slowing down the fan. The airspeed was calibrated using a hot wire anemometer to match the generators airspeed of 7.5 m/s.

3.4.2 Ash Dispersal System Design

Dispersal of the ash required a device which could provide a sustained fall rate over an extended period. The device must also be variable, to allow a range of ash fall rates to be tested.

The final design for the dispersal mechanism (ash shaker) was a wooden box measuring 400 x 400 x 100 mm with a stainless steel mesh base. Two aperture sizes were used for the mesh base dependant on the ash size (480 and 1,000 µm). The shaker was struck at varying rates by a hammer located on the side of the box (Figure 3.6). The vibration induced by each strike allowed a consistent amount of ash to be dispersed.

The hammer was powered by a crank attached to a 12v steeper motor. The steeper motor is computer controlled, allowing the device to rotate at a range of speeds, including stepping in 0.5° increments, with infinite pauses between steps. This study used computer code to control the motor, therefore the relative timing/strike of hammer (Appendix A).

Ash Fall Rates and Calibration

As indicated earlier, ash fall rate is a key variable in testing, as such the ash dispersal system required detailed calibration for changes in desired ash fall rates and induced changes between pseudo ashes (i.e. grain size differences, particle morphologies). To calibrate the delivery of ash, a petri dish was located below the mesh; the motor was then programmed to disperse ash at a set number of strikes per minute, with the dish weight recorded at 20 minute intervals, using an analytical scale. The calibration was repeated using the three ash types, at a number of speeds. The data was used to produce curves to indicate the strike rate required to achieve a particular fall rate, for each ash type.

It was also noted that ash fall rate was subject to variation when the hopper (ash dispersal box storage) contained less than 50mm of ash. It was therefore necessary to keep the hopper, above this level during testing, and begin testing with a minimum 100mm depth.

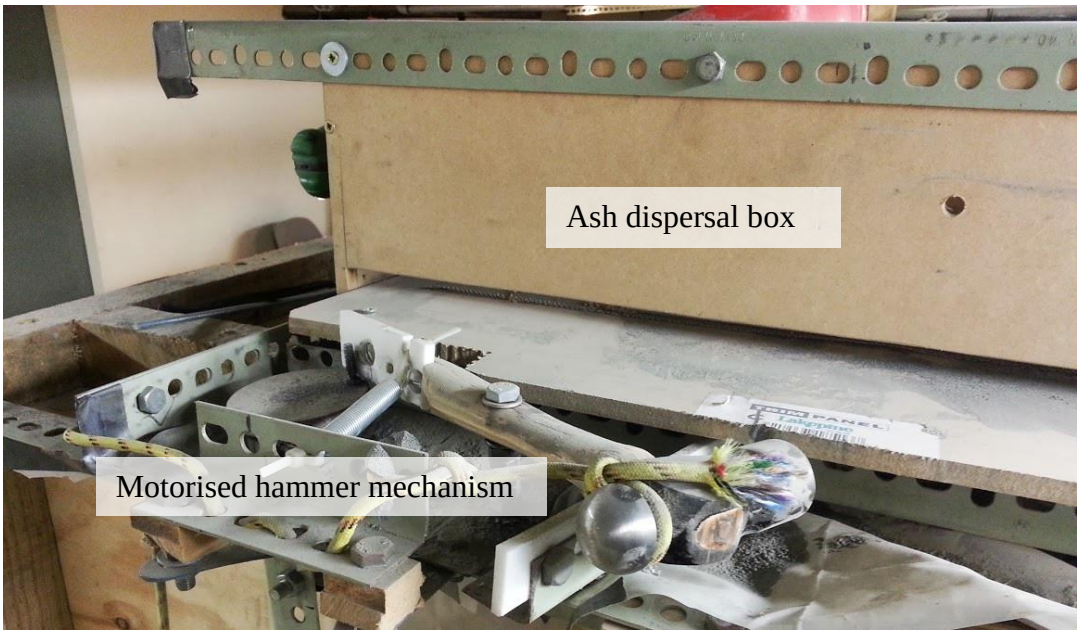

Figure 3.6: Image showing the hammer mechanism of the ash shaker with the mesh based ash box at the rear.

3.5 Monitoring Instruments and Methods

To monitor the AGA for performance losses during the tests, several pieces of monitoring equipment (hot wire anemometer, particle tracker) were strategically positioned (**Figure 3.7**) Details of these devices and data sets to be recorded are introduced below. Physical measurements were also taken via the collection of ash from areas where ash was deposited (testing chamber, ARM measure if filtration), and weight measurements of critical

components (ARMs and particle tracker filters). Further analytical methods involved macro photographs, microscope analysis (micro photographs),

Hot Wire Anemometer

An anemometer records air flow changes, the anemometer used in this testing is an ATP USB logging hot wire anemometer, which is capable of measuring air speeds between 0.1 and 25 m/s, with an accuracy of ±5%. The device measures airflow by monitoring changes in the temperature of a filament, heated to 80°C. This measurement method is superior to a traditional mechanical anemometer, as it can measure very low air speeds with a high degree of accuracy. The device logs to a computer via a USB cable, allowing air speed to be recorded once per second. In testing the anemometer was positioned on the reverse side of the grill, within the testing chamber, to determine the speed of air passing though and to monitor changes as ARM became obstructed with ash.

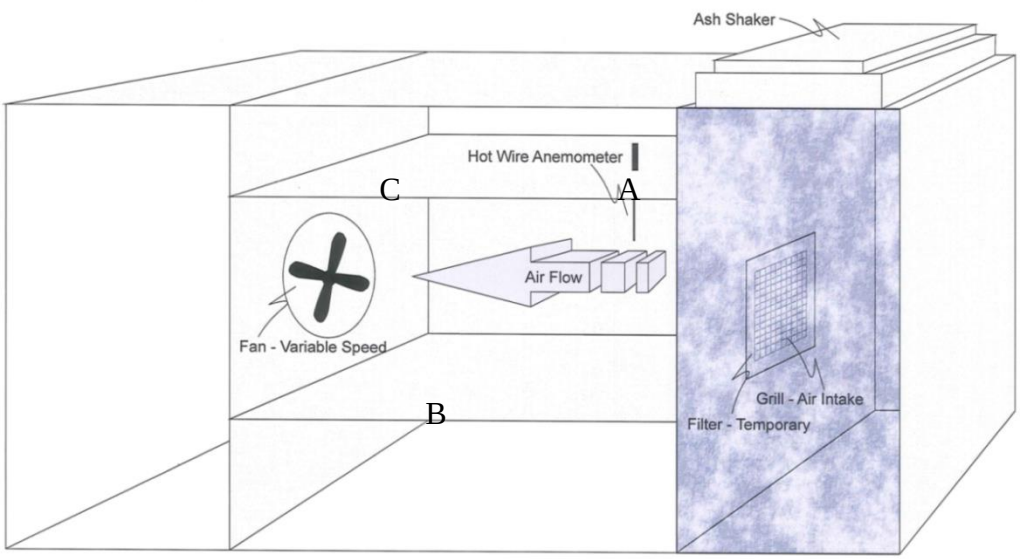

Figure 3.7: Diagram of AGA showing the locations of the anemometer (A), the particle tracker (B) and the engine air intake (C).

Particle Tracker

A particle tracker records the particle concentration within the testing chamber. The device used in this testing was a high flow particle tracker, supplied by Department of Geography, University of Canterbury.

Particle concentrations within the chamber were used to determine the effectiveness of each ARM. The tracker is calibrated to draw a consistent 10 m^3/min through filter paper. The filter paper was weighed on an analytical scale before and after testing. Changes in weight, combined with the volume of air which passed through the device, provide an average concentration of suspended particles within the testing chamber during testing.

3.6 Ash Reduction Methods (ARM)

Ash reduction methods (herein referred to as ARM) are components or methods that can be utilised to reduce or eliminate the ingestion of volcanic ash in generators. Each ARM was evaluated on its ability to reduce the volume of ingested ash sufficiently, while not significantly reducing air flow, and real life application (readily available and easily applied in an emergency situation).

In reviewing potential ARM's the following classification were identified methods used to exclude or reduce airborne particles from either generators or air handling units such as HVAC (heating, ventilation and cooling) units: material filtration, deflection, cyclonic filtration, water based ash removal and baffles. The following is a brief review of each ARM and its application based on rapid deployment during a volcanic crisis. If significant time is required to source and apply an ARM it may result in the method being deemed unviable.

Material filtration includes filters specifically designed for air filtration, but also includes any material which can be applied to reduce ash ingestion. Examples include hessian material, cotton and foam. Material filtration is used extensively for the purpose of particle exclusion and is widely available. The simple nature of material filtration makes it easy to apply. These qualities resulted in it proceeding to initial testing.

Deflection uses an object to provide separation between the ash fall and the air intake. It consists of a sheet or hard material (plastic or metal) projecting out from the top of the grill at an angle. Material is formed along the sides of the sheet, creating a hood. Deflection hoods are simple to construct and can be made by folding and cutting a single sheet of metal. The nature of a hood means it does not suffer from obstruction, reducing maintenance. The ease of use and low maintenance costs, resulted in deflection hoods being considered during initial testing.

Cyclonic filtration uses a mix of centrifugal and gravitational forces, to remove solids from gasses. The device spins air in a vertical chamber, drawing particulate matter to the edge and

out of the main air flow. The particles then move down the chamber under the force of gravity until they exit through an opening in the base. While cyclonic filtration is currently used in mines and other environments which particle reduction is required, it is not easily obtained, making it impractical for rapid deployment in a volcanic crisis. As a result it did not proceed to initial testing

Water based ash removal uses a curtain of water to remove particles as they move through the chamber. The particles are then washed out of the chamber by the water, while the clean air continues into the air intake. Water based ash removal and baffles were also excluded. While literature showed they are effective at removing particles from air (Sanchez, 1999), their performance is significantly degraded at the high airflows needed for a generator to function.

Baffles employ similar methods to cyclonic filtration. The airflow is forced to travel up and down, over and under baffles which line a box. The force needed to raise the particles up each baffle, causes some of the particulates to drop out of the airflow, reducing the concentration of particles ingested.

3.6.1 ARM Selection

ARM exclusion was based on three criteria, literature review, expert judgment and initial testing. Each ARM was analysed in all three stages and excluded if it failed any stage. **Table 3.7** details the ARMs considered for testing.

The project aim is to provide methods to mitigate the ingestion of ash which can be applied rapidly during a volcanic crisis. If significant time is required to source and apply an ARM it may result in the method being deemed unviable.

Material filtration is used extensively for the purpose of particle exclusion and is widely available. The simple nature of material filtration makes it easy to apply. These qualities resulted in it proceeding to initial testing. Deflection hoods are simple to construct and can be made by folding and cutting a single sheet of metal. The nature of a hood means it does not suffer from obstruction, reducing maintenance. The ease of use and low maintenance costs, resulted in deflection hoods being considered during initial testing.

While cyclonic filtration is currently used in mines and other environments which particle reduction is required, it is not easily obtained, making it impractical for rapid deployment in a

volcanic crisis. As a result it did not proceed to initial testing. Water based ash removal and baffles were also excluded. While literature showed they are effective at removing particles from air, their performance is significantly degraded at the high airflows needed for a generator to function.

Table 3.6: ARM considered for testing.

Filter type	Tested or excluded
Deflection Hood	Tested
Hessian Material	Tested
Windbreak Material	Tested
Polyurethane Foam	Tested
Vehicle Air Filter	Tested
Foam	Tested
Cyclonic Filtration	Excluded
Baffles	Excluded
Water Based Ash Removal	Excluded

ARMs selected for testing are outlined in the **Table 3.7**, also included are initial air speed results, defined using a hot wire anemometer during preliminary testing (Section 3.5). Each selected ARM to be utilised in testing are presented in **Table 3.8**.

.

Table 3.7: ARM used for testing, showing initial air speed reduction.

Filter type	Initial air speed reduction
Deflection Hood	25%
Hessian Material	27%
Windbreak Material	27%
Polyurethane Foam	69%
Vehicle Air Filter	89%
Foam	88%

Table 3.8: Description of ARM used in testing

ARM	Description	Ash Reduction Measure
Deflection	Single sheet of stainless steel was folded by bending the edges 90° and cutting off half of the resulting flaps.	ARM 1
Filtration	Hessian cloth with an open weave	ARM 2
Filtration	Windbreak material constructed from high density polyethylene	ARM 3
Filtration	45ppi polyurethane filtration foam with an open cell structure	ARM 4
Filtration	Paper vehicle air filter – Ryco A1523	ARM 5
Filtration	25 mm thick bedding foam	ARM 6

3.7 Testing Procedure

Each test was run for a six hour period. The test length was determined by the time available in the testing schedule. Testing, data collection and analysis followed a defined protocol, as outlined in the following series of bullet points;

Pre Test

- Whole AGA (especially drop and testing chambers) cleaned to ensure no ash was left over from the previous test
- Hopper filled to 100 mm in depth to ensure a stable ash fall rate
- A petri dish was placed at the top of the drop chamber to ensure the ash fall rate was correct during the test
- ARM to be tested was weighed (excluding the deflection hood) before being fitted to the air intake grill
- Filter for the particle tracker was weighed on an analytical scale to determine the start weight. The flow value on the particle tracker was recorded
- Hot wire anemometer was tuned on; power saving mode turned off and software was opened on the computer. A check was made to ensure software was receiving data
- Fan switched on and flow rate calibrated using anemometer
- The ash fall rate set by predefined script in the software (calibrated for ash type and required fall rate)

During each test:

- The particle tracker and hammer mechanism were turned on simultaneously and a stop watch was started
- Every 20 minutes the petri dish was weighed and analysed to check the ash fall rate. The dish was cleared and reset after each weighing

At the end of the test

- Components of the system switched off simultaneously
- Detailed photographs were taken of insitu ARM and deposited ash
- Petri dish was weighed to determine final fall rate
- ARM and the particle tracker's filter photographed under the binocular microscope
- The filter in the particle tracker was weighed and the flow value recorded to determine contamination levels within the testing chamber
- The anemometer software file was saved showing the flow rate profile during the test
- Ash from the drop and testing chambers was collected and weighed to determine the distribution of ash deposition.
- Collected ash was analysed to determine grain size

At the end of testing, all data was recoded in a spreadsheet for analysis. A checklist was produced to ensure all steps were performed in order and to provide a physical backup of key data. The checklist can be found in Appendix (C)

3.8 Outline of Testing Regimes

The following outlines the key tests that were undertaken and the key data presented in Chapter 4. A number of tests were performed to determine the effectiveness of the selected ARM. A matrix of these tests is shown in and includes additional tests with ARM 4 including a combination ARM 1 + 4 test and two tests at higher fall rates.

Table 3.9: Matrix displaying the combination of ARM and ash type for each test.

Ash Reduction Measure	Ash A	Ash B	Ash C
Control	Test 1	Test 11	Test 18
ARM 1	Test 2	Test 12	Test 19
ARM 2	Test 3	Test 13	Test 20
ARM 3	Test 4	Test 14	Test 21
ARM 4	Test 5	Test 15	Test 22
ARM 5	Test 6	Test 16	Test 23
ARM 6	Test 7	Test 17	Test 24
ARM 1+4	Test 8		
ARM 4 @ 1000g/m2/hr.	Test 9		
ARM 4 @ 1000g/m2/hr.	Test 10		

Chapter 4 Results

4.1 Overview

Chapter Four details data gathered during testing of six ARMs and a control, with three different ash types. The structure of the chapter follows the progression of the ingested ash from the drop chamber, through to the test chamber (**Figure 4.1**). Results include: fall rates, air speed data, particle concentration levels, grain size distributions and filter mass data. Over the testing period the laboratory's average temperature was 17.9°C with a standard deviation of 0.09°C. The average relative humidity was 72% with a standard deviation of 3.7%.

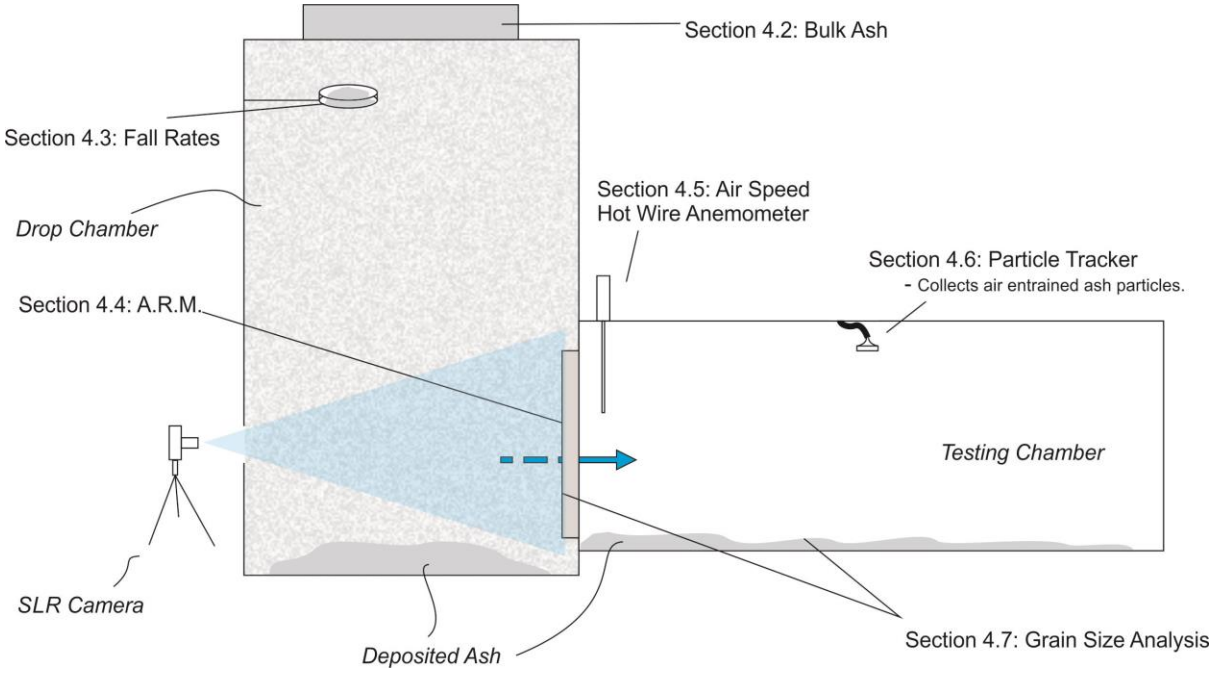

Figure 4.1: Diagram of test setup and data collection devices. Blue arrow indicates the flow of air from the drop chamber (on left) to the testing chamber (on right). Light blue triangle indicates the SLR camera's field of view.

4.2 Bulk Ash

Grain size analysis was performed on all bulk ash samples (Section 3.3.5) (**Figure 4.2**). The results show Ash B and C are bimodal and have a similar distribution. Ash C is enriched with

coarse particles and slightly depleted of fine particles when compared to Ash B. Ash A has a wider distribution and is significantly more enriched with finer particles than either Ash B or C (**Figure 4.2**).

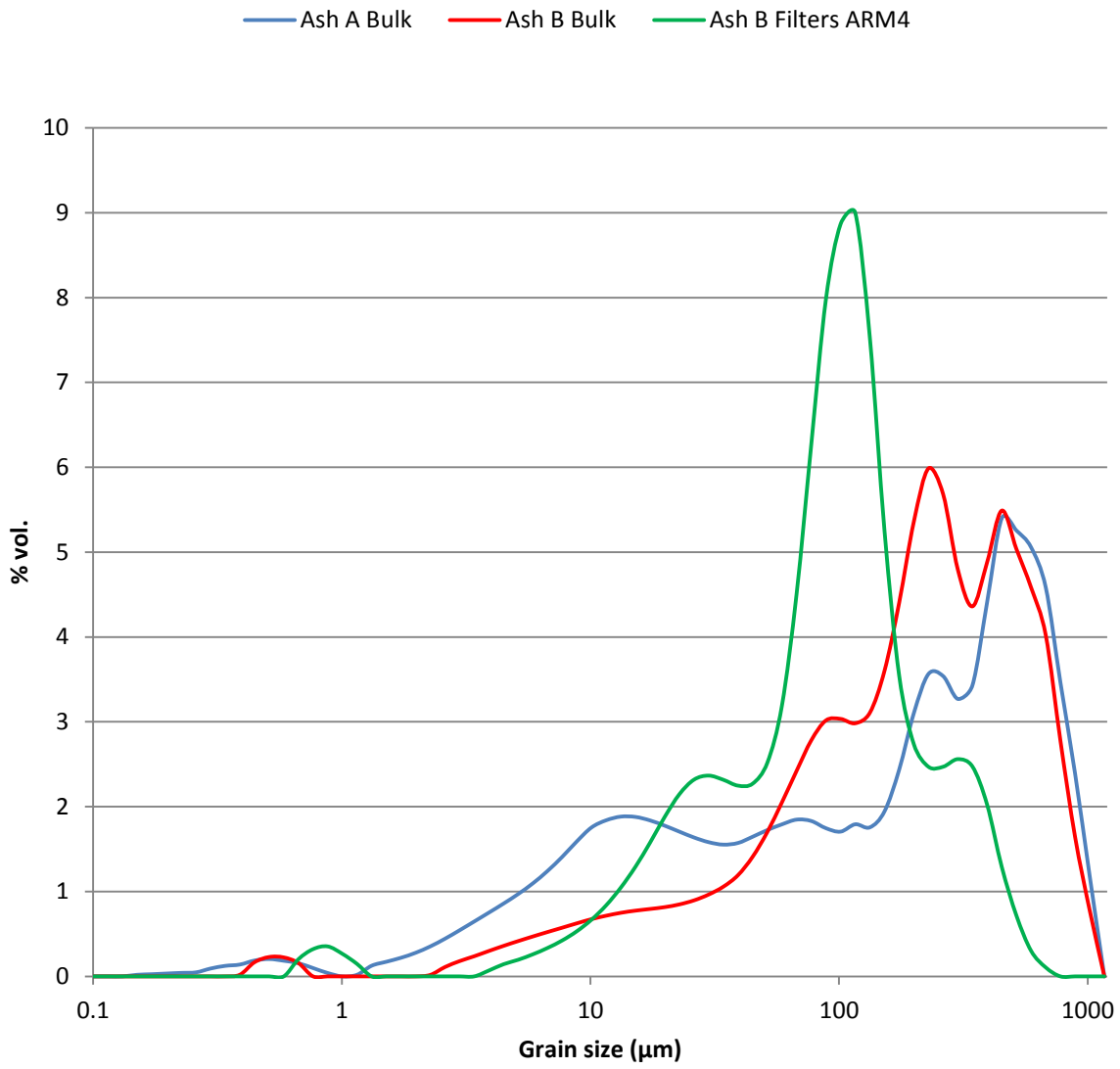

Figure 4.2: Grain size distribution for the bulk ash types A, B and C

4.3 Ash Fall Rates

Fall rates (Figure 4.3) were recorded using the petri dish method as outlined in Chapter 3. Results are reported as the mass of ash, deposited over one square metre in 60 minutes. **Table 4.1** contains the average fall rate and standard deviation for each ash type. An overall average and standard deviation are provided at the bottom of the table.

While every effort was made to ensure the fall rates were consistent, the nature of the various ash types resulted in variation between tests. Variations were due to smaller grain sizes; primarily in Ash C, requiring a small aperture mesh (~500 µm) to be fitted in the ash shaker.

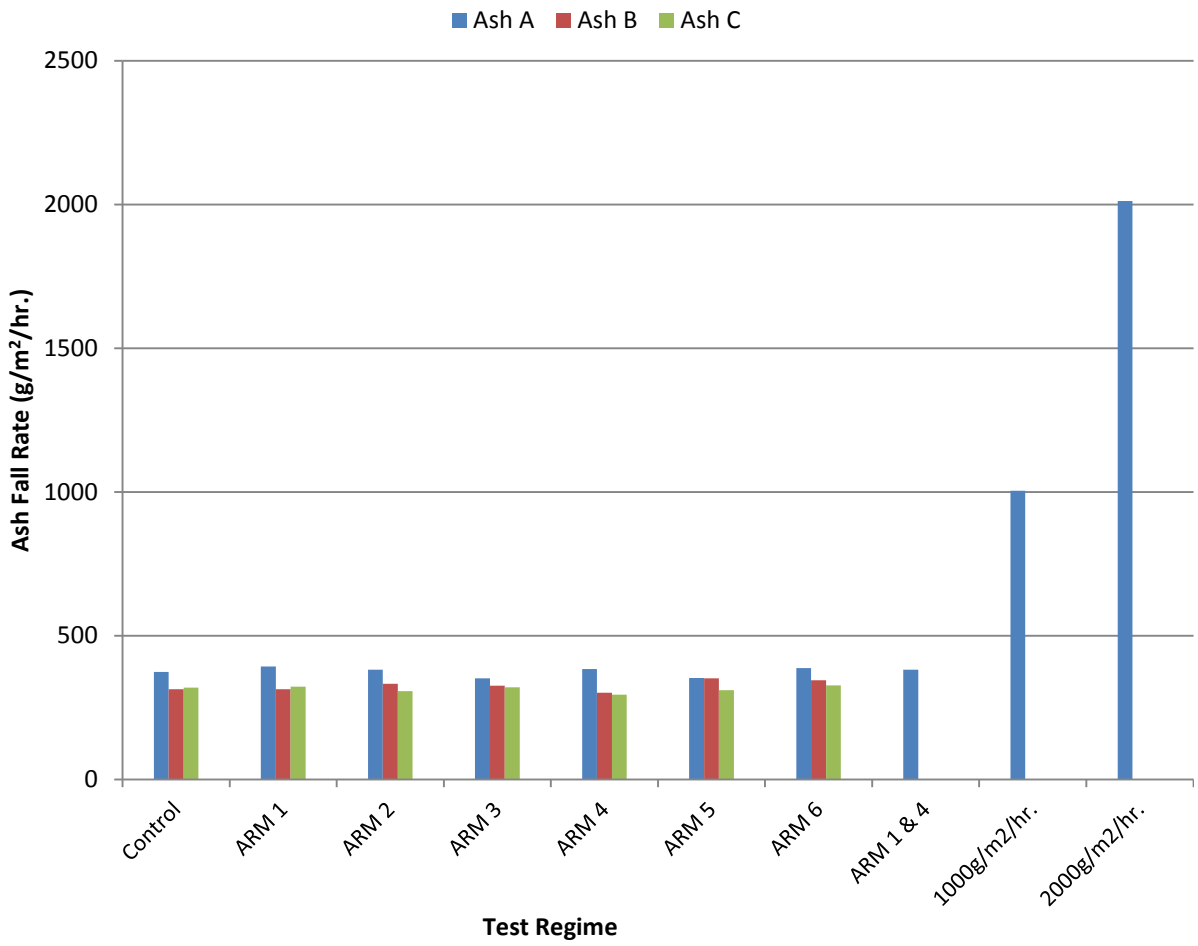

Figure 4.3: Ash fall rates recorded during testing. The testing period was 6 hours, over which an average of 2,000 g of ash was deposited. Control and ARM 1-6 were part of stage one testing. The ARM 1 + 4 combination, 1000 g/m^2/hr. and 2000 g/m^2/hr. tests were part of a second stage of testing informed by results obtained during stage one.

Table 4.1: Average and standard deviation of fall rates of each of the three ash types. Two additional tests involving higher fall rates (1,000 and 2,000 g/m^2/hr.) are excluded from these calculations.

Ash Type	Average fall rate (g/m^2/hr.)	Standard deviation (g/m^2/hr.)
Ash A	375.0	15.33
Ash B	327.0	16.74
Ash C	315.0	10.33
Overall	339.0	29.85

4.4 Ash Reductions Measures ARM

Ash Reduction Measures (ARM) were fitted between the drop chamber and testing chamber (**Figure 4.1**). The following sections divides ARM into mass data and photographs of each ARM. The data provides both quantitative and qualitative means of assessing ARM performance.

4.4.1 ARM Weights – Before and After Testing

ARM which contain a method of physically stopping/intercepting ash particles, underwent weighing prior to and post testing. ARM 1 is not included in this section as it operates by deflection rather than physically obstructing ash ingestion. Pre and post-test values were used to calculate the mass of ash lodged within each ARM. The mass was then weighted by the density multiple of the particular ash (1.79, 1.57 and 1.1 for Ash A, B and C respectively), to account for the bulk density of each ash type (**Figure 4.4**). The mass of lodged ash varies significantly between filters but is relatively consistent between ash types.

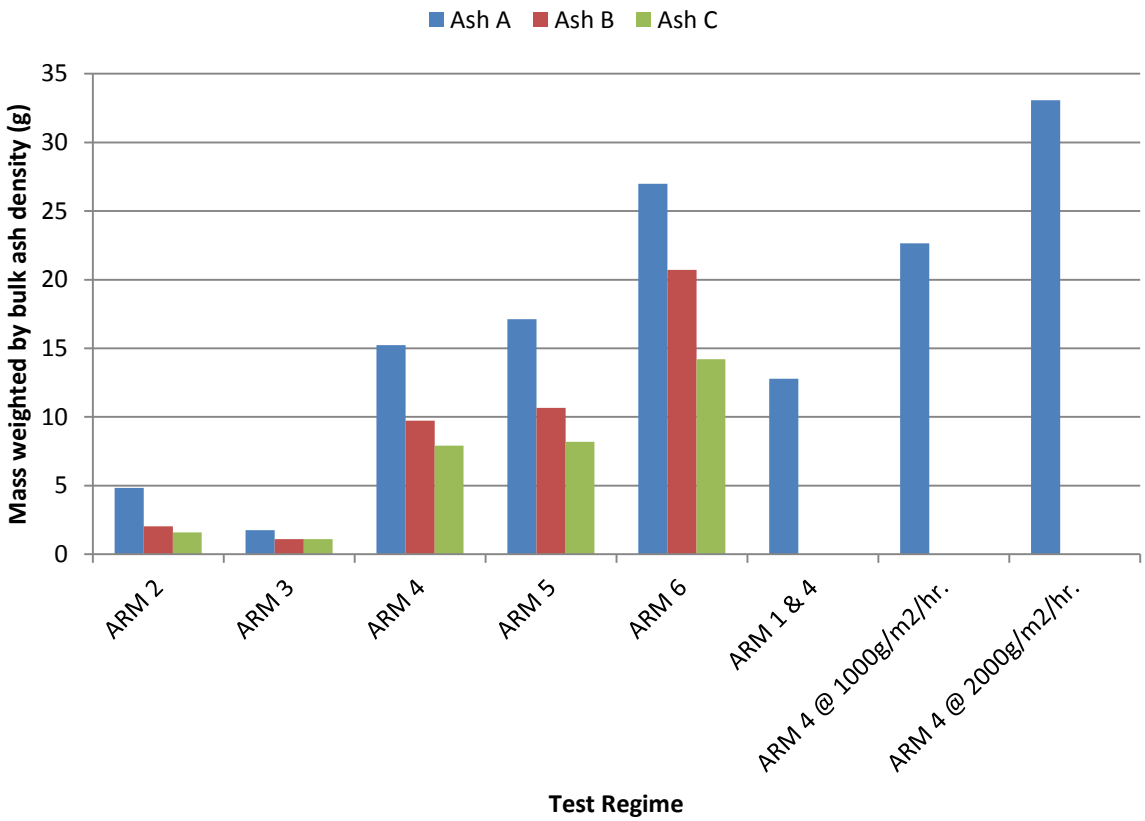

Figure 4.4: Change in the mass of individual ARM as a result of ash ingestion during testing. Mass for each ARM has been modified to account for variations in the bulk density of each ash type, allowing for direct comparison. The bulk density of Ash A is 1,790 kg/m^3, Ash B 1,568 kg/m^3 and Ash C 1,100 kg/m^3

4.4.2 ARM Photos

In addition to previously outlined methods, photographs of ARM were taken at two stages and at two scales after each test, 1) in situ macro photographs with an SLR camera (**Figure 4.5**), perpendicular to the filters surface, through a hole cut in the drop chamber; and 2) filter photographs under a binocular microscope, allowing a close examination of deposited ash.

In addition to gaining perspective by using different scales, in situ photographs were used to account for loss of ash which may have occurred during the un-mounting and transportation of the filters to the microscope. In detail, this process involved careful removal of the ARM from its housing to preserve deposited ash and placement of the ARM in a sealed container, ash side up. Care was taken during transfer to the binocular microscope. The following presents data sets at these two different scales.

4.4.2.1 SLR Camera in Situ Photographs

Ash in the ARM 2 test adhered to both the primary fibres of the materials weave and to smaller 'frayed' fibres which partially fill the space between the primary fibres (**Figure 4.5**). Ash A is the most contaminated, while Ash B is the least. ARM 3 retained minimal quantities of ash. ARM 4 is coated with a fine grain layer of ash which is deposited through the top few layers of the open cell foam structure. ARM 5 accumulated large amounts of material. Ash A and C caked the ARM, while Ash B formed a moderate layer of ash on the surface. ARM 6 was caked with ash in all three tests. The ash formed a thick covering on the surface of the ARM, changing the foam's colour to grey, orange and brown for Ash types A, B and C respectively.

4.4.2.2 ARM Binocular Microscope Photographs

Microscope images for each ARM were taken at two magnifications, 0.7x and 4.5x (Figure 4.6). Levels of ash in the microscope images are consistent with SLR photographs (Figure 4.5), supporting limited to low loss of ash during the removal and transportation of the ARM. The photographs indicate ARM tested with Ash A and C accumulated more ash than ARM tested with Ash B.

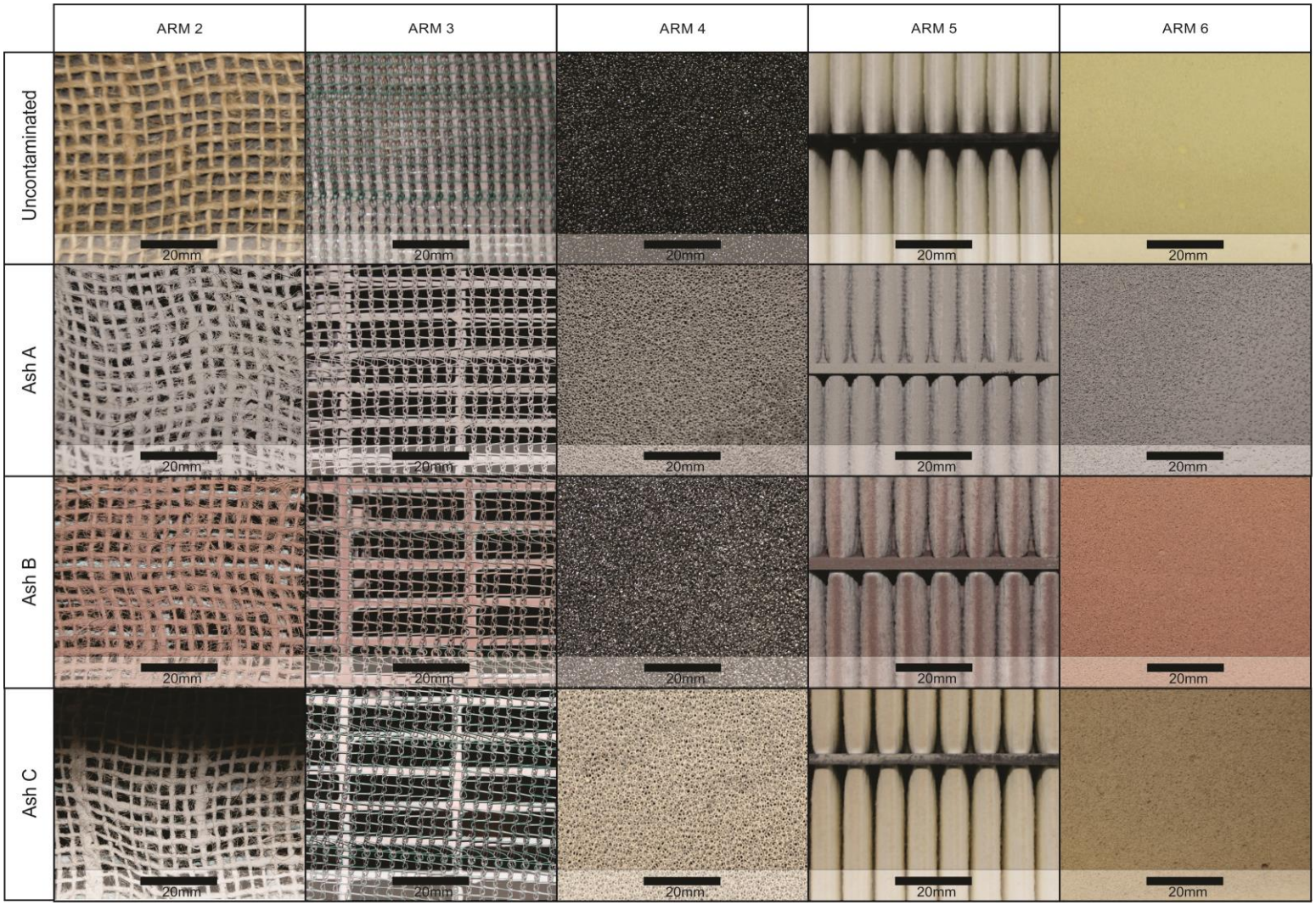

Figure 4.5: Table of in situ SLR photographs taken of ARM with material filtration. Photographs show ARM before testing and after testing with Ash A, B and C. See **Table 3.8** for description of material used in each ARM.

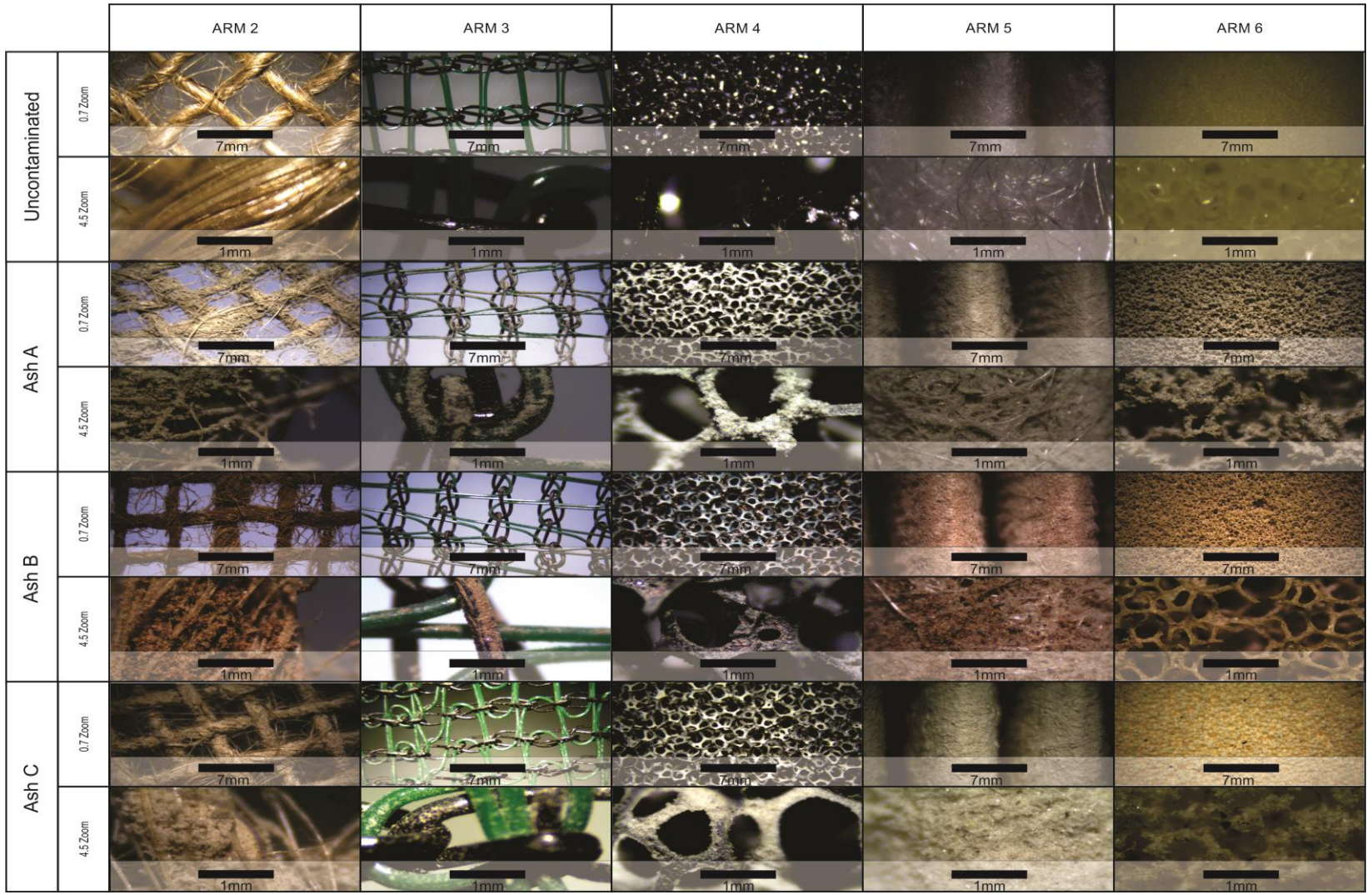

Figure 4.6: Micro-photographs taken of all ARM with material filtration. Photographs show ARM at two zoom levels (0.7x and 4.5x), before testing and after testing with Ash A, B and C. See **Table 3.8** for description of material used in each ARM.

4.5 Air Speed

Air speed was recorded once per second, during each test, using a hot wire anemometer. Variability exists between initial airspeed values, involving the same ARM with different ash types; however these variations are minimal (i.e. ARM 1 in **Figure 4.7** and **Figure 4.8**) and are probably due to small movements of the anemometer between tests.

Air speed results are presented according to ash type, with airspeed for each ARM plotted on representative figures (**Figure 4.7** - **Figure 4.10**).

4.5.1 Ash A

Ash A was introduced into this testing regime at an average of 375 g/m^2/hr. (**Table 4.1**). The control test involved measuring the air speed through the unimpeded intake grill, averaging ~7.4 m/s, fluctuating between 7.3 and 7.5 m/s. Fluctuations were observed in tests involving little or no obstruction of the flow of air and appear to be the result of turbulent air flow (i.e. when no material filter type ARM is in place). ARM 1 reduces airflow by ~2 m/s relative to the control, and like the control ARM 1 produces turbulent airflow as it is a deflection device rather than a material filter. ARM 2 is the first of the material filtration measures. The airflow is similar to ARM 1 but has fewer fluctuations. ARM 3 reduces the air speed by ~3 m/s relative to the control, with air speed slightly increasing over the test period. ARM 4 reduces airflow to less than half of the control airspeed over the first 60 minutes, before plateauing for the remainder of the test. ARM 5 reduces air speed to just over 1 m/s over the test period. Air speed decreases over the first 200 minutes, before increasing again. ARM 6 increases air speed over the first 100 minutes (0.7 to 0.79 m/s), before becoming stable for the rest of the test. The ARM 1 & 4 combination recorded approximately the same average air speed as ARM 4 alone (~2.4 m/s); however the air speed rose, over the test period, by approximately 0.3 m/s.

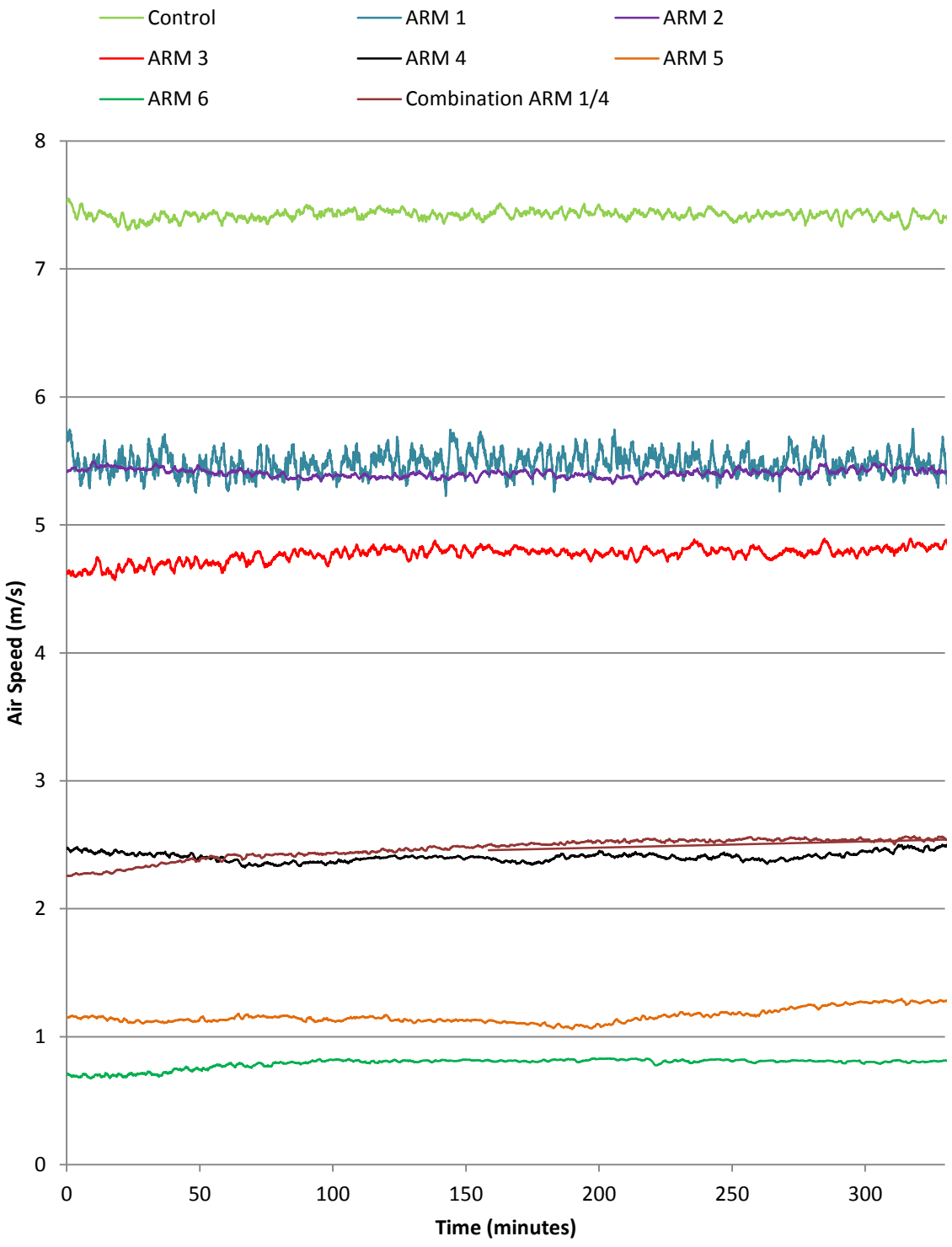

Figure 4.7: Airspeeds recorded once per seconds for each test involving Ash A. Test run time is 360 minutes. Ash fall rate during test was ~375 g/m^2/hr.

4.5.2 Ash B

Ash B was introduced into this testing regime at an average of 327g/m^2/hr. (**Table 4.1**). The control test has a high degree of fluctuation (±0.25m/s). The air speed of ARM 1 fluctuates significantly (±0.5m/s) and slowly reduces during the test. ARM 2 increases air speed during the first 100 minutes of the test, before slowly decreasing until ~200 minutes, where it begins to increase slowly again. ARM 3 begins and ends at approximately 4.7m/s but decreases air speed during the middle of the test. ARM 4 shows a smooth and slow reduction in air speed over the test period. ARM 5 is highly variable but shows an overall air speed reduction. ARM 6 maintains a smooth plot throughout the test, decreasing airflow very slowly.

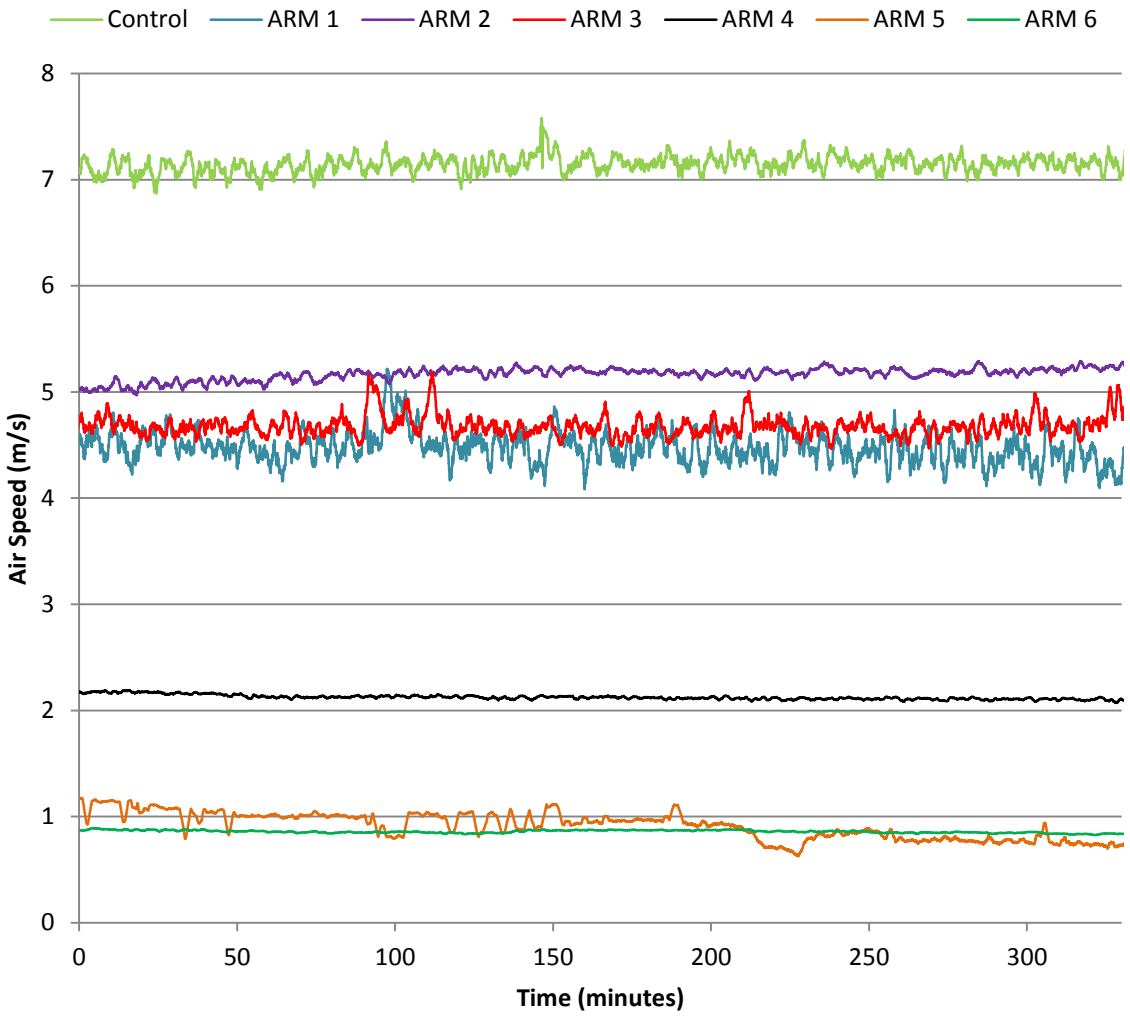

Figure 4.8: Airspeeds recorded once per seconds for each test involving Ash B. Test run time is 360 minutes. Ash fall rate during test was ~327 g/m^2/hr.

4.5.3 Ash C

Ash C was introduced into this testing regime at an average of 315 g/m^2/hr. (**Table 4.1**). The control test averaging ~6.7 m/s and fluctuated between 6.6 and 6.8 m/s. ARM 1 has large variations and includes a significant increase at ~150 minutes. ARM 2 has a smooth and gradual reduction in air speed. The ARM 3 average air speed remains stable over the test, despite fluctuations. ARM 4 starts and finishes the test at approximately the same air speed but has a sudden reduction and recovery between 75 and 110 minutes. ARM 5 records an air speed reduction over the test period; reducing air speed by approximately 0.8 m/s. ARM 6 maintains a smooth plot with a slight reduction in air speed.

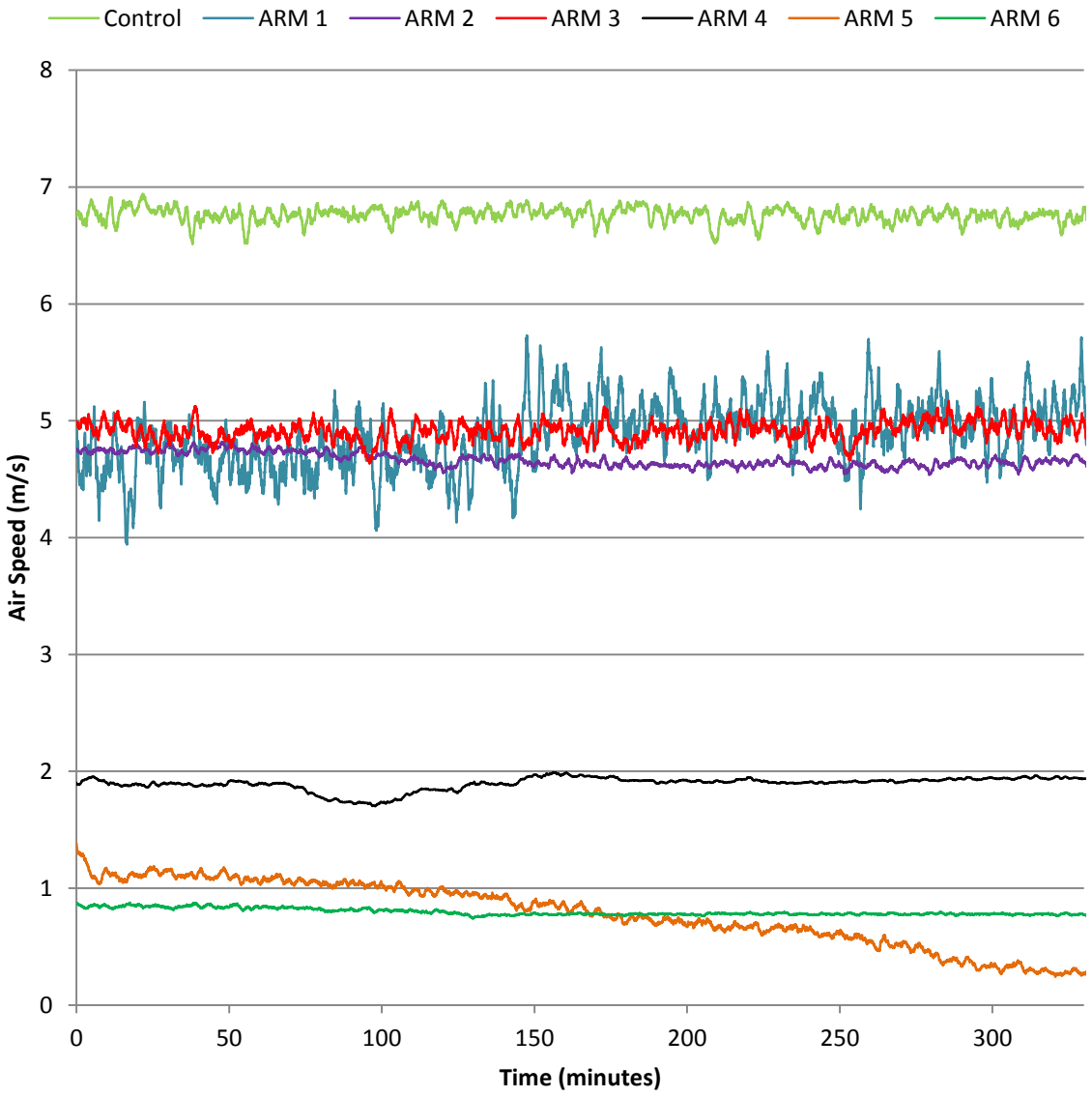

Figure 4.9: Airspeeds recorded once per seconds for each test involving Ash C. Test run time is 360 minutes. Ash fall rate during test was ~315 g/m^2/hr.

4.5.4 High Fall Rates

Ash A was introduced into this testing regime at higher fall rates of 1000 and 2,000 g/m^2/hr. The 1,000 g/m^2/hr. test showed a slow steady decline in airspeed from ~2.7 to 2.5 m/s over the 360 minute test period; fluctuations were minimal. The 2000 g/m^2/hr. tests reduced airspeed by approximately 0.3 m/s over the duration of the test and recorded episodic higher and lower air speed values over the test period, fluctuating ~0.2 m/s. ARM 4 at the standard fall rate (~375 g/m^2/hr.) is plotted for comparison.

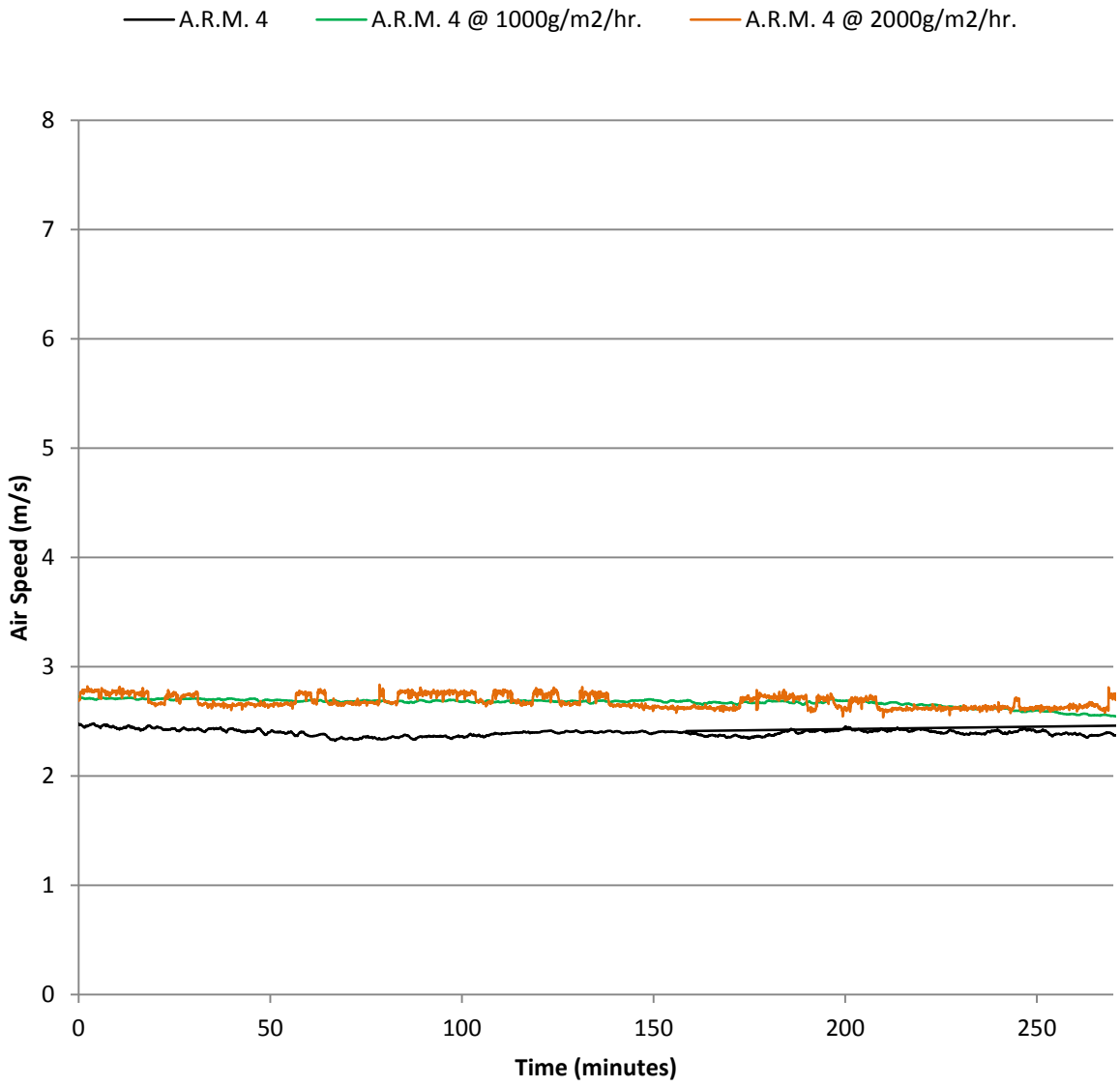

Figure 4.10: Airspeeds recorded once per seconds for high fall rate tests involving Ash A. Test run time is 360 minutes. Ash fall rate during test was ~1000 and ~2000 g/m^2/hr. for the two tests.

4.6 Particle Tracker

A particle tracker was used to determine the concentration of suspended material in the testing chamber. After testing, filters within the particle tracker were weighed and photographed; results are presented in Section 4.6.1 and 4.6.2.

4.6.1 Particle Tracker: Particle Concentration

Particle concentration (Figure 4.11) is displayed as mg/m^3 for each ash type. The concentration is measured in the testing chamber and provides an indication of the effectiveness of the ARM. Particle concentration is lower in tests involving ARMs with lower levels of filtration. The concentration is measured by dividing the change in mass of the tracker filter by the volume of air which passes through the filter over the 360 minute test period.

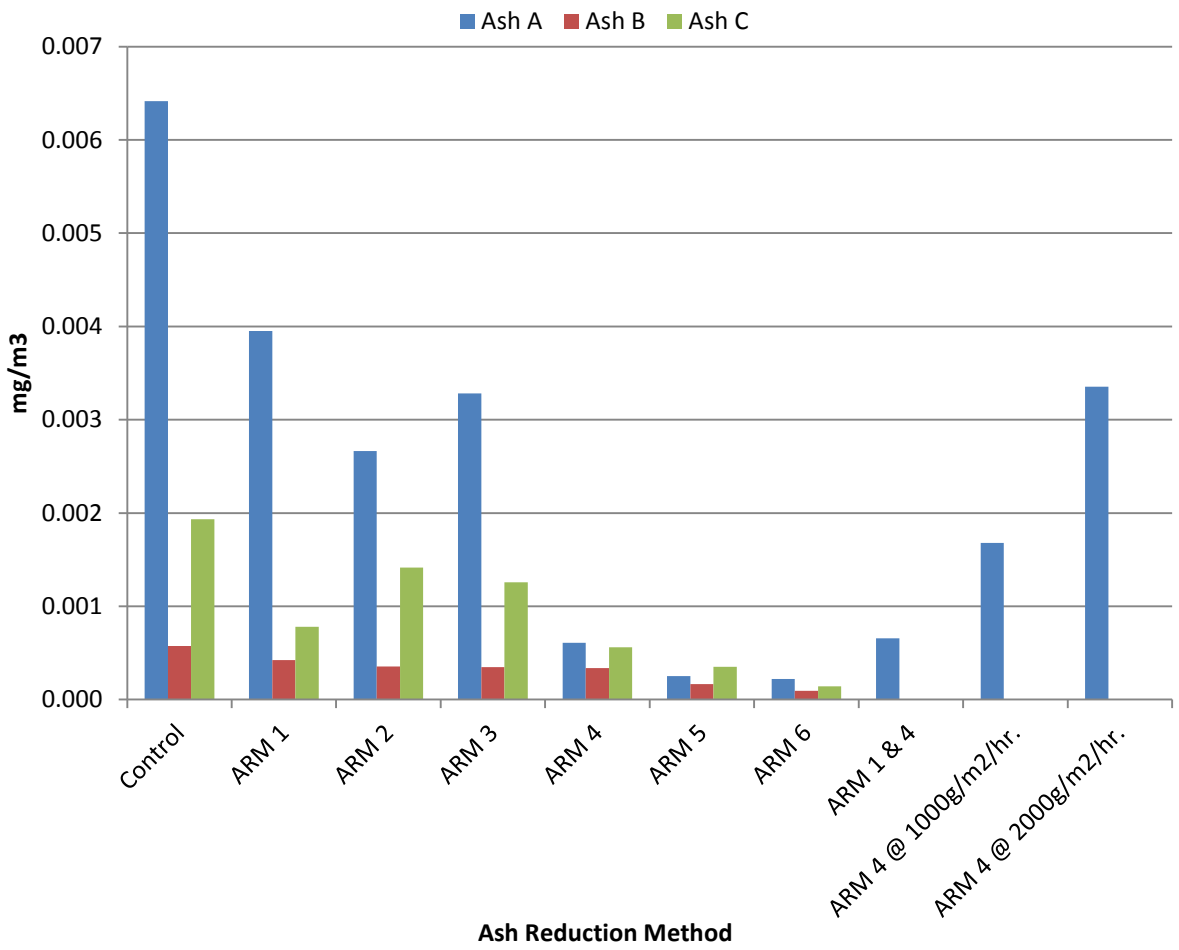

Figure 4.11: Particle concentration within the testing chamber for each ash type. Absolute particle concentration is calculated by measuring change in weight of the particle tracker's tracking filter and dividing by the volume of air which passed through the tracker over the test period (360 minutes).

4.6.2 Particle Tracker: Binocular Microscope Photographs

Photographs taken with a binocular microscope (**Figure 4.12**), act as a visual confirmation of the particle concentration data (Figure 4.11). Photographs of new uncontaminated filters are displayed to provide a reference point for assessment of the test filters (Figure 4.12). Varying lighting and white balances between the images mean colour cannot be used to compare the filters.

In control tests, the filters have recorded the greatest particle concentration (Figure 4.11) and are visually caked with ash material. The images show individual grains with a finer grain background which in general indicate Ash A had the most adhered particles, while filters used with Ash B and C had slightly less particles adhered.

ARM 1 is also caked with ash material, however individual large grains are less visible than in the control test. Filters used with Ash A are caked with ash. The Ash B filters are moderately soiled but areas of the white filter can be seen. Ash C's filter also has a high degree of contamination but is less contaminated than the filter from Ash A. Filters used with ARM 2 are similar to ARM 1 filters. There is no noticeable difference in the level of contamination or the quantity and size of the particles lodged on the filters. Filters in ARM 3 tests have a similar level of contamination as those used with ARM 1 and 2. The filter used with Ash B is the only filter to be noticeably more contaminated, having approximately three times more grains on its surface than the preceding two ARMs. The ARM 4 filters used with Ash A and B are significantly less contaminated than any of the preceding filters. The filters appear to be devoid of the fine grain particles which caked the preceding filters, having only a few grains present on the surface of the largely clean filter. Ash C differs in this test; its contamination level is more significant than Ash C in ARM 3, but has no visible individual grains. ARM 5 & 6 filters for all three ash types are clean with only a few large grains present on each filter.

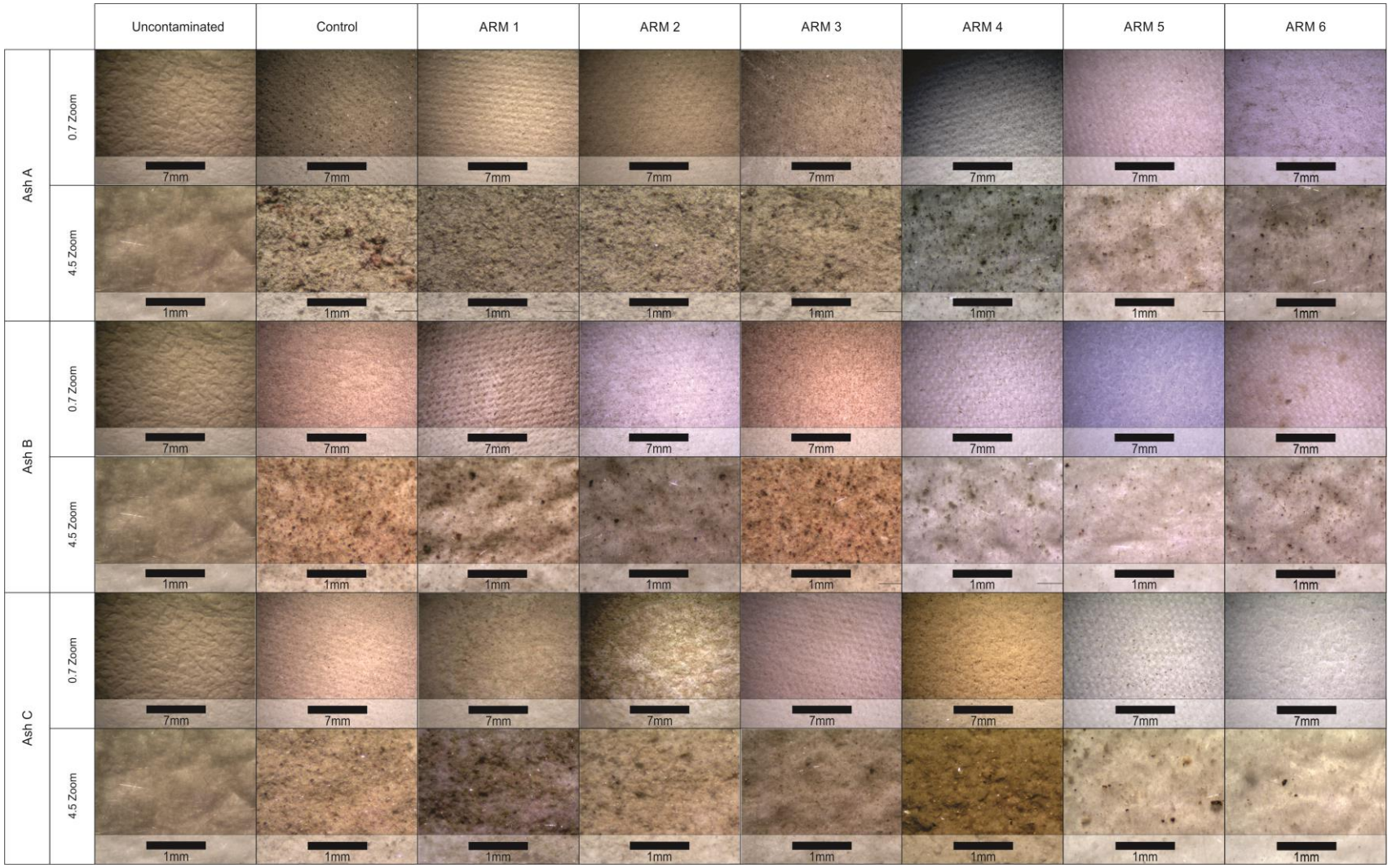

Figure 4.12: Micro-photographs of the particle tracker's filter. The figure displays all tracking filters used in tests involving Ash A, B and C and includes uncontaminated filters for comparison. Varying lighting and white balances between images means colour cannot be used to compare the filters.

4.7 Photographs from Combination ARM and High fall Rate Testing

Photographs were taken of the additional combination and high fall rates tests using an SLR camera for macro photographs and a binocular microscope for micro photographs (**Figure 4.13**).

The macro photograph of ARM used in the combination ARM 1+4 test shows the ARM is covered with ash, coating the open cell structure of the foam. The high fall rate tests have a similar appearance but more ash can be seen blocking the cells. Photographs from the 2,000 g/m^2/hr. test show large amount of ash filling the cells.

Micro photographs of the ARM confirm the observations made at macro scale. The ARM 1+4 combination has a coating of ash on its surface. The moderate higher fall rate test (1,000 g/m^2/hr.) has a coating of ash while the highest fall rate test (2,000 g/m^2/hr.) is covered in ash. Micro photographs of the tracker's filter show only light soiling of the filter in the combination ARM 1+4 test. The 1,000 g/m2/hr. test has a light covering of ash on the surface of the filter. The highest fall rate's filter is caked with ash.

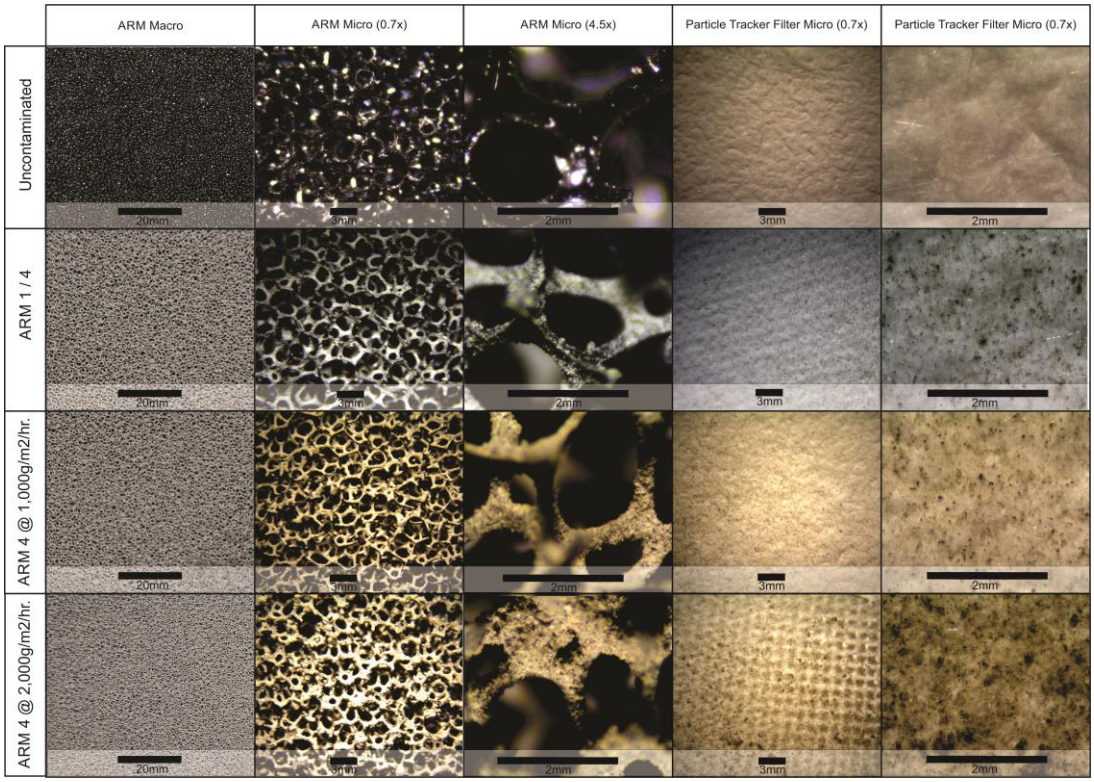

Figure 4.13: Micro and macro photographs from a binocular microscope and SLR camera. Varying lighting and white balances between images means colour cannot be used to compare.

4.8 Grain Size Analysis

Grain size analysis is presented in the following eight figures (**Figure 4.15** - **Figure 4.22**) to provide detail of the filtration properties of each ARM. Each figure covers one test regime (Control, ARM 1-6, combined ARM and the high fall rate tests). The graphs are displayed as a set three graphs, stacked vertically which provide an easy means of comparison, without the confusion which may be caused if all lines for a given ARM were plotted on one graph. The graphs can be used to determine the maximum particle size in: 1) the chamber of the control test 2) the chamber when the ARM is fitted 3) lodged within the ARM (**Figure 4.14**). With the exception of the combined ARM 1+4/high fall rate graph (**Figure 4.22**) all figures are stacked with Ash A (top), Ash B (middle) and Ash C (bottom).

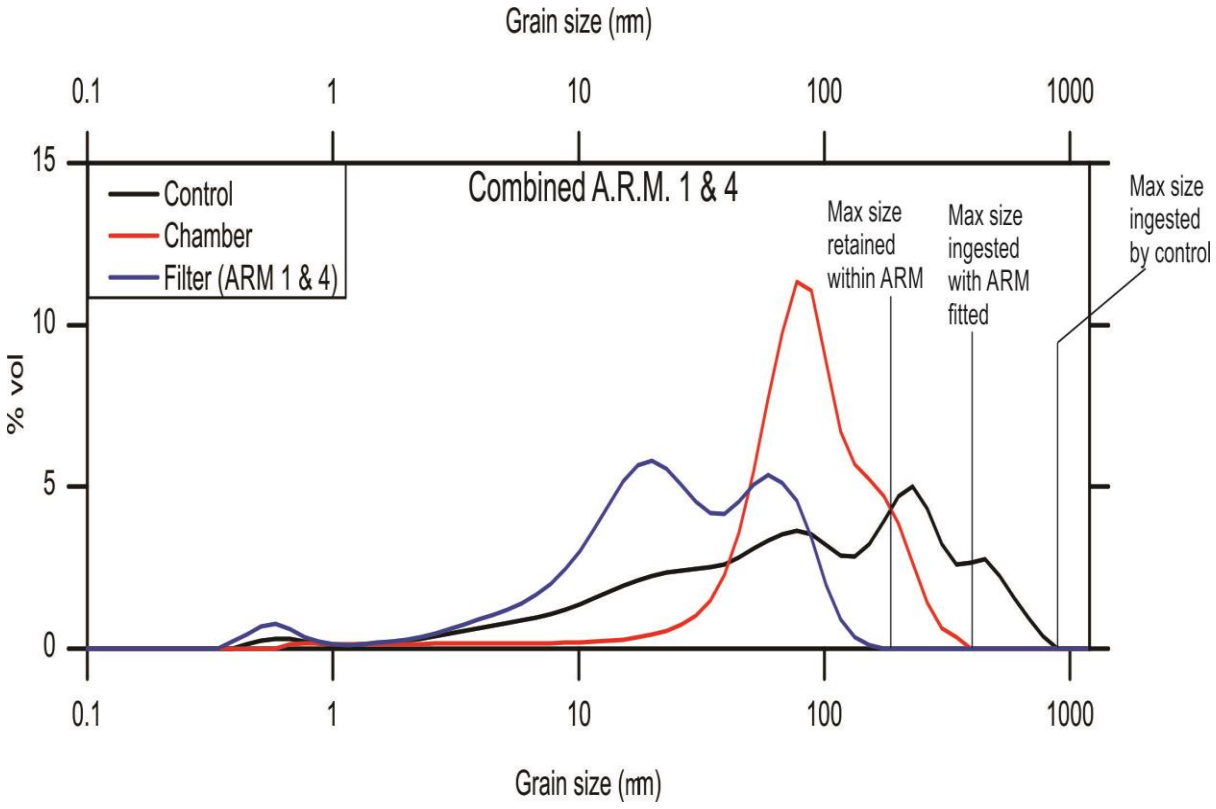

Figure 4.14: Example grain size distributions displaying maximum particle size ingested by: the control chamber; chamber with ARM fitted; and combined ARM 1 and 4.

4.8.1 Control

Control ash tests were undertaken for each ash type, without any ash reduction measures in place, providing a baseline for the comparison of each ARM. Grain size analysis of ash types A, B and C show the testing chamber, without protection, preferentially ingests finer particles, resulting in the deposition of a fine grain subset of the bulk ash within the testing chamber.

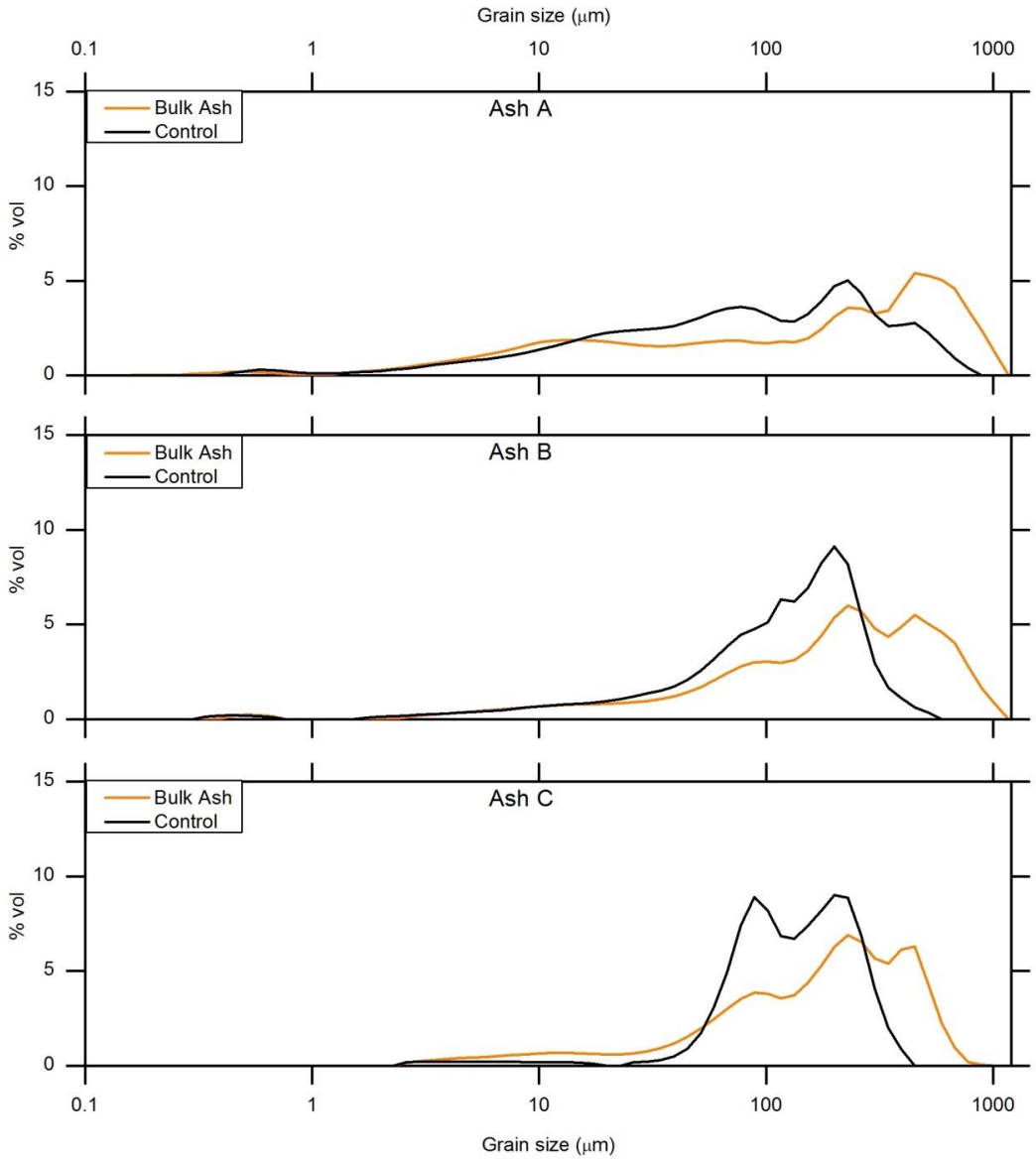

Figure 4.15: Grain size distributions for ash collected from the testing chamber during the control test, with Ash A (top), Ash B (middle), and Ash C (bottom). Distributions are compared against the bulk ash to determine the particle size distribution ingested without ash reduction measures.

4.8.2 Ash Reduction Measure One (ARM 1)

ARM 1 is not a material filtration method, so only ash from the chamber was analysed. The ARM 1 distributions vary, dependant on the ash type. The chamber grain size distribution for Ash A has a narrower distribution than the control; with a peak at approximately 100 µm. Ash B has a similar profile, while Ash C is less modified, following the control distribution closely.

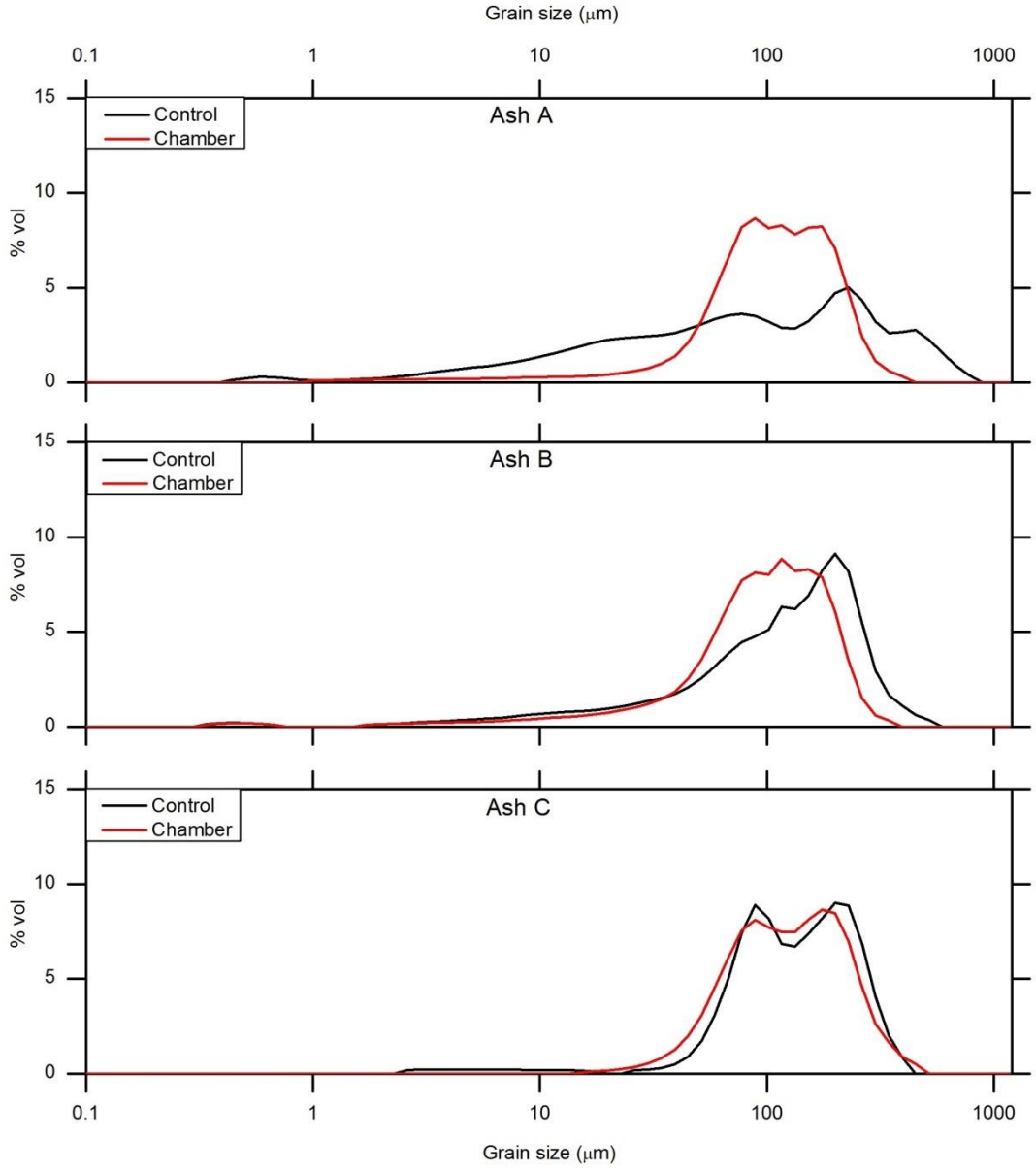

Figure 4.16: Grain size distributions for ash collected from the testing chamber during testing of ARM 1 with Ash A (top), Ash B (middle), and Ash C (bottom). Distributions are compared against control ash ingested without ash reduction measures (Figure 4.15).

4.8.3 Ash Reduction Measure Two (ARM 2)

ARM 2 is a material ash reduction measure, so grain size data for the chamber ash and filter ash was collected. The ash types collected from the testing chamber have a narrower distribution than the control with the exception of Ash C which follows the control distribution closely. Ash B is coarser than the control, in this test. The filter ash is all finer than the control with Ash B the least modified.

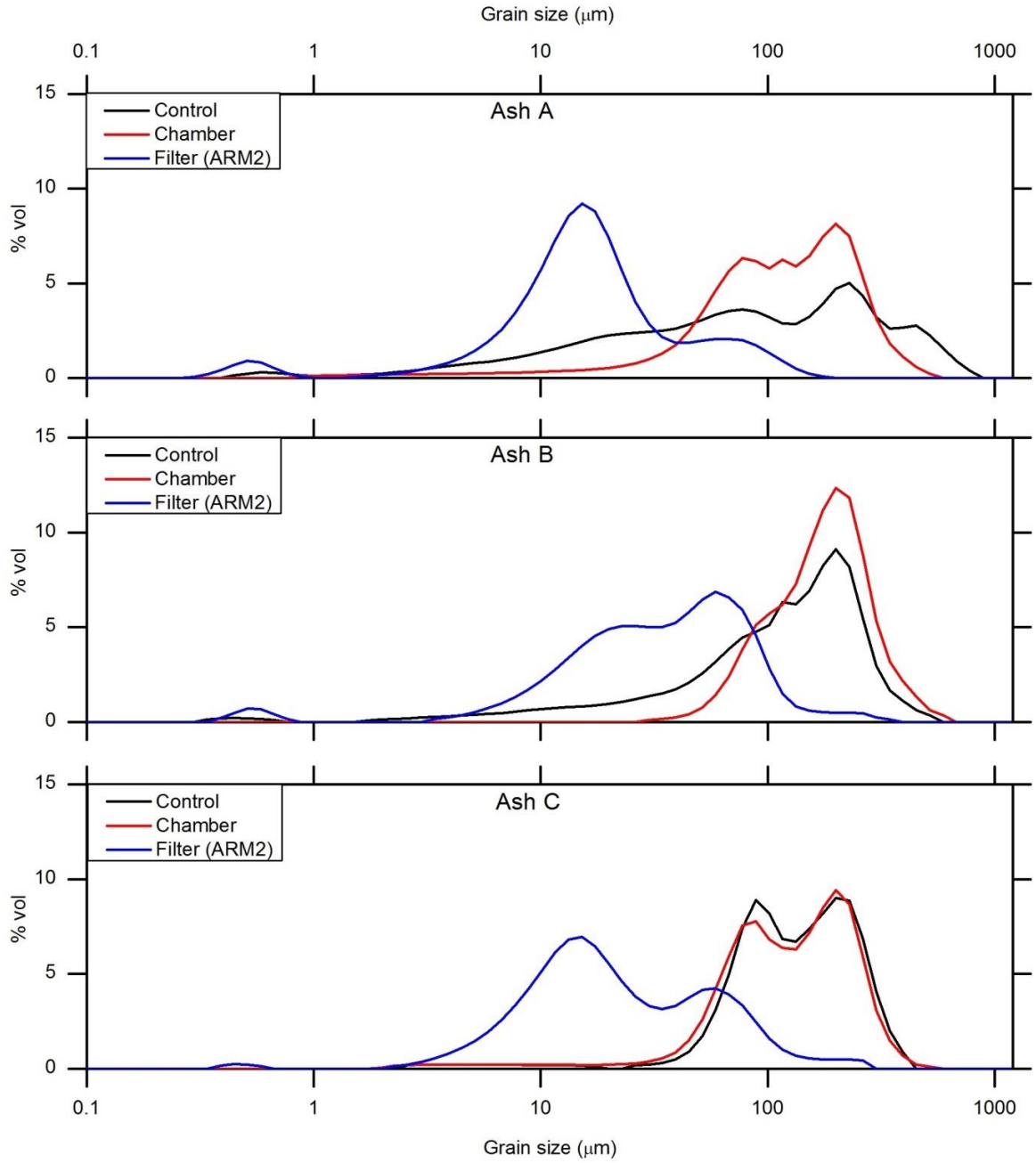

Figure 4.17: Grain size distributions for ash collected from the testing chamber during testing of ARM 2 with Ash A (top), Ash B (middle), and Ash C (bottom). Distributions are compared against control ash ingested without ash reduction measures (Figure 4.15).

4.8.4 Ash Reduction Measure Three (ARM 3)

ARM 3 is a material filtration measure but has a very open weave which did not collect sufficient filter ash for analysis. Chamber ash was collected and is compared with the control in Figure 4.18. The ash has been modified to different degrees by ARM 3, dependant on the ash type. Ash A has a narrower distribution than the control and has become enriched with ~100 µm particles. Ash B is similar to the control but has become enriched with ~80 µm particles and depleted of smaller particles, strengthening the bimodal nature of the ash. Ash C is also similar to the control but has reduced the ~80 µm peak, while increasing the ~250 µm peak, making the ash coarser overall.

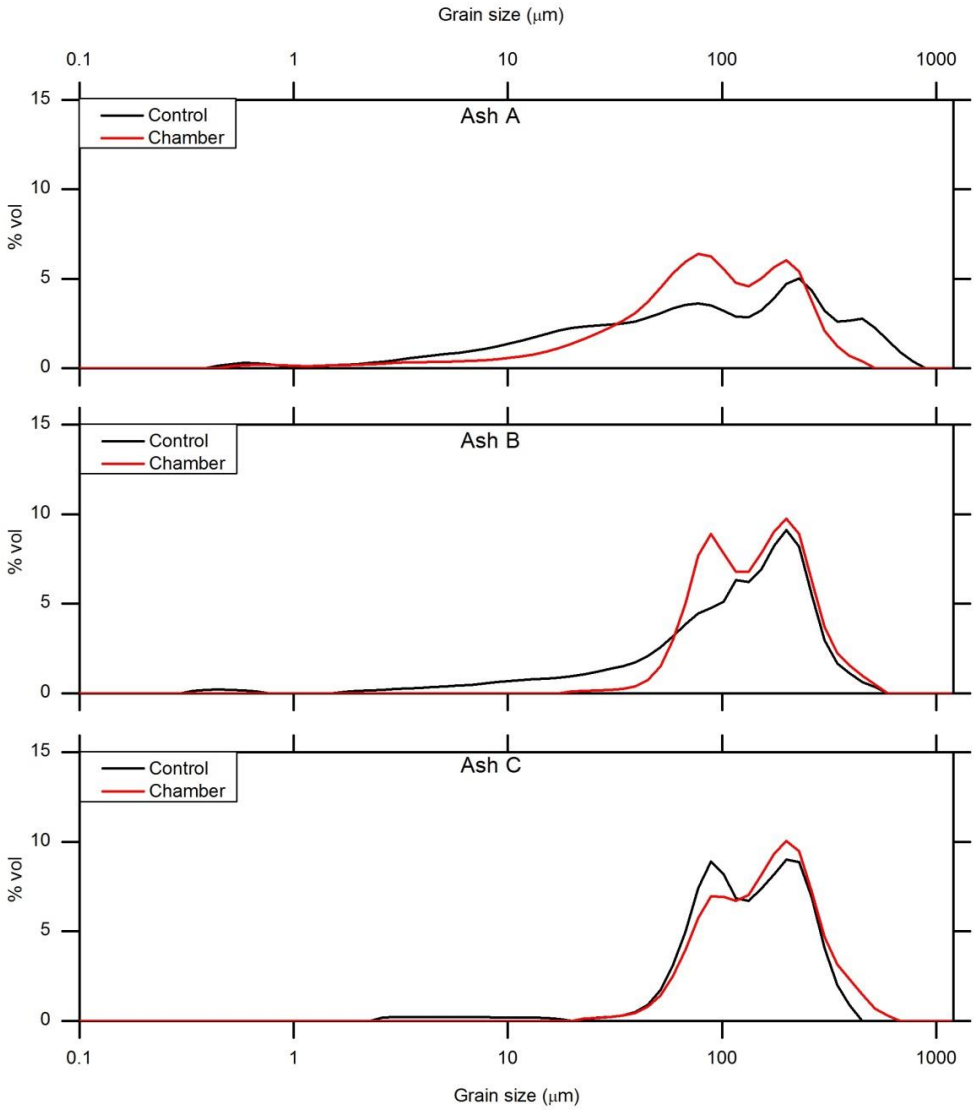

Figure 4.18: Grain size distributions for ash collected from the testing chamber during testing of ARM 3 with Ash A (top), Ash B (middle), and Ash C (bottom). Distributions are compared against control ash ingested without ash reduction measures (Figure 4.15).

4.8.5 Ash Reduction Measure Four (ARM 4)

ARM 4 modified the ash distribution of the control significantly in Ash A, moderately in Ash B and to a minor degree in Ash C. Chamber ash collected from the Ash A test had a narrower distribution than the control and was more concentrated in particles between ~80-300 µm. Ash B was also enriched in a similar range but to a lesser degree. Ash C was less enriched in this range and became less bimodal. Filter ash was finer than the control in all three ash types. Ash C showed the greatest modification, followed by Ash A, with Ash B the least modified.

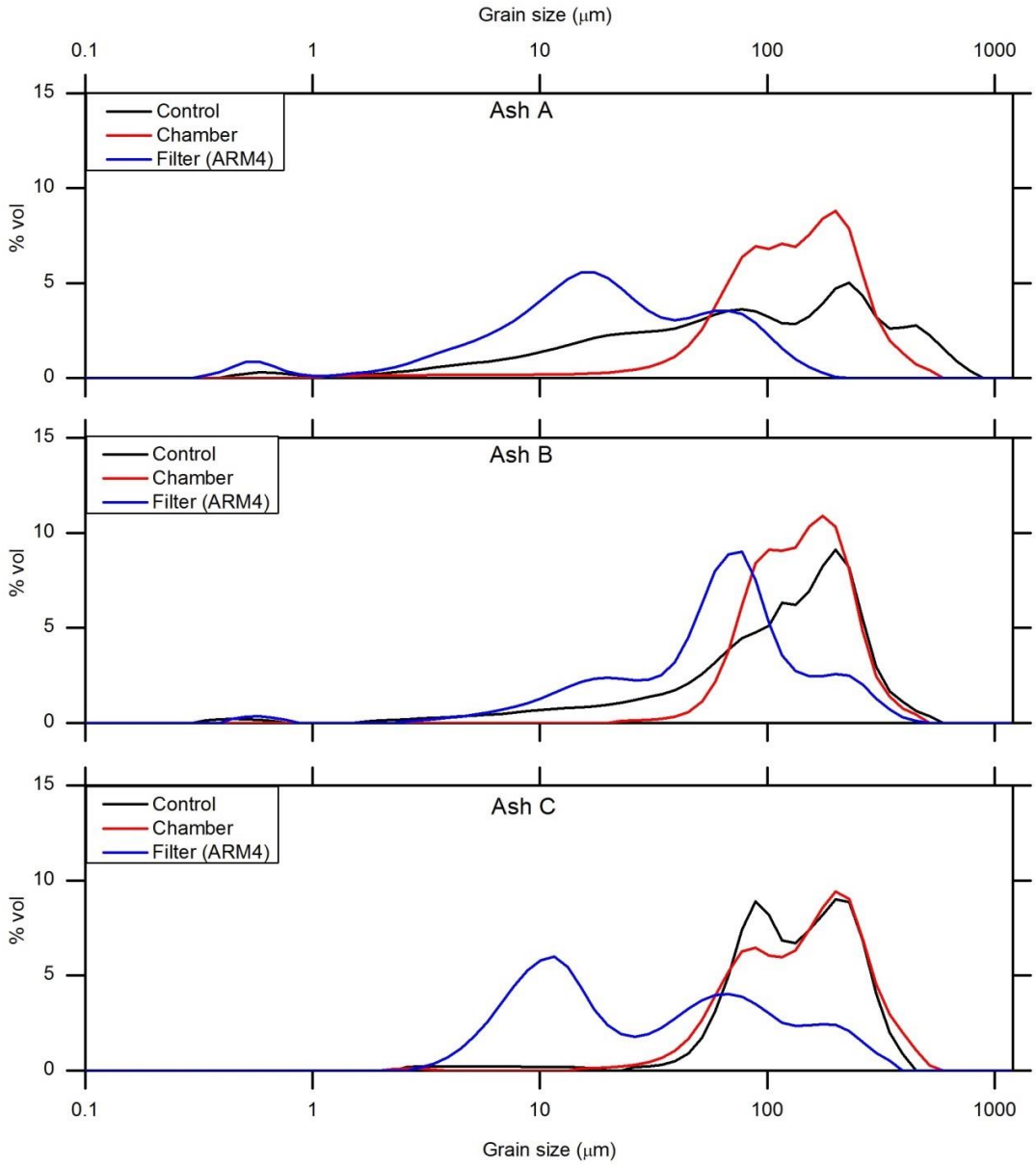

Figure 4.19: Grain size distributions for ash collected from the testing chamber during testing of ARM 4 with Ash A (top), Ash B (middle), and Ash C (bottom). Distributions are compared against control ash ingested without ash reduction measures (Figure 4.15).

4.8.6 Ash Reduction Measure Five (ARM 5)

ARM 5 did not allow sufficient ash to pass into the chamber for analysis during tests with Ash A or B; however sufficient quantities were collected during the test of Ash C. All ash types were collected from the filter for analysis. In all cases the filter ash was finer than the control. Ash A and B maintained a similar grain size range, compared against the control while Ash C narrowed to form a peak at ~70-80 µm. Chamber ash, collected during testing with Ash C, had a very similar distribution to the control but was slightly enriched in coarse particles and depleted of ~200 µm particles.

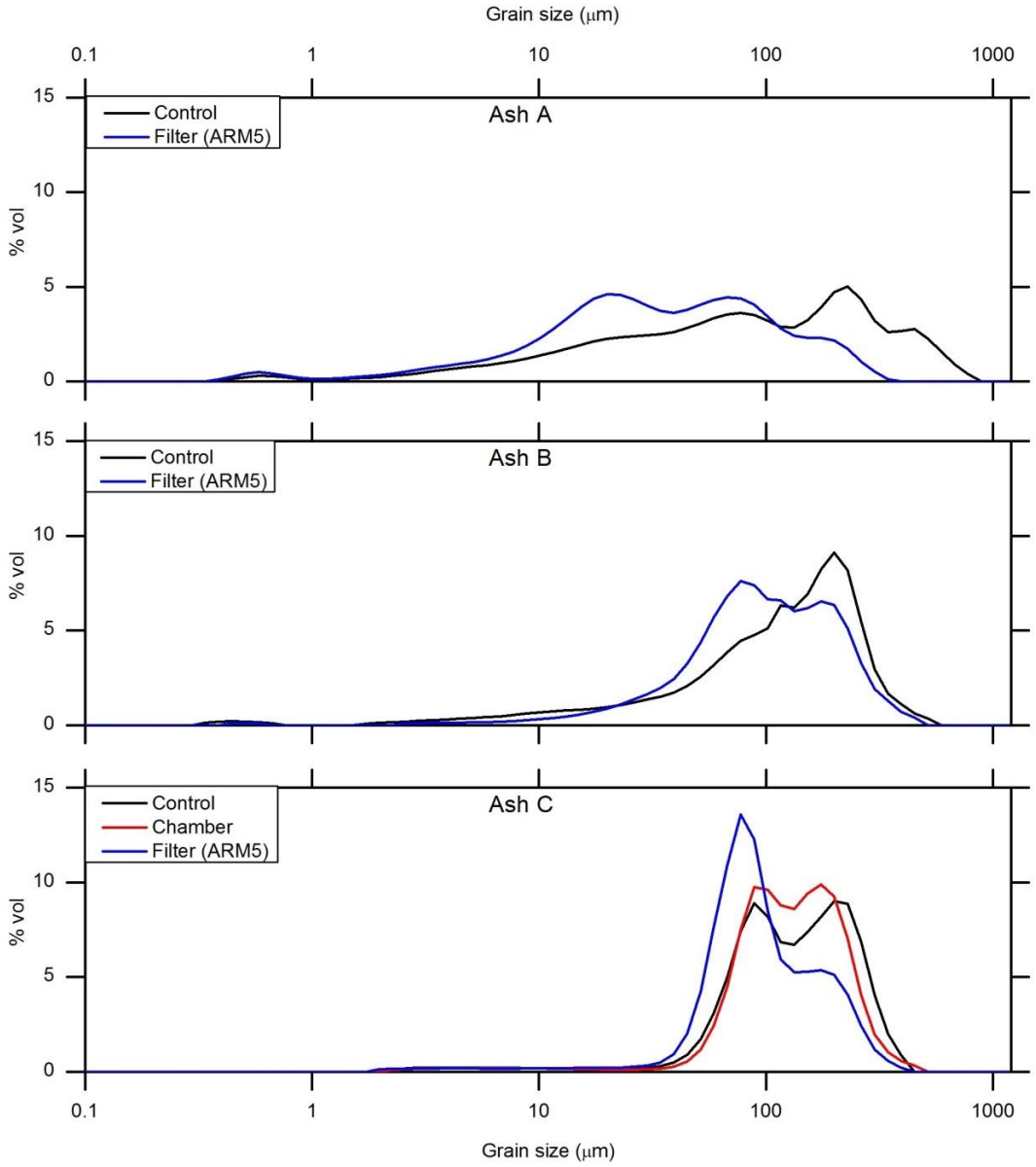

Figure 4.20: Grain size distributions for ash collected from the testing chamber during testing of ARM 5 with Ash A (top), Ash B (middle), and Ash C (bottom). Distributions are compared against control ash ingested without ash reduction measures (**Figure 4.15**).

4.8.7 Ash Reduction Measure Six (ARM 6)

ARM 6 was a dense filter and did not allow sufficient ash to pass to the testing chamber for analysis. Filter ash collected was all enriched in fines compared to the control. Ash A and B maintained similar distribution ranges but shifted to the finer end of the spectrum. Ash C was less modified but became slightly enriched in particles around 80 µm and 500 µm but depleted in particles around 300 µm.

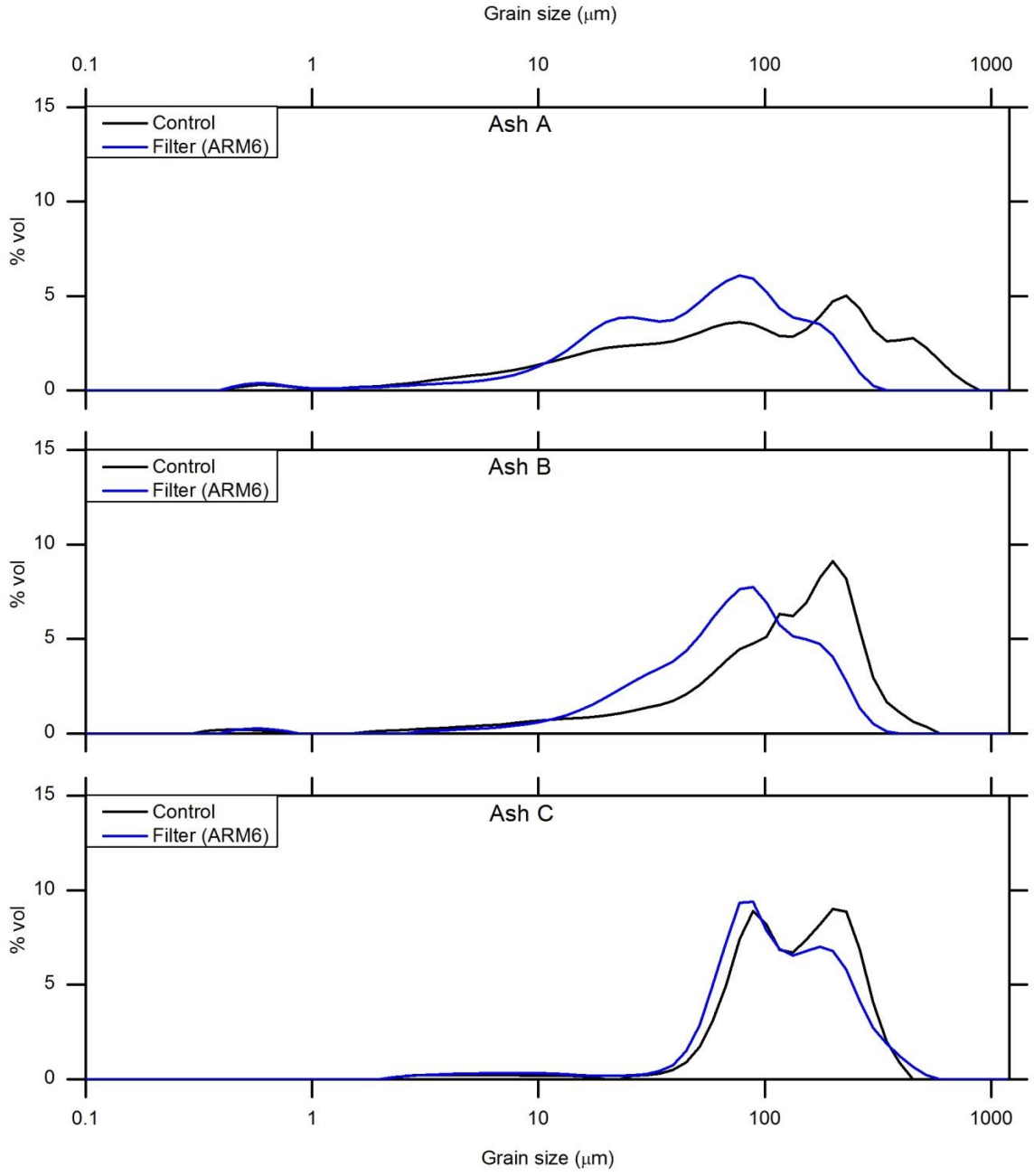

Figure 4.21: Grain size distributions for ash collected from the testing chamber during testing of ARM 6 with Ash A (top), Ash B (middle), and Ash C (bottom). Distributions are compared against control ash ingested without ash reduction measures (**Figure 4.15**).

4.8.8 Additional Testing

Extra testing, involving the combination ARM 1 & 4, caused a higher level of modification of the chamber ash than ARM 1 or 4 alone. Chamber ash became enriched with ~100 µm particles. Filter ash was finer that the control with a peak at around 10 – 40 µm. Chamber ash from the two high fall rate tests had similar distributions which were significantly finer than the control, with a peak between 80 and 300 µm. The filter ash from these tests was also finer than the control, with a peak at around 20 µm.

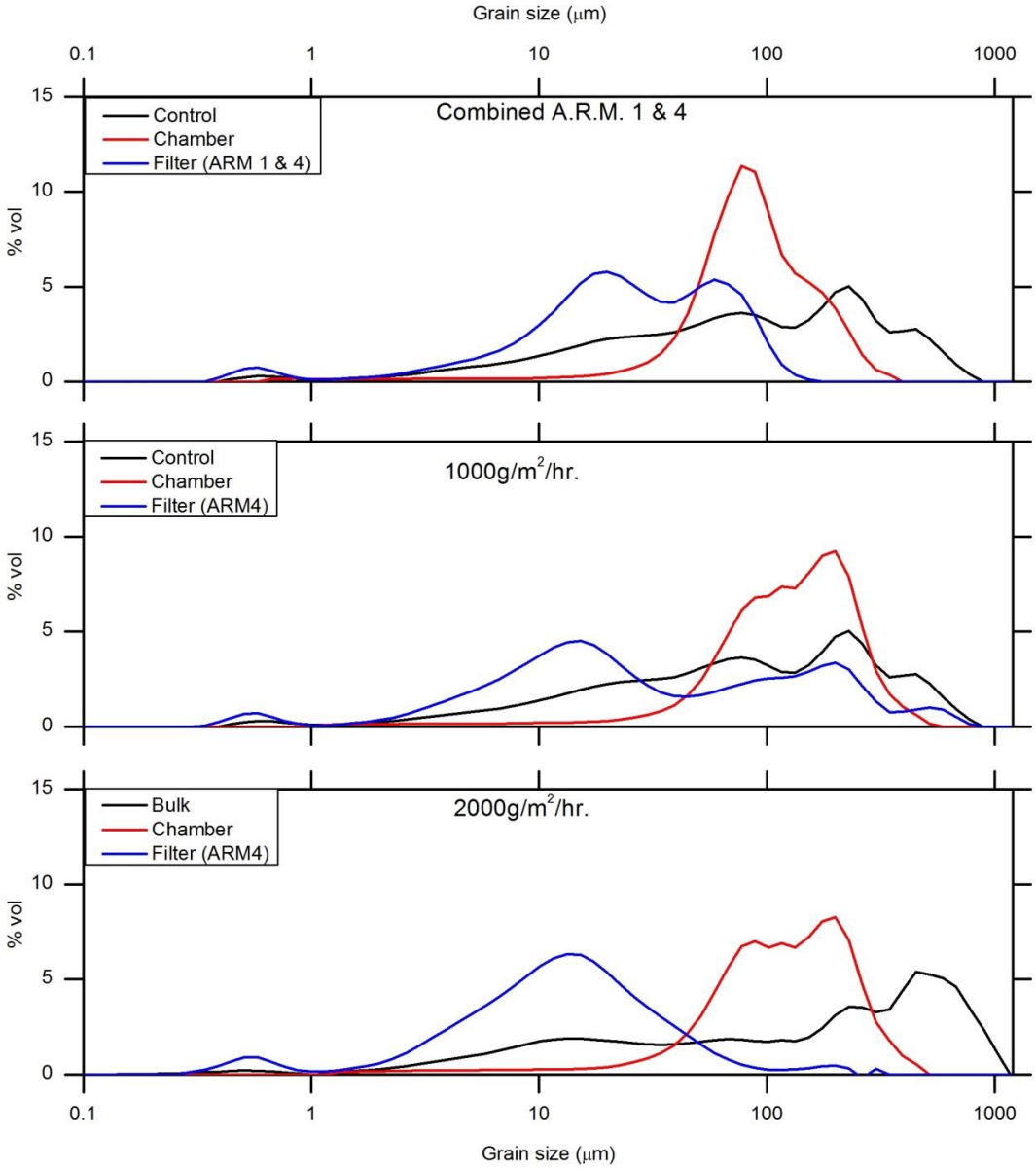

Figure 4.22: Grain size distributions for ash collected from the testing chamber during testing of ARM 1&4 combination, 1,000 g/m^2/hr. and 2,000 g/m^2/hr. Tests involved Ash A (top), Ash B (middle), and Ash C (bottom). Distributions are compared against control ash ingested without ash reduction measures (**Figure 4.15**).

4.9 Grain Size Summary

Median grain size and the standard deviation of each of the tests was provided during the laser particle analysis. Dashes indicate the ash was not analysed, either because the filtration of the ARM was highly effective, preventing sufficient ash passing into the testing chamber or the ARM did not retain sufficient ash.

Table 4.2: Median particle size of all tests. Where no value is provided, ash was not collected because either: 1) the ARM tested did not allow ash to pass to the testing chamber or 2) the ARM collected insufficient ash for analysis.

Ash Type	Ash Reduction Measure	Chamber Ash Median (μm)	Filter Ash Median (μm)
Ash A	Bulk Ash	131.7	-
	No ARM	77.7	-
	ARM 1	99.5	-
	ARM 2	110.4	14.7
	ARM 3	79.7	-
	ARM 4	122.4	17.2
	ARM 5	-	31.4
	ARM 6	-	51.4
Ash B	Bulk Ash	189.1	-
	No ARM	118.4	-
	ARM 1	92.5	-
	ARM 2	166.2	33.9
	ARM 3	134.7	-
	ARM 4	133.1	60.2
	ARM	-	90.6
	ARM 6	-	69.6
Ash C	Bulk Ash	184.6	-
	No ARM	134.1	-
	ARM 1	116.1	-
	ARM 2	132.0	17.9
	ARM 3	149.1	-
	ARM 4	138.5	24.9
	ARM 5	120.2	82.8
	ARM 6	-	102.8
Additional Test Regimes (Ash A)	Combined	78.5	22.5
	1000	123.2	27.5
	2000	110.3	11.7

4.10 Summary

Test results presented in this chapter allow analysis of the ARM performance. The data will be discussed in Chapter Five to determine the more effective filtration measure, accounting for: air speed performance, mass of ash ingested, particle concentrations and grain size change between tests.

Chapter 5 Discussion

5.1 Introduction

Chapter Five analyses the performance of the Ash Reduction Measures (ARM) to address the thesis aims of reducing ash ingestion by large format generators. The chapter analyses results from the empirical laboratory experiments presented in Chapter 4. The results are discussed in the context of failure modes identified in Chapter 2. Limitations of the research methodology (Chapter 3) are also discussed.

5.2 ARM Performance Metrics

The following sections (5.2.1 - 5.2.6) discuss the results of each metric individually to determine the best preforming ARM. **Table 5.1** reviews the metrics recorded in Chapter 4, providing an overview of their application.

Table 5.1: Metrics collected during testing (Chapter Four) and a description of their application for assessing ARM performance.

Metric	Application of Metric to ARM Performance
Particle tracker data	The particle tracker provides information on the concentration of ash particles within the test chamber. This metric provides an indication of the concentration of airborne ash which is available for ingestion by the generator's engine air intake and may cause the generator to stall.
Air speed data	Provides information on the initial air speed reduction induced by the ARM alone and further reduction as ARM becomes obstructed with ash. Provides information on the failure mode of overheating and stalling.
Location of deposited ash	Provides information on the distribution of ash inside and outside the generator casing, allowing assessment of the ARM's filtration performance. This data is key to the understanding of the secondary failure modes (abrasion & corrosion)
ARM mass	Provides information on the filtration performance of the ARM,

	recording the mass of ash retained. It supports assessment of the primary and secondary failure mechanisms as it influences air speed and controls the mass of ash ingested into the testing chamber.
Grain size data	Provides an indication of filtration performance by identifying the particle size ranges which pass into the chamber. Smaller ash particles are less likely to deposit while passing though the chamber reducing the risk of secondary failure mechanisms; however these particles are more likely to be ingested into the engine air intake potentially stalling the engine

5.2.1 Particle Tracker

Particle concentration data (Section 4.6.1), has been further analysed by calculating the particle concentration as a percentage of the control test for each ash type. The calculated data is presented as a graph in **Figure 5.1**. Processing the data as a percentage of the control test, allows data from different ash types to be compared, without the need to compensate for the range of bulk density values of the ashes types introduced. Without percentage compensation, variations in the bulk density would cause denser ash types such as Ash A to appear more contaminating.

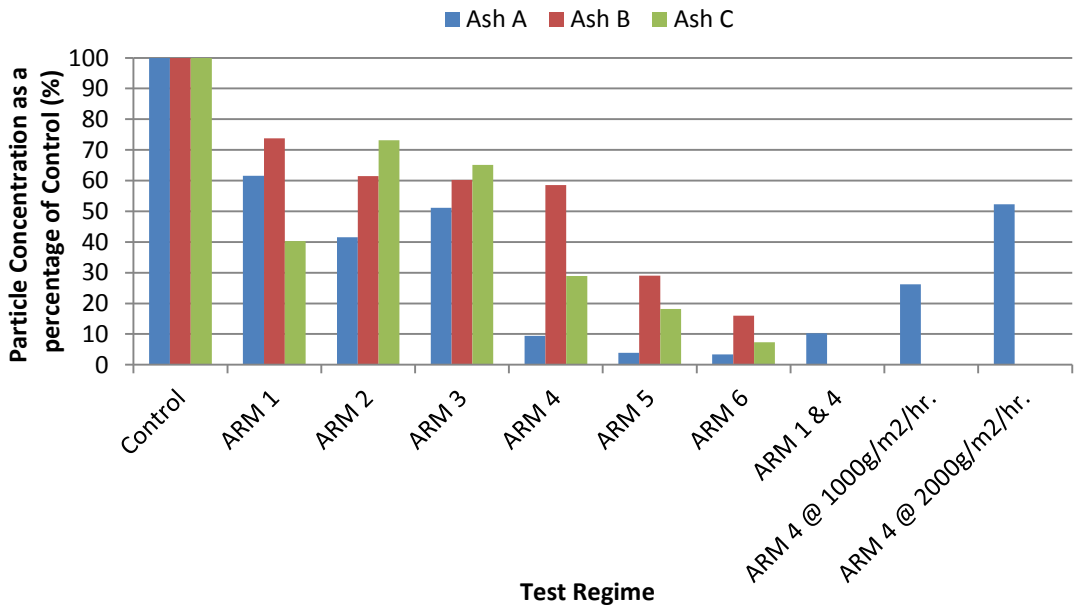

Figure 5.1: Particle concentration within the testing chamber as a percentage of the control test for each ash type. Absolute particle concentration is calculated by measuring change in weight of the particle tacking filter and dividing by the volume of air which passed through the tracker over the test period (6 hours).

In setting the control at a level representing 100% ash being ingested into the testing chamber, the level of effectiveness of each ARM is clearly evident. Most effective, in reducing ash by an average of 91.5% was ARM 6 for all ash types. The data indicated a variation between ash types tested with the same ARM. The variation is largely consistent across the ARM types tested. Ash B is the most contaminating followed by Ash C, then Ash A. The exceptions are ARM 3 & 4 where Ash C is more contaminating than Ash B. The data shows ARMs with an open weave or no material filtration, such as ARM 1, 2 and 3 allows higher levels of contamination than foam or paper filters with open or closed cell structures such as ARM 4, 5 and 6. (See Section 4.4.2.1 for ARM photographs). To aid analysis ARMs were assigned qualitative filtration levels, based on the quantitative particle concentrations within the testing chamber during the test of each ARM (**Table 5.2**). The quality of filtration follows the ARM naming convention; ARM 1 has the lowest filtration and ARM 6 the highest.

Table 5.2: Particle concentration recorded during the testing of each ARM. Filtration levels used in the discussion are noted below.

Reduction Measure	ARM 1	ARM 2	ARM 3	ARM 4	ARM 5	ARM 6
Particle Conc. (mg/m^3)	0.0040	0.0027	0.0025	0.0006	0.0002	0.0002
Description	Lowest filtration-------- Moderate filtration --------- Highest filtration					

5.2.2 Air Speed

Air speed was recorded to determine the initial reduction induced by each ARM and any further impedance due to ash retention within the ARM. Initial air speed values for individual ARM are provided in **Table 3.7**. Individual ARM which reduced initial airspeed by more than 50% were ARM 4, 5 and 6 which reduced air speed by 69, 89 and 88% respectively.

During testing, small rises and falls of airspeed were recorded, but in most cases they were less than degree of variability. For example ARM 4 tested with Ash C (**Figure 4.9**) reduces slightly over the test period (0.18 m/s) but records variability of 0.1 m/s over a period of 2 minutes. The only ARM to show a significant reduction in airspeed during the test was ARM 5 tested with Ash C which reduced the air speed by 1.18 m/s over the test period; however magnitude of this decrease was not mirrored in tests with the other ash types.

The data suggests that over the period of testing (360 min) any air speed reductions induced by ingestion of ash were less than the error margin of the monitoring device or could not be effectively identified due to fluctuations in the data. It is possible a longer testing period may help to identify ash related air speed reduction.

The general trend identified within the airspeed data was that airspeed has a direct trade off with contamination levels. The rankings for airspeed are a direct inversion of those for contamination indicating the most effective ARM may lie in the middle ground where it does not impede the air speed significantly but can reduces ash ingestion appreciable.

The air speed data also showed some cyclical increase and decrease of airspeed with some ARMs. These were characterised as steep airspeed reduction followed by stable airspeed then followed by a steep increase in airspeed and another stable period; the pattern then repeats. The 2,000 $g/m^2/hr.$ fall rate tested with ARM 4 most clearly displays this behaviour (**Figure 4.10**). It is possible that these periodic high and low airspeeds relates to the blocking and unblocking of pore spaces within the filter which has an open cell structure; however this is only one possibility and cannot be corroborated by an of the other data recorded.

A limitation to note when considering airspeed is the pressure drop potential of the fan. The lower pressure drop potential of the small fan used caused the airspeed to reduce at a lower level of impedance than a full scale fan. Unfortunately in order to replicate the full scale fan, a large fan must be used. The larger fan will have a higher air flow which would then require a large aperture to achieve the same airspeed. The logical end point, in order to achieve the correct pressure drop, is full scale.

The reduced ability to induce a pressure drop, allows the ARM to impact airspeed at a lower threshold. In this situation, the fan used is only sustaining the current pressure drop, preventing it from drawing any extra air through the ARM. The implication of this limitation is that results are relative rather than absolute. i.e. ARM 1 can be determined to have a better performance than another ARM but cannot be used to state the filter will last a specific period of time based on a specific ash fall rate and ash type.

5.2.3 Ash Fate: Locations of Ash Deposition during Testing

The deposition on ash was monitored at the locations specified in **Figure 5.2**. To understand the impact of ash on generators and the influence of each ARM on mitigating ash ingesting, the fate of ash within the system is critical. To understand ash ingestion, it is necessary to determine the spatial distribution of the total deposited ash.

For each testing regime ash mass was recorded/monitored (**Table 5.3**) providing a detailed datasets on the amount of ash at locations I to IV. The locations represent: I) Ash deposited on the floor of the drop chamber, II) ash retained within the ARM, III) ash deposited within the testing chamber and IV) ash remaining entrained in the airflow. **Table 5.3** details the average mass and the percentage of total ash deposited at each location for each of the three ash types.

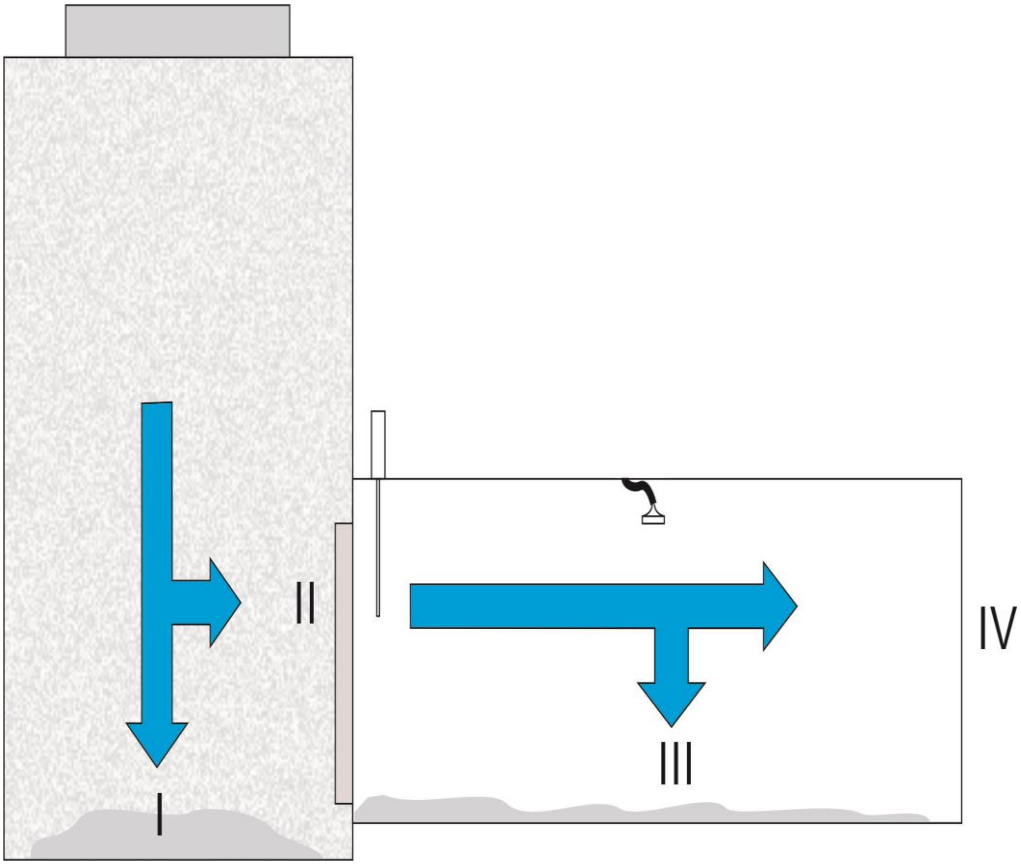

Figure 5.2: Schematic of test setup detailing the four monitored locations.

Table 5.3: Mass of ash deposited at monitored locations during the test period.

	Control (%)	ARM 1 (%)	ARM 2 (%)	ARM 3 (%)	ARM 4 (%)	ARM 5 (%)	ARM 6 (%)	ARM 1+4 (%)	1000 $g/m^2/hr.$ (%)	2000 $g/m^2/hr.$ (%)
Location I										
Ash A	97.81	98.2	98.22	98.0	98.2	98.1	98.0	98.2	99.08	99.21
Ash B	98.32	98.3	98.42	98.2	98.1	97.8	98.4	--	--	--
Ash C	98.13	98.3	98.09	98.1	97.0	97.9	97.3	--	--	--
Location II										
Ash A	--	--	0.12	0.05	0.37	0.45	0.65	0.31	0.00	0.00
Ash B	--	--	0.03	0.13	0.10	0.66	0.14	--	--	--
Ash C	--	--	0.05	0.11	1.14	0.41	1.06	--	--	--
Location III										
Ash A	0.86	0.50	0.35	0.47	0.08	0.04	0.03	0.10	0.08	0.08
Ash B	0.09	0.07	0.05	0.05	0.01	0.02	0.01	--	--	--
Ash C	0.30	0.12	0.23	0.20	0.09	0.06	0.02	--	--	--
Location IV										
Ash A	1.34	1.27	1.31	1.42	1.30	1.42	1.29	1.31	0.50	0.25
Ash B	1.59	1.59	1.50	1.53	1.66	1.42	1.45	--	--	--
Ash C	1.57	1.55	1.63	1.56	1.70	1.61	1.53	--	--	--

In all tests, including the control, a relatively small amount of ash was ingested into the ARM and test chamber, the majority of ash (~98%) was deposited on the floor of the drop chamber, which represents the outside environment of a real generator. The ingested ash was divided between the ARM (location II and the testing chamber (location III) depending on the ARM and ash type. On average Ash A was deposited evenly between the two locations while Ash B and C were mostly retained within the ARM, ingesting just a fraction of the ash into the testing chamber.

In all cases, ash ingestion at location III, as a percentage of the total, was reduced relative to the control test. In all tests ash masses recorded at location II and III combined were less than the control mass recorded at location III (within the test chamber). This indicates that either the presence of the ARM causes less ash to be deflected from the drop chamber toward the air intake, possibly due to reduced air speed, or the ARM has lost particles which were ingested while it was transported from the AGA to the scales. The fact that ARM 1, which has no material filtration to retain ash, has reduced the ingested mass at location III suggests that less ash is being deflected into the drop chamber by the airflow when an ARM is fitted

but does not eliminate the possibility that ash mass lost from the ARM during transport has impacted the results.

Based on the results presented, the ARM which ingested the least ash into location III (test chamber) was ARM 6. This measure reduced ingestion by an average of 96.2% over the three ash types tested.

5.2.4 ARM Weights

The mass gain of ARMs during testing can be used as a further method to determine ARM performance. The mass gained by the ARM during testing is likely to represent ash which would otherwise be ingested. This method only applied to ARM with material filtration which retains ash; as a result ARM 1 is excluded.

The data has been weighted by bulk density to allow for reasonable comparison between ash types (**Figure 4.4**). The results show Ash A is the most contaminating ash type in all tests, followed by Ash B and then Ash C. Filter mass increases are larger in ARMs with higher filtration; however the fall rate also controlled the mass increase with the largest increase recorded during the testing of ARM 4 at 2,000 $g/m^2/hr$.

5.2.5 Grain Size Analysis

Grain size data can be used to determine the size range preferentially excluded by the ARM. This is useful when determining which type of ARM which is most suited to a particular ash type. **Figure 4.14** explains the way in which the grain size graph can be used to determine the excluded grain sizes. The graph shows the maximum particle size ingested by testing chamber in the control test was 777.1 µm, the second point of interest is the maximum size ingested into the testing chamber when the ARM was fitted (344.2 µm). The graph also shows the largest grain size retained within the ARM was 152.5 µm. This process was carried out on each of the graphs (**Figure 4.15** to **Figure 4.22**), the data are summarised in **Table 5.4**.

The data showed ash at location III was coarser than location II in all tests for which data was recorded at both locations. This indicated the ARM retains fine particles while allowing coarse particles to reach the test chamber. A possible explanation is that larger particles which are stopped by the filter, are too heavy to be retained within the filter when the fan is switched off, falling back into the drop chamber. Unfortunately, the higher levels of filtration

(ARM 5 and 6) prevent sufficient ash from reaching the testing while ARMs with poor levels of filtration do not collect sufficient ash within the ARM to allow for analysis. As a result only ARM 4 has a complete data set at location II and III, making comparisons between ARMs difficult.

Comparisons can be drawn between ash types for the tests of ARM 4 where Ash B has the largest particle retained within the ARM (location II) and the smallest deposited within the testing chamber (location III) This appears to be a reflection of the bimodal nature of the Ash B.

Table 5.4: Maximum particle size recorded at three locations within the testing chamber. Black - Ash A, red – Ash B, green – Ash C. Deflection indicates the ARM has not material filtration to retain ash, preventing analysis.

Ash Reduction Measure	Location I Max Particle Size (µm)	Location II Max Particle Size (µm)	Location III Max Particle Size (µm)
Control	1019.5	No ARM	777.1
	1019.5	No ARM	517.2
	890.1	No ARM	394.2
ARM 1	1019.5	Deflection	394.2
	1019.5	Deflection	344.2
	890.1	Deflection	451.6
ARM 2	1,019.5	174.6	517.2
	1,019.5	344.2	592.4
	890.1	trace	517.2
ARM 3	1,019.5	trace	451.6
	1,019.5	trace	517.2
	890.1	262.4	592.4
ARM 4	1,019.5	344.2	517.2
	1,019.5	451.6	451.6
	890.1	344.2	517.2
ARM 5	1,019.5	344.2	trace
	1,019.5	451.6	trace
	890.1	394.2	451.6
ARM 6	1,019.5	300.5	trace
	1,019.5	344.2	trace
	890.1	517.2	trace
ARM 1/4	1,019.5	152.5	344.2
ARM 4 at 1,000g/m^2/hr.	1,019.5	777.1	517.2
ARM 4 at 2,000g/m^2/hr.	1,019.5	300.5	451.6

As the performance is dependent on the grain size of the ash it is difficult to use this data to determine the best ARM; however the data can be used to: 1) match the grade of filtration to the grain size of the ash which is of concern and 2) identify ARM which reduce the grain size significantly, as fine grain ash is more likely to remain entrained within the airflow passing through the chamber without depositing on the generator.

5.2.6 Photographs

Photographs were used to record the contamination of the particle tracker's filter and the ARM at both micro and macro scales (see Sections 4.4.2.1 and 4.6.2). Photographs of filters used in the particle tracker shows a progression towards lighter, less soiled filters as the filtration level of the ARM increases (**Figure 4.12**). Photographs of ARMs, both in situ and under the microscope (**Figure 4.5** and **Figure 4.6**) show the level of ash retention increases as filtration levels increase. Photographs of the particles tracker's filter display a progression toward less soiled filters as filtration levels increase. For example photographs of ARM 5 in **Figure 4.5** and **Figure 4.6** shows a significant build-up of ash on the ARM in all the ash types tested. The corresponding particle tracking filters in **Figure 4.12** are mostly clean with only a few large grains present on the surface.

Based on the dataset, the ARMs which performed the best were ARM 5 and 6 as ash retention on the ARM was high while soiling of particles tracker's filter was low.

5.2.7 Summary of Metrics

A summary of the best performing metrics from the preceding sections is shown in **Table 5.5**. ARM 1 and 6 had the highest performance levels in five of the six metrics reviewed.

Table 5.5: Summary of ARM performance

Method	Ash reduction measure
Particle Tracker	ARM 6
Airspeed	ARM 1
Ash Location	ARM 6
ARM Mass	ARM 6
Grain Size	Inconclusive
Photographs	ARM 6

5.3 Analysis of ARM

This section attempts to bring together all metrics (Table 5.5), allowing each ARM's performance to be compared. For each metric discussed, the relevant data set (figures) are referenced (**Table 5.6**). Each ARM is discussed in the flowing sections.

Table 5.6: List of reference figures for metrics discussed during analysis of ash reduction measures.

Metric	Reference
Particle Tracker	Figure 4.11
Air Speed	Figure 4.7, Figure 4.8, Figure 4.9 and Figure 4.10
Ash Fate	
	Table 5.3
ARM Mass Gain	Figure 4.4
Grain Size Analysis	Figure 4.15 - Figure 4.22
Photographs	Figure 4.5, Figure 4.6 and Figure 4.12

ARM 1: Deflection Hood

ARM 1, a deflection hood, had the least impact on recorded ingested ash, reducing the average mass deposited at location III by 41% and the average particle concentration by 58%, over the three ash types. Ash B was most reduced followed by Ash A. The ARM had the lowest impedance, reducing airspeed by ~69%. The photographs of the particles trackers are the most contaminated of any of the ARMs. The grain size at location III is moderately reduced compared with the other ARMs tested. Based on this analysis ARM 1 has a moderate effect on reducing the ingestion of volcanic ash. Overall the function of a deflection measure is beneficial as it has the least impact on airspeed of all ARMs tested.

ARM 2: Hessian

The hessian filter had the second lowest reduction of ingested ash but had the second highest airspeed. The mass of ash deposited at location III was also slightly lower than the test of ARM 1 but higher than all other tests. Maximum grain size at location III was less modified with ARM 2 than ARM 1, but more modified than all other ARMs. Photographs show the particle tracker's filter is soiled to a similar degree as ARM 1. ARM 2 gained a small amount of mass during the experiment and was most significant during the test of Ash A (5 g increase). Based on this analysis ARM 2 has a moderate effect on reducing the ingestion of

volcanic ash. Overall the function as a filtration measure is appropriate at reducing ash ingestion with limited impact on air speed.

ARM 3: Windbreak

ARM 3 is a material filtration measure with an open weave, which in most tests, did not retain sufficient ash within the ARM for analysis. The exception was where the ARM was tested with Ash C, where more ash adhered to polyurethane weave. The air speed reduction induced by ARM 3 was similar to ARM 1 and 2 and less than ARM 4, 5 and 6. Particle tracker analysis indicates this measure was more efficient at reducing ash ingestion than ARM 1 and 2 but less effective than ARM 4, 5 or 6. The deposited ash mass at location III is consistent with the particle tracker. Maximum grain sizes at location II were reduced to a similar degree as tests with ARM 1 and 2. The ARM gained an average mass of ~1 g over the test period. Photographs show trace amount of ash on the ARM. Photographs of the tracker's filter are less soiled than those used with ARM 1and 2 but more soiled than those used with ARM 4, 5 and 6. Overall the filtration measure was effective but came with the cost of a reduced airspeed.

ARM 4: Polyurethane Filter

The open cell structure of the polyurethane filter significantly reduced the particle concentration during testing of all three ash types. It was most effective with Ash A (9.46% of the control). The airspeed was reduced to a much larger degree with ARM 4 than ARM 1, 2 and 3 but less than tests of ARM 5 and 6. The maximum grain sizes at location II were larger than ARM 2 and 3. At location III the maximum grain size was similar to the ARM 3. Photographs show a large amount of ash was deposited within the ARM, this is supported by the ARM mass gain which averaged 10 g over the three tests. Photographs of the tracker's filter are less soiled than the preceding ash types and the mass of ash at location III is less than half the mass deposited during the test of ARM 3. Ash A was most significantly impacted, reducing ash at location III by 83% compared to ARM 3. The measure was very effective at reducing a particle ash ingestion but reduces air speed substantially. Overall the measure was effective.

ARM 5: Vehicle Air Filter

The vehicle filter reduced particle concentration at location III to a significant degree in all tests. Like tests involving ARM 4, Ash A was reduced to the largest degree (3.9% of the

control). The airspeed in these tests was significantly impacted (~13.6% of the control). Only trace amounts of ash were ingested into the chamber, preventing grain size analysis. Photographs of the particle tracker's filter shows a largely clean filter containing only a few grains of ash. Photographs of the ARM show significant quantities of retained ash. The ARM gained an average of ~10 g of ash over the three tests. Overall the filter was not effective, while it significantly reduced ash ingestion; the resulting air seed reduction was substantial.

ARM 6: Foam Filter

The foam of ARM 6 was the most effective measure tested, reducing particle concentration by up to 96.4% (Ash A); however the ARM reduces the airspeed significantly (~11% of the control). The ARM let so little ash through, that grain size analysis and the mass of ash deposited at location III could not be calculated. Photographs of the particle tracker's filter show a clean filter while photographs of the ARM show significant ash retention. The filter gained an average of 20 g of ash during the tests, much more than any other ARM tested. Overall, like ARM 5 the filter was not effective due to the significant air speed impedance.

Combination ARM 1+4: Deflection Hood and Polyurethane Filter

The combination ARM has a similar impact on air speed as ARM 4 alone (30% of control). The particle concentration is also similar (10.2% vs 9.46%); however the maximum ash size at both locations II and III is significantly less (152.5 µm compared with 344.2 µm and 344.2 µm compared with 517.2 µm). The mass of ash recorded at location III was also similar. Photographs of the ARM and the particle tracker's filter are similar as those from the test of ARM 4; however the mass gained by the ARM is significantly less (13 g compared with ~20 g). Overall the filtration measure was effective; however it was not substantially more effective than ARM 4 alone.

High Fall Rate 1,000 g/m^2/hr. with ARM 4: Polyurethane Filter

ARM 4, the polyurethane filter, was tested at approximately three times the standard fall rate (375 g/m^2/hr.) and had a similar air speed as the standard ARM 4 test; however the maximum grain size recorded at location III was smaller. The particle concentration was also higher (276% higher) but this is consistent with the increased fall rate (260% higher). Ash deposited within the chamber is also similar to ARM 4 at the standard fall rate, suggesting extra ash ingested, as indicated by the particle tracker is not being deposited within the testing

chamber. Photographs of the tracker's filter show it has more ash than the standard ARM 4 test. The ARM has gained 22 g which is almost 33% more than the standard ARM 4 test. Photographs of the ARM show it contains more ash. Overall the test showed the relationship between fall rate and the level of contamination is linear indicating ARM 4 was not better or worse at reducing ash ingestion at higher fall rates.

High Fall Rate 2,000 g/m^2/hr. with ARM 4

The polyurethane filter, ARM 4, when tested at 2,000 g/m^2/hr. also had a scaled relationship compared with the standard ARM 4 test. The airspeed and maximum particle size was similar; however particle concentration was 52.3% of the control. This is also consistent with the scale relationship as it is 550% higher than the standard ARM 4 test while the fall rates is 530% higher. Ash mass at location III is consistent with other ARM 4 tests. Photographs of the particle tracker's filter show more ash than the other ARM 4 tests. Mass gain of the filter is almost twice as much as the standards ARM 4 test and this is supported by photographs showing that the ARM is caked with ash. Overall this test came to the same conclusion as the preceding test.

5.4 Overall Ash Reduction Measures Performance

In reviewing the literature (Section 2.7) two categories of failure modes, short term (stalling and overheating) and long term (corrosion and conduction) were identified. The various metrics aid the understanding of one or both failure modes as outlined in **Table 5.1**. After reviewing the metrics and considering the failure modes, it was decided that particle concentration and airspeed were the most valid metrics to assess the performance of the ARMs. The validity of these data sets is based on the fact that the particle tracker and airspeed were both automated means of recording the variables and therefore less open to error or observational bias e.g. subjective analysis of photographs or loss of ash from ARM in transport. The review of airspeed and particle concentration also allows quantitative assessment of the trade-off between ash ingestion and air speed.

The process to identify the best performing ARM involved two stages. First the best ARM was identified using the air speed and particle concentration data, and second, supplementary metrics were considered to determine if they support the findings made in stage one.

Stage 1

To aid in the identification of the best ARM, the air speed and particle concentration data was further analysed as a percentage of the control for each ash type, and ranked by air speed (**Table 5.7**).

Table 5.7: Absolute and relative measures for ash contamination and air speed. Percentage values are relative to the control test for each ash type. Extra test ARM 1 and 4 is relative to Ash A control.

Ash Type	ARM	Air Speed		Particle Concentration	
		Air Speed (m/s)	% of Control	Mass (mg/m^3)	% of Control
ASH A	Control	7.1	100.00	0.00642	100.00
	ARM 1	5.47	77.15	0.00395	61.57
	ARM 2	5.41	76.30	0.00266	41.53
	ARM 3	4.75	66.95	0.00328	51.18
	ARM 4	2.41	34.01	0.00061	9.46
	ARM 1 & 4	2.15	30.25	0.00066	10.21
	ARM 5	1.15	16.29	0.00025	3.91
	ARM 6	0.79	11.11	0.00022	3.42
ASH B	Control	7.1	100.00	0.00057	100.00
	ARM 2	5.15	72.43	0.00035	61.48
	ARM 3	4.69	65.97	0.00035	60.23
	ARM 1	4.47	62.88	0.00042	73.79
	ARM 4	2.13	29.93	0.00034	58.51
	ARM 5	0.93	13.02	0.00017	29.04
	ARM 6	0.86	12.10	0.00009	15.98
ASH C	Control	7.1	100.00	0.00642	100.00
	ARM 3	4.91	69.19	0.00126	65.08
	ARM 1	4.87	68.57	0.00078	40.33
	ARM 2	4.67	65.81	0.00141	73.17
	ARM 4	1.90	26.72	0.00056	28.92
	ARM 5	0.83	11.73	0.00035	18.22
	ARM 6	0.80	11.25	0.00014	7.32

Due to the trade-off it is likely the best ARM will lie in the middle ground where a reasonable air speed is maintained but a sufficient amount of ash is blocked. Data from **Table 5.7** was plotted on opposing axes to explore the trade-off and determine the best ARM (**Figure 5.2**).

The points are plotted using colour, to identify the ARM, and shape to identify the ash type (**Figure 5.2**). Regions have been drawn around each ARM grouping, indicting the range of performance values the ARM may occupy, dependant on the grain size and density of the ash type. The vertical axis displays contamination reduction as a percentage. For the purpose of identifying the best ARM, a minimum reduction of 50% or greater is required. Similarly, the horizontal axis indicates air speed reduction as a percentage; reductions of <80% are determined to be sufficient. These minimum levels or thresholds have been implemented based on this author's interpretations, air speed is at a level that is at an acceptable lower limit of initial air flow (no ash blockage) while particle concentration is at a level that substantially reduces occurrence of the failure modes.

While these limits are based on the author's interpretation, they help frame the ARMs which are most likely to perform well. The limits emplaced by these restrictions form an area of acceptable performance, accounting for the trade-off between air speed and particle concentration (**Figure 5.2**).

It is important to note the pressure drop potential issues of the scaled down fan, discussed in Section 5.2.2, mean the air speed reduction induced by the impedance of the ARM may not be as significant at full scale. Therefore, the contamination level was given more weight in the comparison, resulting in the rectangular shape of the sufficient air speed and particle concentration zone (high performance zone).

Three ARMs involving five tests fall within the acceptable zone. These are: ARM1 - Ash C, ARM 2 – Ash A, ARM 4 – Ash A and B and ARM 1+4 combination – Ash A.

The number of ARMs falling within the high performance zone indicates there may be a range of ARMs which are suitable for use as temporary filtration and that the choice of ARM may be dependent on factors such as the grains size and the fall rate of ash. Light ash falls may require a lower levels of protection e.g. ~50% particle reduction; in which case ARM 1 or 2 would be more appropriate than ARM 4 as it can maintain a higher air speeds.

In heavy ash fall the best performing ARM was ARM 4 as it had the highest overall ash reduction of any ARM above the air speed cut-off value of 80%. In addition ARM 4 was the only measure to record more than one ash type within the high performance zone.

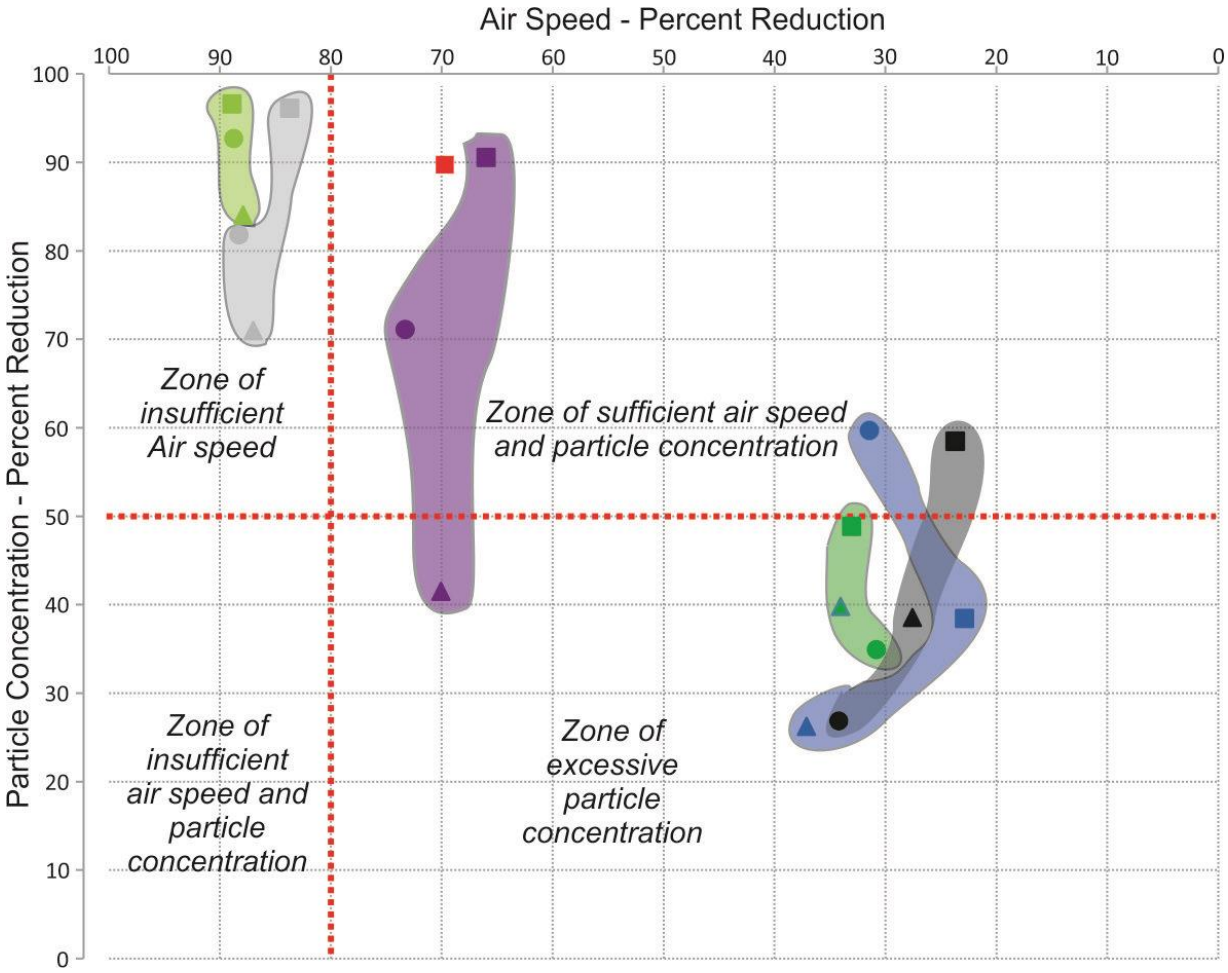

	Ash A	Ash B	Ash C
ARM 1	■	▲	●
ARM 2	■	▲	●
ARM 3	■	▲	●
ARM 4	■	▲	●
ARM 5	■	△	○
ARM 6	■	△	○
ARM 1 & 4	■		

Figure 5.2: Graph of air speed and particle concentration values relative to control test. Lines and labels indicate areas of acceptable performance. Shapes around the ARM groupings indicate the possible range of effective values with other ash types which are within the density and grain size ranges of the ash types tested.

Stage 2

As outlined above, the best performing ARM identified in stage one were further verified using the supplementary metrics, as outlined in the following section. **Table 5.8** details the range of supplementary metrics for ARM 4.

Table 5.8: ARM 4 - performance of supplementary metrics.

Supplementary Metric	ARM 4 Performance
Ash mass at location III	The deposited mass of ash at location III in the testing of ARM 4 (Table **5.3**) are significantly lower than ARM 1, 2 or 3 (at least 50%). Ash mass values for ARM 5 and 6 are not substantially lower than ARM 4 but come with the cost of reduced airspeed.
ARM mass gain	The mass gain of ARM 4 is slightly lower than ARM 5 and 6 and does not have the cost of the reduced air speed (Figure 4.4). The ARM mass of ARM 4 is significantly higher than ARM 2 and 3. ARM 1 does not retain ash mass as it is a deflection measure.
Photographs	Photographs of the particle tracker's filter show the ARM filter is significantly cleaner than ARM 1, 2 and 3 (Figure 4.12). ARM 4 is slightly more soiled than ARM 5 and 6.
Laser grain size analysis	The maximum grain sizes at location II were larger than ash recorded while testing ARM 1, 2 and 3. Ash tested with ARM 5 and 6 similar to ARM 4's ash. At location III the maximum grain size was similar to the ARM 1, 2 and 3. ARM 5 and 6 recorded only trace amount of ash.

5.4.1 Performance of ARM 4 at High Ash Fall Rates

Two tests involving ARM 4 with higher fall rates are consistent with the effectiveness of ARM 4 alone when the higher fall rates are accounted for (Section 5.3). These tests recorded contamination levels which were ~3 and 6 times the contamination recorded during the

standard ARM 4 test, which is consistent with the fall rates which were also ~3 and ~6 times the standard rate. This data can be used to show the performance and service life of temporary filter may be predictable using the fall rate.

5.5 Combination ARM

It was expected in this study that pairing up two of the better performing ARMs would provide additional performance gains; however the combination of deflection hood and polyurethane filter, ARM 1 and 4 respectively, plots in a similar location to ARM 4 (**Figure 5.2**). Based on this analysis, the combination of ARMs (1 and 4) appears to offer limited, if not reduces the benefits of ARM 4 on its own; however the combined measure does significantly reduced grain size at location III (~45% of ARM 4). The particle concentration determined by the particle tracker is a measure of suspended ash, the reduced grain size which results from the combination ARM is more likely to remain suspended than larger grain sizes, reducing deposited ash which can cause corrosion

5.6 Influence of Volcanic Ash Density

Patterns or groupings which occur within **Figure 5.2** may indicate ARM performance is modified by grain size and density. Two groupings are present in the figure. 1) ARMs which are grouped in the top left of the graphs (ARM 4, 5 and 6), and 2) ARM which were grouped in the centre right (ARM 1, 2 and 3).

ARMs grouped in the top left were more effective with Ash A, followed by Ash C, with ash B the least modified. ARM 1 and 2, grouped in the centre right, are also most effective with Ash A; however Ash B and C are in opposite positions to the order determine by the fist grouping, with Ash C now the least effectively reduced. The deflection hood, ARM 1 does not appear to follow either pattern.

The orders displayed by ARM 4, 5 and 6 are potentially controlled by grain size and/or density. The ingested mass of Ash A, the largest grain size and highest density, is most effectively reduced while Ash C, the smallest grain size and lowest density ash is less reduced. The exception is Ash B, the medium grain size/density ash which is the most reduced. This appears to contradict the earlier implication that large grain sizes and higher densities are more effectively reduced: however Ash B is a highly bimodal ash (see section 4.8) and as such it is possible the ash has reduced qualities of the medium grain sizes which

are being picked up by the tracker, i.e. the large grains of the ash are not drawn into the chamber while the fine grains are easily expelled by the chamber.

Figure 5.3 indicates possible particle pathways through the chamber. A stratified ash column is likely to form as air is drawn through the chamber. Low density ash with smaller grain sizes are likely to remain entrained as move high in the chamber. The medium grain size/density ash is likely to be drawn through the middle of the chamber while the coarse grain, high density ash is likely to saltate along the bottom of the chamber. This ash has the greatest chance of depositing within the chamber.

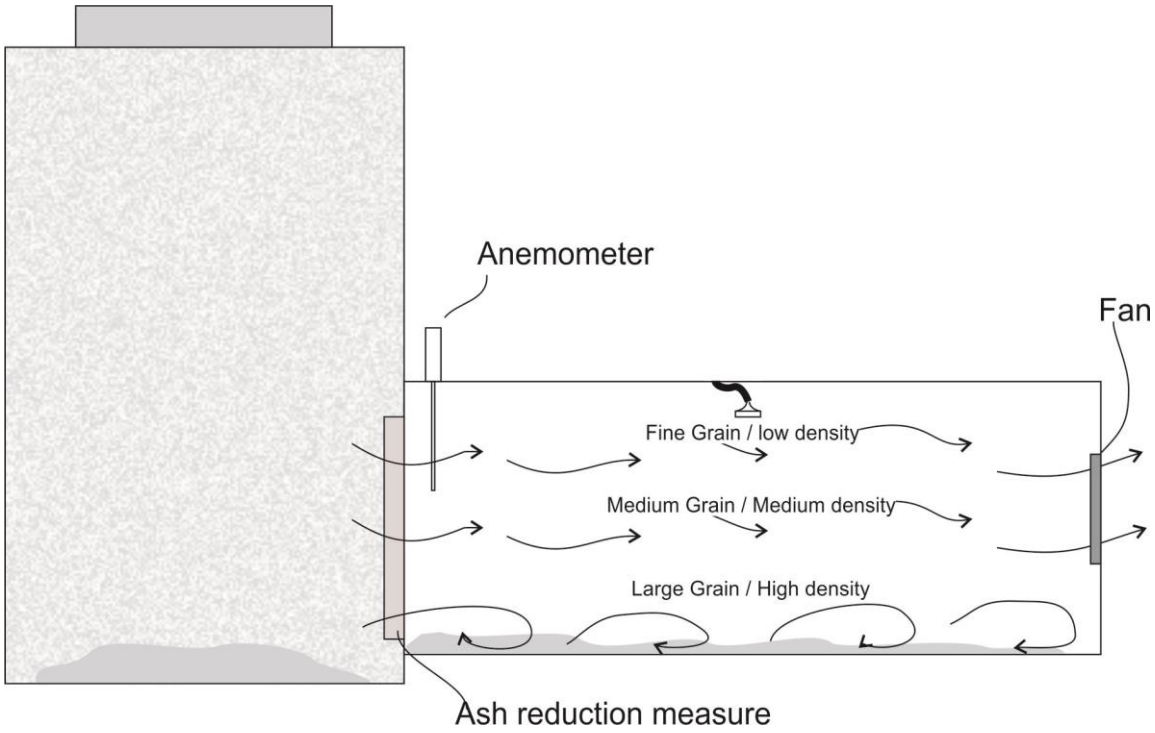

Figure 5.3: Diagram of the AGA indicating possible particle pathways through the testing chamber.

5.7 Limitations of study

A number of limitation act to restrict the application of the results as an absolute measures of ARM performance. However the data's potential to be use in relative terms, i.e. as a measure of comparing ARM, is not impacted. The two primary limitations were the capacity of the fan and the variations in fall rates during the test.

5.7.1 Fan Capacity

The lower pressure drop potential meant air speed was rescued at a lower level of airflow impedance (see Section 5.2.2).

5.7.2 Fall Rate Variation

Fall rates across each ash type were variable due to differences in the grain sizes, densities, and cohesiveness of particles. Variations meant modifications were needed to ensure ash fall rates were as close to the 340 g/m^2 per hour target as possible. The modifications included altering the shacker box's strike mechanism to allow for less forceful impacts and swaping out the 1,000 µm mesh for mesh with apatures of 480 µm. In addition the strike rate was reduced by modifing the controling code to increasing the delay between hits and decreaseing the rotation speed of the motor.

5.7.3 Future Modifications

A repeat of testing would see a number of modifications. The primary modification would be a larger, more powerful fan. Although the fan used cannot be equivalent to a large format generator for the reasons outlined in Section 5.2.2, a larger fan would make the air speed results more reliable as an absolute measure of airspeed performance.

A second modification would be made to the ash dispersal mechanism. The current design is highly sensitive to small variations in the force of the hammer and strike rate. In addition, clumping of the particles or compaction of the ash due to vibration of the hammer mechanism can reduces the test rate both within and between tests. The amount of ash in the hopper also controlled the fall rate. A repeat of the test would use a chamber angled at 45°. In the middle of the chamber a container of ash with an auger would dispense small amount of ash into the chamber. A fan mounted at the bottom would send the ash/air mixture up the chamber and into the fall chamber producing a continuous ash fall which falls under its own weight in a turbulent environment.

Testing of ARMs which were excluded due to the time constrains and difficulty of testing could be useful. In particular cyclonic filtration may be an effective measure as it is currently used to reduce particulate ingestion in generators used in dusty environments.

Grain size and fall rates were determined using a range of eruptive sources due to time constrains and difficulty obtaining relevant data for the Auckland region. Future work in this area should focus on fall rates and grain sizes which have impacted Auckland in the past to ensure the study accurately models expected ash fall characteristics.

All testing involved dry ash, in the future testing with moist ash would be useful to determine any variations moisture may cause to the ingestion and adherence of volcanic ash. Based on previous work it is likely that moisture will reduce the ingestion of ash but increase its adherence to surfaces (Barnard, 2010).

Lastly modification of the pseudo ash would be beneficial. The bulk density of the ash is much higher than that of real volcanic ash due to the solid rock used to produces it. A lower density ash would better replicate volcanic ash but further work is needed to determine a way to achieve this.

5.8 Summary

The discussion provided a comparison of ARM performance using different ash types and fall rates. The various metrics from Chapter 4 were used to determine the impact of the outlined failure modes from Chapter 2 and identity the ARM which best mitigates the short term and long term modes. The next chapter provides conclusions and recommendations based on the discussion to achieve the thesis air of identifying the most effective temporary filtration measure for operating large format generators in environments which high levels of suspended ash.

Chapter 6 Conclusions and Recommendations

6.1 Conclusions

In this study, a range of mitigation measures were trialled to determine the best method to reduce ash ingestion by large format generators. It found that all filtration measure trialled reduced the ingestion of ash; however increased airflow impedance was associated within high filtration performance. Thus filters which were effective at reducing ash ingestion may cause failure of the generator by restricting ingress of air for engine aspiration.

The literature review identified a range of impacts of volcanic ash, in particular the impacts of ash on the generators of Bariloche, Argentina, at two large scale generator facilities. The review enabled the identification of four failure modes: stalling, overheating, corrosion, conduction. These modes fall into two categories: 1) short term failure modes which may occur in the hours to days following ash fall (i.e. overheating and stalling), and 2) long term modes which may occur in the weeks to months following the eruption (i.e. corrosion and conduction).

Laboratory experimentation involving 24 tests was undertaken using six ash reduction measures and three distinct pseudo-ashes. Each six hour test was recorded and monitored to provide a range of metrics which could be used to identify the best mitigation measure. Testing found the measures had a range of performance characteristics. While all ash reduction measures reduced ash ingestion by at least 25%, some severely impeded airflow, reducing airspeed through the intake grill by up to 90%; however air speed reduction can only be used as a relative measure of performance due to the reduced pressure drop potential of the fan used. The conclusion of this study was that any of the filtration measure trialled are suitable for use during ash fall, dependant on the airspeed and filtration requirements of the generator in question and the availability of filtration materials. Deflection hoods were particularly effective as they reduced ingestion by ~50% with minimal air speed reduction.

Long-term experimentation was not undertaken due to time constraints but the results suggest that ash reduction measures, with the exception of the deflection hood, may suffer further air speed reductions as ash obstructs the filter. This effect will be more pronounced in measures which were most efficient at reducing particle concentration within the testing chamber. Further experimentation involving longer run tests (more than six hours) may allow identification of the maximum service life of the filter and provide information of the timing of cleaning and replacement of temporary measures.

6.2 Implications for Generator Operation in the Auckland Region

The results of the study were considered in the context of the Auckland region (Table 6.1). Ash types which could potentially impact Auckland (detailed in section 2.3.1) are reviewed in light of test results and analysis (**Table 6.1**), providing guidelines on suggested ARM application for each eruption scenario.

Table 6.1: Table of ash types which may impact the Auckland region. Potential mitigations measures are outlined for each ash type.

Eruption Source	Ash Types	Mitigation Method
Wet AVF Style Eruption or Distal Basaltic Eruption	A wet eruption in a proximal location is likely to result in a fine grain ash. Ash A analogue.	The best mitigation method will have good filtration capabilities. ARM 4 in particular was shown to be effective with Ash A which is the most appropriate analogue for this type of ash.
Dry AVF Eruption	A dry AVF eruption will likely produce coarse particles. While the particles are likely to be coarser than those used in this experiment, the best ash analogue is Ash B.	In the event of coarse ashfall the deflection hood is likely to be the most effective measure as it distances the falling ash without high levels of filtration which may be unnecessary with larger particles.
Distal Rhyolitic Eruption	Distal eruption of a rhyolitic source will produce fine, low density particles similar to Ash B.	The most effective measure in this case was ARM 4 which removed ~42% of the ash ingested by the control.

6.3 Recommendations

Recommendations have been divided into two categories below. Those which can be implemented prior to an eruption and those which can be used during ash fall to limit ingestion

6.3.1 Pre Ash Fall Planning and Mitigation

Steps should be taken to mitigate ash ingestion in regions where ash fall is possible. Mitigation steps can be applied to pre-existing generators or ideally, included in the planning stages of generator installation.

Generator air intakes should face away from the prevailing wind direction or have a barrier to reduce the ingestion of remobilised ash. Air intakes should not be located on the top of the generator housing to avoid ash depositing directly into intakes. Intakes should be located well off the ground (>0.5 m) to avoid ingestion of deposited ash or ash build-up around the intake. Air intakes should be fitted with deflection hood(s) as a preventative measure. If possible the generator should be elevated (>0.2 m) to prevent ash build up around the base of the casing.

6.3.2 Mitigation during Ash Fall

Where possible, the generator intakes should be fitted with material filtration. Testing found that filters with an open weave or open cell structure preformed best as these material can reduce ash ingestion while maintaining airflow. When filtration is applied, the generator should be monitored to ensure the airflow is sufficient to prevent the generator overheating. This can be done by consulting the generator's manual to determine the necessary airflow and monitoring using a standard anemometer. Automated monitoring of generators with a digital connected anemometer which is routinely monitored may also be useful to pre-empt failure. Monitoring is essential in timing the replacement of ARM filters.

Key details of recommended actions (pre and during ash fall) for facilities managers is outlined in the poster section.

6.3.3 Poster

An ash impacts poster (**Figure 6.1**) was a key output of the research as is part of an ash impacts series produced by the Department of Geological Sciences to help communicate ash impacts to stakeholders in an easy digestible manner. The poster series was commissioned by

the Auckland Engineering Lifeline Group (www.aelg.org.nz). The poster drew on recommendations from (Barnard, 2010) to advise on the use of HVAC units. The poster was published prior to the completion of testing and is to be updated based on the results presented (**Figure 6.2**).

6.4 Summary

This study tested the effectiveness of temporary mitigation measures for the air intakes of large format generators. Testing was required, due to the unique characteristics of volcanic ash. The study has shown material filtration is effective at mitigating the risk. In addition, a deflection hood is shown to be effective and suitable for installation as a preventative measure. The final aspect of the risk management framework is the treatment of the risk. In the context of this study, risk treatment has been undertaken by providing accessible outputs such as the poster which can be consulted easily during an ash fall crisis.

ADVICE FOR FACILITIES MANAGERS: GENSETS AND HVAC

VOLCANIC ASH IS: HARD, HIGHLY ABRASIVE, MILDLY CORROSIVE AND CONDUCTIVE WHEN WET.

AIRBORNE ASH CONCENTRATIONS CAN BE AS HIGH AS 9 G M^{-3}, SEVERAL TIMES GREATER THAN SAND AND DUST STORMS

IMPACTS ON GENERATOR SETS AND HVAC SYSTEMS

A volcanic ashfall can cause electricity outages (see companion poster on transmission/distribution). Therefore use of emergency power generation equipment on electrical transmission (Generator Sets or GenSets) may be necessary. Air intakes on GenSets are vulnerable to airborne ash and need to be protected. Air intakes on heating, ventilation and air-conditioning (HVAC) systems are similarly vulnerable.

COMMON IMPACTS:

- **Ash Ingress through air intake and condenser units:** ash ingress may cause ash accumulation in the radiator and air filters, reducing air flow and and HVAC condenser system performance. Reduced airflows may cause stalling and overheating:
  - » High humidity significantly increases ash adhesion and thus blockage
  - » Filters are generally not designed to cope with the suspended particle volumes seen in volcanic ash falls
  - » HVAC systems with low fan speeds block more readily
  - » Horizontal air-intakes and condensers ingest significantly less ash than vertical systems
- **Ash may cause accelerated corrosion and wear,** usually over timescales of weeks to months:
  - » Exposed, sensitive components outside the GenSet or HVAC casing, such as fuel valves or electrical switches, can be vulnerable to wear, contamination and corrosion
  - » Ingestion of ash into the engine is rarer, but can wear moving parts and block fuel filters, lines and valves

See companion posters on Advice for Electrical Transmission and Distribution Managers and Advice for Power Station Managers for additional information on effects of ash on power supply systems.

Adaptations to protect GenSet equipment in Bariloche, Argentina, from repeated airborne ash exposure following 2011-2012 eruption of Cordon Caulle volcano, Chile.
Top: sealed fuel valve. Bottom: hood to protect air intake.

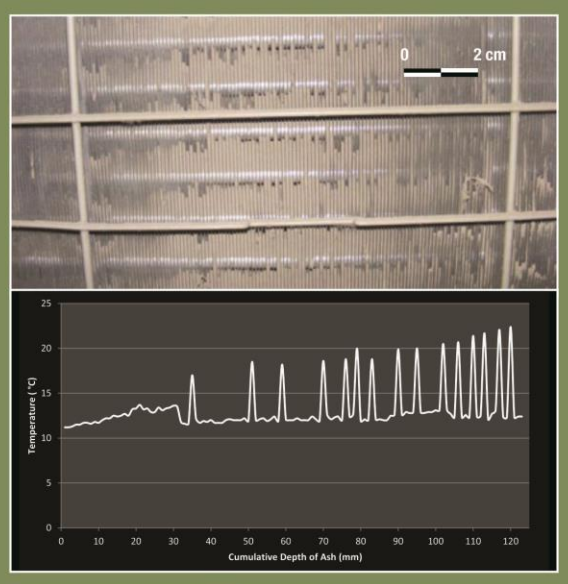

Top: Ash accumulation on a HVAC condenser after 11 hours of simulated high-humidity ashfall (1.5 mm/hr; max. 2 g m^{-3}). Ash with a mean grain size of ~100 µm was deposited in the fins (1.5 mm separation). Bottom: Increasing accumulation of moist ash on air conditioner condenser fins leads to increased frequency of shutdowns as compressor overheats.

RECOMMENDED ACTIONS

WHERE TO FIND WARNING INFORMATION

See www.geonet.org.nz for ashfall forecasts in the event of an explosive eruption.

HOW TO PREPARE

At-risk facilities should develop operational plans for managing ash fall events, including a priority schedule and standardised procedures for inspecting/maintaining/cleaning:

Physical mitigation options:

- Install hoods over air intake to reduce direct ash ingestion (see bottom left figure)
- Add temporary filtration to external air intakes, monitor and replace as needed
- Seal or cover sensitive equipment, such as external fuel valves and switches

Cleaning Guidance:

- Vacuum or gently (30 psi or less) blow away excess ash from air intakes or condensers, then wipe down with a cloth. Air filters should be removed before cleaning
- Wet methods for ash cleanup are not recommended, as they may promote clogging of radiator fins, or cause short-circuits

HOW TO RESPOND

- Initiate priority schedule for inspection, cleaning and preventative maintenance
- Regularly check and service air and fuel intakes and filters (stock spares)
  - » Frequency of air filter replacement could be as high as every 30 minutes during high rates of ash fall. In this case, step up preventative maintenance
- Maintain a clean site, especially in front of air intakes, to reduce remobilisation of ash
  - » Use dry methods where possible. See companion "Advice for Urban Clean-Up Operations" poster
  - » Store collected ash in bags to prevent remobilisation
  - » Ensure stockpiled ash is well clear of equipment and air intakes
- Beware wet ash maybe conductive. Isolate and earth energised apparatus as appropriate
- Advise customers/users not to clean electrical equipment and to limit the use of water in clean up, and to be careful when cleaning near electrical equipment.

MORE INFORMATION

THE FOLLOWING RESOURCES PROVIDE FURTHER INFORMATION ON VOLCANIC HAZARDS:

http://www.geonet.org.nz
http://www.gns.cri.nz
http://volcanoes.usgs.gov/ash/index.html
http://www.ivhhn.org

DRAFTED BY DANIEL HILL, TOM WILSON, CAROL STEWART, SAM HAMPTON AND JOHNNY WARDMAN.

20 September 2013

Figure 6.1: Advice for facilities managers: Gensets and HVAC poster produced part way through this study. Information on the performance of HVAC units used in the poster are based on the work of (Barnard (2010)

ADVICE FOR FACILITIES MANAGERS: GENSETS AND HVAC

VOLCANIC ASH IS: HARD, HIGHLY ABRASIVE, MILDLY CORROSIVE AND CONDUCTIVE WHEN WET.
AIRBORNE ASH CONCENTRATIONS CAN BE AS HIGH AS 9 g m^{-3}, SEVERAL TIMES GREATER THAN SAND AND DUST STORMS

VOLCANIC ASHFALL

IMPACTS ON GENERATOR SETS AND HVAC SYSTEMS

A volcanic ashfall can cause electricity outages (see companion poster on transmission/distribution). Therefore use of emergency power generation equipment on electrical transmission (Generator Sets or GenSets) may be necessary. Air intakes on GenSets are vulnerable to airborne ash and need to be protected. Air intakes on heating, ventilation and air-conditioning (HVAC) systems are similarly vulnerable.

COMMON IMPACTS:

- **Ash Ingress through air intake and condenser units:** ash ingress may cause ash accumulation in the radiator and air filters, reducing air flow and and HVAC condenser system performance. Reduced airflows may cause stalling and overheating:
  - » High humidity significantly increases ash adhesion and thus blockage
  - » Filters are generally not designed to cope with the suspended particle volumes seen in volcanic ash falls
  - » HVAC systems with low fan speeds block more readily
  - » Horizontal air-intakes and condensers ingest significantly less ash than vertical systems
- **Ash may cause accelerated corrosion and wear**, usually over timescales of weeks to months:
  - » Exposed, sensitive components outside the GenSet or HVAC casing, such as fuel valves or electrical switches, can be vulnerable to wear, contamination and corrosion
  - » Ingestion of ash into the engine is rarer, but can wear moving parts and block fuel filters, lines and valves

See companion posters on "Advice for Electrical Transmission and Distribution Managers" and "Advice for Power Station Managers" for additional information on effects of ash on power supply systems.

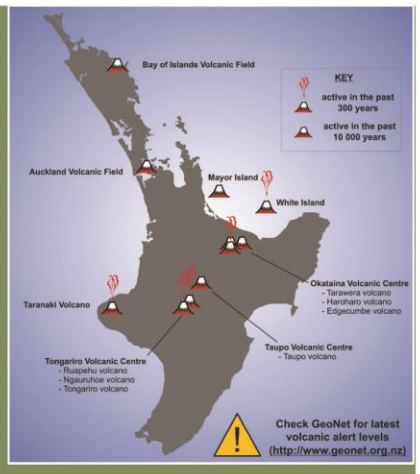

Adaptations to protect GenSet equipment in Bariloche, Argentina, from repeated airborne ash exposure following 2011-2012 eruption of Cordon Caulle volcano, Chile.
Top: sealed fuel valve. Bottom: hood to protect air intake.

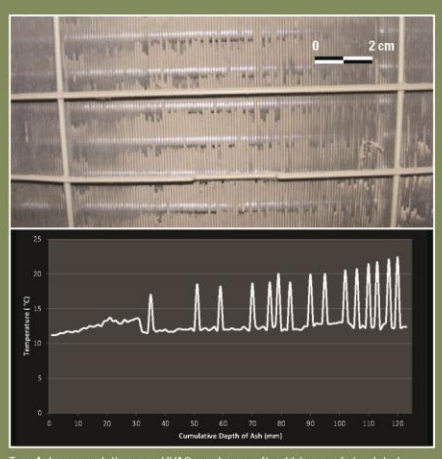

Top: Ash accumulation on a HVAC condenser after 11 hours of simulated high-humidity ashfall (1.5 mm/hr; max. 2 g m^{-3}). Ash with a mean grain size of ~100 µm was deposited in the fins (1.5 mm separation). Bottom: Increasing accumulation of moist ash on air conditioner condenser fins leads to increased frequency of shutdowns as compressor overheats.

Change existing graph for particles concentration graph.

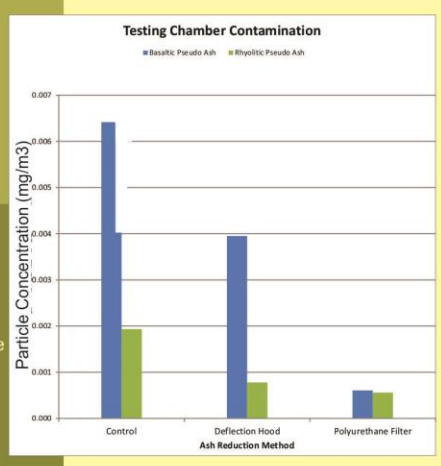

RECOMMENDED ACTIONS

WHERE TO FIND WARNING INFORMATION

See www.geonet.org.nz for ashfall forecasts in the event of an explosive eruption.

HOW TO PREPARE

At-risk facilities should develop operational plans for managing ash fall events, including a priority schedule and standardised procedures for inspecting/maintaining/cleaning:

Physical mitigation options:

- Install hoods over air intake to reduce direct ash ingestion (see bottom left figure)
- Add temporary filtration to external air intakes, monitor and replace as needed
- Seal or cover sensitive equipment, such as external fuel valves and switches

Cleaning Guidance:

- Vacuum or gently (30 psi or less) blow away excess ash from air intakes or condensers, then wipe down with a cloth. Air filters should be removed before cleaning
- Wet methods for ash cleanup are not recommended, as they may promote clogging of radiator fins, or cause short-circuits

HOW TO RESPOND

- Initiate priority schedule for inspection, cleaning and preventative maintenance
- Regularly check and service air and fuel intakes and filters (stock spares)
  - » Frequency of air filter replacement could be as high as every 30 minutes during high rates of ash fall. In this case, step up preventative maintenance
- Maintain a clean site, especially in front of air intakes, to reduce remobilisation of ash
  - » Use dry methods where possible. See companion "Advice for Urban Clean-Up Operations" poster
  - » Store collected ash in bags to prevent remobilisation
  - » Ensure stockpiled ash is well clear of equipment and air intakes
- Beware wet ash maybe conductive. Isolate and earth energised apparatus as appropriate
- Advise customers/users not to clean electrical equipment and to limit the use of water in clean up, and to be careful when cleaning near electrical equipment.

MORE INFORMATION

THE FOLLOWING RESOURCES PROVIDE FURTHER INFORMATION ON VOLCANIC HAZARDS:

http://www.geonet.org.nz
http://www.gns.cri.nz
http://volcanoes.usgs.gov/ash/index.html
http://www.ivhhn.org

DRAFTED BY DANIEL HILL, TOM WILSON, CAROL STEWART, SAM HAMPTON AND JOHNNY WARDMAN.

20 September 2013

UC University of Canterbury Te Whare Wānanga o Waitaha Christchurch New Zealand
Auckland Engineering Life Lines
Massey University
GNS Science Te Pū Ao

- *Stockpile genuine and recommended filters*
- *Cover exposed inlets while cleaning the filters*
- *Move Cleaning section into "how to respond" section*
- *Face air intakes away from the prevailing wind*
- *Install barrier in front of generator to reduce wind blown ash*
- *Elevate generators to prevent accumulation of ash around casing*
- *Add coarse filters over engine air intakes.*
- *Install recommended temporary filtration over external air intakes*
- *Monitor air flow*

Figure 6.2: Advice for facilities managers: Gensets and HVAC poster produced part way through this study with modifications noted on the figure to identify changes to be made upon conclusion of testing. Information on the performance of HVAC units used in the poster are based on the work of (Barnard (2010).

References

ALIDIBIROV, M. & DINGWELL, D. 2000. Three fragmentation mechanisms for highly viscous magma under rapid decompression. *Journal of Volcanology and Geothermal Research,* 100**,** 413-421.

ALLEN, S. R. & SMITH, I. E. M. 1994. Eruption styles and volcanic hazard in the Auckland Volcanic Field, New Zealand. 20**,** 5-14.

AUKER, M., SPARKS, R., SIEBERT, L., CROSWELLER, H. & EWERT, J. 2013. A statistical analysis of the global historical volcanic fatalities record: Journal of Applied Volcanology, v. 2.

BARNARD, S. T. 2010. The vulnerability of New Zealand lifelines infrastructure to ashfall.

BEAVERS, J. E. 2003. *Advancing Mitigation Technologies and Disaster Response for Lifeline Systems: Proceedings of the Sixth US Conference and Workshop on Lifeline Earthquake Engineering, August 10-13, 2003, Long Beach, California*, ASCE Publications.

BLONG, R. 1996. Volcanic hazards risk assessment. *Monitoring and mitigation of volcano hazards.* Springer.

BLONG, R. 2000. Volcanic Hazards and Risk Management. *In:* SIGURDSSON, H., HOUGHTON, B. F., MCNUTT, S. R., RYMER, H. & STIX, J. (eds.) *Encyclopedia of Volcanoes.* San Diego: Academic Press.

BONADONNA, C., ERNST, G. & SPARKS, R. 1998. Thickness variations and volume estimates of tephra fall deposits: the importance of particle Reynolds number. *Journal of Volcanology and Geothermal Research,* 81**,** 173-187.

BONADONNA, C., GENCO, R., GOUHIER, M., PISTOLESI, M., CIONI, R., ALFANO, F., HOSKULDSSON, A. & RIPEPE, M. 2011. Tephra sedimentation during the 2010 Eyjafjallajökull eruption (Iceland) from deposit, radar, and satellite observations. *Journal of Geophysical Research: Solid Earth (1978–2012),* 116.

BROOM, S. 2010. *Characterisation of "pseudo-ash" for quantitative testing of critical infrastructure components with a focus on roofing fragility.* Unpublished BSc (Hons) thesis, University of Canterbury, Christchurch, New Zealand.

BROWNE, P. & LAWLESS, J. 2001. Characteristics of hydrothermal eruptions, with examples from New Zealand and elsewhere. *Earth-Science Reviews,* 52**,** 299-331.

CAREY, S. & BURSIK, M. 2000. Volcanic Plumes. *In:* SIGURDSSON, H., HOUGHTON, B. F., MCNUTT, S. R., RYMER, H. & STIX, J. (eds.) *Encyclopedia of Volcanoes.* San Diego: Academic Press.

CASHDOLLAR, K. L. 1996. Coal dust explosibility. *Journal of Loss Prevention in the Process Industries,* 9**,** 65-76.

CASHMAN, K. V., STURTEVANT, B., PAPALE, P. & NAVON, O. 2000. Magmatic Fragmentation. *In:* SIGURDSSON, H., HOUGHTON, B. F., MCNUTT, S. R., RYMER, H. & STIX, J. (eds.) *Encyclopedia of Volcanoes.* San Diego: Elsevier Inc.

CATERPILLAR ELECTRIC POWER 2014. Diesel Generator Sets (9 kW to 17,460 kW).

COATES HIRE 2014. CONTAINER STYLE GENERATORS - 650 TO 1400KVA.

COLE, J., GRAHAM, I., HACKETT, W. & HOUGHTON, B. 1986. Volcanology and petrology of the Quaternary composite volcanoes of Tongariro volcanic centre, Taupo volcanic zone. *Royal society of New Zealand bulletin,* 23**,** 224-250.

COLE, J., SPINKS, K., DEERING, C., NAIRN, I. & LEONARD, G. 2010. Volcanic and structural evolution of the Okataina Volcanic Centre; dominantly silicic volcanism associated with the Taupo Rift, New Zealand. *Journal of volcanology and geothermal research,* 190**,** 123-135.

CROSWELLER, H. S., ARORA, B., BROWN, S. K., COTTRELL, E., DELIGNE, N. I., GUERRERO, N. O., HOBBS, L., KIYOSUGI, K., LOUGHLIN, S. C. & LOWNDES, J. 2012. Global database on large magnitude explosive volcanic eruptions (LaMEVE). *Journal of Applied Volcanology,* 1**,** 1-13.

CUMMINS. 2013. *Diesel generator set QST30 series engine* [Online]. Available: http://www.cumminspower.com/www/Commercial/Diesel/d-3332.pdf [Accessed 04/06/2013 2013].

EMEIS, S., FORKEL, R., JUNKERMANN, W., SCHÄFER, K., FLENTJE, H., GILGE, S., FRICKE, W., WIEGNER, M., FREUDENTHALER, V. & GROß, S. 2011. Measurement and simulation of the 16/17 April 2010 Eyjafjallajökull volcanic ash layer dispersion in the northern Alpine region. *Atmos. Chem. Phys,* 11**,** 2689-2701.

FINK, J. H. & ANDERSON, S. W. 2000. Lava Domes and Coulees. *In:* SIGURDSSON, H., HOUGHTON, B. F., MCNUTT, S. R., RYMER, H. & STIX, J. (eds.) *Encyclopedia of Volcanoes.* San Diego: Academic Press.

FOWLER, W. & LOPUSHINSKY, W. 1986. Wind-blown volcanic ash in forest and agricultural locations as related to meteorological conditions. *Atmospheric Environment (1967),* 20**,** 421-425.

HANSELL, A., HORWELL, C. & OPPENHEIMER, C. 2006. The health hazards of volcanoes and geothermal areas. *Occupational and environmental medicine,* 63**,** 149-156.

HEIKEN, G. 1972. Morphology and petrography of volcanic ashes. *Geological Society of America Bulletin,* 83**,** 1961-1988.

HEIKEN, G. Volcanic ash: what it is and how it forms. Volcanic Ash and Aviation Safety—Proceedings of the First International Symposium on Volcanic Ash and Aviation Safety, 1994. 39-45.

HEIKEN, G. & WOHLETZ, K. 1985. *Volcanic ash*, University Presses of California, Chicago, Harvard & MIT.

HOUGHTON, B., WILSON, C., MCWILLIAMS, M., LANPHERE, M., WEAVER, S., BRIGGS, R. & PRINGLE, M. 1995. Chronology and dynamics of a large silicic magmatic system: central Taupo Volcanic Zone, New Zealand. *Geology,* 23**,** 13-16.

HOUGHTON, B. F., WILSON, C. J. N., WEAVER, S. D., LANPHERE, M. A. & BARCLAY, J. 2010. *Mayor Island Geology*. [Online]. Available: http://www.gns.cri.nz/Home/Learning/Science-Topics/Volcanoes/New-Zealand-Volcanoes/Volcano-Geology-and-Hazards/Mayor-Island-Geology [Accessed 7 February 2014.

HURST, T. & SMITH, W. 2004. A Monte Carlo methodology for modelling ashfall hazards. *Journal of volcanology and geothermal research,* 138**,** 393-403.

HURST, T. & SMITH, W. 2010. Volcanic ashfall in New Zealand–probabilistic hazard modelling for multiple sources. *New Zealand Journal of Geology and Geophysics,* 53**,** 1-14.

INDEC 2012. Instituto Nacional de Estadística y Censos de la Republica Argentina (2010).

ISO, I. 2009. 31000: 2009 Risk management–Principles and Guidelines. *International Organization for Standardization, Geneva, Switzerland*.

JENKINS, S., SPENCE, R., FONSECA, J., SOLIDUM, R. & WILSON, T. 2014. Volcanic risk assessment: Quantifying physical vulnerability in the built environment. *Journal of Volcanology and Geothermal Research,* 276**,** 105-120.

JOHNSTON, D. M. 1997. *Physical and social impacts of past and future volcanic eruptions in New Zealand: a thesis presented in partial fulfilment of the requirements for the degree of Doctor of Philosophy in Earth Science, Massey University, Palmerston North, New Zealand.*

KIENLE, J. & SWANSON, S. E. 1980. Volcanic Hazards from Future Eruptions of Augustine Volcano, Alaska. *Geo-physica! Institute, University of Alaska, Fairbanks, AK*.

KIENLE, J. & SWANSON, S. E. 1985. *Volcanic hazards from future eruptions of Augustine volcano, Alaska*, Geophysical Institute, University of Alaska.

KLUG, C. & CASHMAN, K. V. 1996. Permeability development in vesiculating magmas: implications for fragmentation. *Bulletin of Volcanology,* 58**,** 87-100.

MAGILL, C. & BLONG, R. 2005. Volcanic risk ranking for Auckland, New Zealand. I: Methodology and hazard investigation. *Bulletin of Volcanology,* 67**,** 331-339.

MAGILL, C., HURST, A., HUNTER, L. & BLONG, R. 2006. Probabilistic tephra fall simulation for the Auckland Region, New Zealand. *Journal of volcanology and geothermal research,* 153**,** 370-386.

MASTIN, L. G. 1995. Thermodynamics of gas and steam-blast eruptions. *Bulletin of Volcanology,* 57**,** 85-98.

MOEBIS, A., CRONIN, S. J., NEALL, V. E. & SMITH, I. E. 2011. Unravelling a complex volcanic history from fine-grained, intricate Holocene ash sequences at the Tongariro Volcanic Centre, New Zealand. *Quaternary International,* 246**,** 352-363.

MOLLOY, C., SHANE, P. & AUGUSTINUS, P. 2009. Eruption recurrence rates in a basaltic volcanic field based on tephra layers in maar sediments: Implications for hazards in the Auckland volcanic field. *Geological Society of America Bulletin,* 121**,** 1666-1677.

MORRISSEY, M., ZIMANOWSKI, B., WOHLETZ, K. & BUETTNER, R. 2000. Phreatomagmatic Fragmentation. *In:* SIGURDSSON, H., HOUGHTON, B. F., MCNUTT, S. R., RYMER, H. & STIX, J. (eds.) *Encyclopedia of Volcanoes.* San Diego: Elsevier Inc.

NAIR, N.-K. C. & ZHANG, L. 2009. SmartGrid: Future networks for New Zealand power systems incorporating distributed generation. *Energy Policy,* 37**,** 3418-3427.

NELLIS, C. & HENDRIX, K. 1980. Progress report on the investigation of volcanic ash fallout from Mount St Helens. Bonneville Power Administration. Laboratory Report ERJ-80-47.

NEWHALL, C. G. & SELF, S. 1982. The Volcanic Explosivity Index (VEI) an estimate of explosive magnitude for historical volcanism. *Journal of Geophysical Research: Oceans (1978–2012),* 87**,** 1231-1238.

NEWNHAM, R. M., LOWE, D. J., GREEN, J. D., TURNER, G. M., HARPER, M. A., MCGLONE, M. S., STOUT, S. L., HORIE, S. & FROGGATT, P. C. 2004. A discontinuous ca. 80 ka record of Late Quaternary environmental change from Lake Omapere, Northland, New Zealand. *Palaeogeography, Palaeoclimatology, Palaeoecology,* 207**,** 165-198.

OEHMEN, J., BEN-DAYA, M., SEERING, W. & AL-SALAMAH, M. Risk Management in Product Design: Current State, Conceptual Model and Future Research. ASME 2010 International Design Engineering Technical Conferences and Computers and Information in Engineering Conference, 2010. American Society of Mechanical Engineers, 1033-1041.

PARFITT, L. & WILSON, L. 2009. *Fundamentals of physical volcanology*, John Wiley & Sons.

PYLE, D. M. 1989. The thickness, volume and grainsize of tephra fall deposits. *Bulletin of Volcanology,* 51**,** 1-15.

RHOADES, D. A., DOWRICK, D. J. & WILSON, C. J. N. 2002. Volcanic Hazard in New Zealand: Scaling and Attenuation Relations for Tephra fall deposits from Taupo Volcano. *Natural Hazards,* 26**,** 147-174.

ROSE, W. & DURANT, A. 2009. Fine ash content of explosive eruptions. *Journal of Volcanology and Geothermal Research,* 186**,** 32-39.

ROSE, W. I., BLUTH, G. J., SCHNEIDER, D. J., ERNST, G. G., RILEY, C. M., HENDERSON, L. J. & MCGIMSEY, R. G. 2001. Observations of volcanic clouds in their first few days of atmospheric residence: the 1992 eruptions of Crater Peak, Mount Spurr Volcano, Alaska. *The Journal of Geology,* 109**,** 677-694.

SANCHEZ, A. 1999. Water-air baffle filter. Google Patents.

SARNA-WOJCICKI, A. M., SHIPLEY, S., WAITT JR, R. B., DZURISIN, D. & WOOD, S. H. 1981. Areal distribution, thickness, mass, volume, and grain size of air-fall ash from the six major eruptions of 1980.

SCASSO, R. A., CORBELLA, H. & TIBERI, P. 1994. Sedimentological analysis of the tephra from the 12–15 August 1991 eruption of Hudson volcano. *Bulletin of Volcanology,* 56**,** 121-132.

SCHAUMKEL, L. 2012. Teachers and students from Tamatea Intermediate School in Napier staying witnessed the eruption while walking part of the Tongariro Crossing. Stuff.co.nz: FairFax New Zealand.

SCHUMACHER, R. & SCHMINCKE, H.-U. 1995. Models for the origin of accretionary lapilli. *Bulletin of Volcanology,* 56**,** 626-639.

SCOTT, W. E. & MCGIMSEY, R. G. 1994. Character, mass, distribution, and origin of tephra-fall deposits of the 1989–1990 eruption of Redoubt Volcano, south-central Alaska. *Journal of Volcanology and Geothermal Research,* 62**,** 251-272.

SIGURDSSON, H., HOUGHTON, B., RYMER, H., STIX, J. & MCNUTT, S. 1999. *Encyclopedia of volcanoes*, Access Online via Elsevier.

SPARKS, R., BRAZIER, S., HUANG, T. & MUERDTER, D. 1983. Sedimentology of the Minoan deep-sea tephra layer in the Aegean and eastern Mediterranean. *Marine geology,* 54**,** 131-167.

TILLING, R. 2003. Volcano Monitoring and Eruption Warnings. *In:* ZSCHAU, J. & KÜPPERS, A. (eds.) *Early Warning Systems for Natural Disaster Reduction.* Springer Berlin Heidelberg.

TRANSPOWER. 2013. *Annual Planning Report* [Online]. Available: https://www.transpower.co.nz/resources/annual-planning-report-2013. [Accessed 12/04/2014.

TURNER, M. B., BEBBINGTON, M. S., CRONIN, S. J. & STEWART, R. B. 2009. Merging eruption datasets: building an integrated Holocene eruptive record for Mt Taranaki, New Zealand. *Bulletin of volcanology,* 71**,** 903-918.

VALENTINE, G. A. & FISHER, R. V. 2000. Pyroclastic Surges and Blasts. *In:* SIGURDSSON, H., HOUGHTON, B. F., MCNUTT, S. R., RYMER, H. & STIX, J. (eds.) *Encyclopedia of Volcanoes.* San Diego: Academic Press.

WALKER, G. 1981. The Waimihia and Hatepe plinian deposits from the rhyolitic Taupo Volcanic Centre. *New Zealand journal of geology and geophysics,* 24**,** 305-324.

WARDMAN, J., WILSON, T., BODGER, P., COLE, J. & JOHNSTON, D. 2012a. Investigating the electrical conductivity of volcanic ash and its effect on HV power systems. *Physics and Chemistry of the Earth, Parts A/B/C,* 45**,** 128-145.

WARDMAN, J., WILSON, T., BODGER, P., COLE, J. & STEWART, C. 2012b. Potential impacts from tephra fall to electric power systems: a review and mitigation strategies. *Bulletin of volcanology,* 74**,** 2221-2241.

WARDMAN, J. B. 2013. *Vulnerability of Electric Power Systems to Volcanic Ashfall Hazards: A Thesis Submitted in Partial Fulfilment of the Requirements for the Degree of Doctor of Philosophy in Hazard and Disaster Management at the Natural Hazards Research Centre (Department of Geological Sciences), University of Canterbury.* University of Canterbury.

WILCOX, R. E. & COATS, R. R. 1959. *Some effects of recent volcanic ash falls with especial reference to Alaska,* US Government Printing Office.

WILSON, G., WILSON, T., COLE, J. & OZE, C. 2012a. Vulnerability of laptop computers to volcanic ash and gas. *Natural hazards,* 63**,** 711-736.

WILSON, J. N. C. & HOUGHTON, B. F. 2000. Pyroclast Transport and Deposition. *In:* SIGURDSSON, H., HOUGHTON, B. F., MCNUTT, S. R., RYMER, H. & STIX, J. (eds.) *Encyclopedia of Volcanoes.* San Diego: Academic Press.

WILSON, L. & HUANG, T. C. 1979. The influence of shape on the atmospheric settling velocity of volcanic ash particles. *Earth and Planetary Science Letters,* 44**,** 311-324.

WILSON, T., COLE, J., STEWART, C., CRONIN, S. & JOHNSTON, D. 2011. Ash storms: impacts of wind-remobilised volcanic ash on rural communities and agriculture following the 1991 Hudson eruption, southern Patagonia, Chile. *Bulletin of Volcanology,* 73**,** 223-239.

WILSON, T. & STEWART, C. 2013. Volcanic Ash. *In:* BOBROWSKY, P. (ed.) *Encyclopedia of Natural Hazards.* Springer Netherlands.

WILSON, T. M., STEWART, C., BICKERTON, H., BAXTER, P., OUTES, V., VILLAROSA, G. & ROVERE, E. 2013. *Impacts of the June 2011 Puyehue-Cordón Caulle Volcanic Complex Eruption on Urban Infrastructure, Agriculture and Public Health,* GNS Science.

WILSON, T. M., STEWART, C., SWORD-DANIELS, V., LEONARD, G. S., JOHNSTON, D. M., COLE, J. W., WARDMAN, J., WILSON, G. & BARNARD, S. T. 2012b. Volcanic ash impacts on critical infrastructure. *Physics and Chemistry of the Earth, Parts A/B/C,* 45**,** 5-23.

WITHAM, C. S., OPPENHEIMER, C. & HORWELL, C. J. 2005. Volcanic ash-leachates: a review and recommendations for sampling methods. *Journal of Volcanology and Geothermal Research,* 141**,** 299-326.

Appendix

A. Appendix A - Arduino Code

```
//////////////////////////////////////////////////////////////

//©2011 bildr

//Released under the MIT License - Please reuse change and share

//Using the easy stepper with your arduino

//use rotate and/or rotateDeg to controll stepper motor

//speed is any number from .01 -> 1 with 1 being fastest -

//Slower Speed == Stronger movement

//////////////////////////////////////////////////////////////

#define DIR_PIN 2

#define STEP_PIN 3

void setup() {

  pinMode(DIR_PIN, OUTPUT);

  pinMode(STEP_PIN, OUTPUT);

}

void loop(){

  //rotate a specific number of degrees

  rotateDeg(360, 1);     //  ← set speed here 0.1-1.0

  delay(1000);   //  ← set delay between rotations here in milliseconds

  rotateDeg(-360, .1);  //reverse
```

```
  delay(1000);
  //rotate a specific number of microsteps (8 microsteps per step)
  //a 200 step stepper would take 1600 micro steps for one full revolution
  rotate(1600, .5);
  delay(1000);


  rotate(-1600, .25); //reverse
  delay(1000);
}
void rotate(int steps, float speed){
  //rotate a specific number of microsteps (8 microsteps per step) - (negitive for reverse movement)
  //speed is any number from .01 -> 1 with 1 being fastest - Slower is stronger
  int dir = (steps > 0)? HIGH:LOW;
  steps = abs(steps);
  digitalWrite(DIR_PIN,dir);
  float usDelay = (1/speed) * 70;
  for(int i=0; i < steps; i++){
    digitalWrite(STEP_PIN, HIGH);
    delayMicroseconds(usDelay);
    digitalWrite(STEP_PIN, LOW);
    delayMicroseconds(usDelay);
  }
```

```
}
void rotateDeg(float deg, float speed){
  //rotate a specific number of degrees (negitive for reverse movement)
  //speed is any number from .01 -> 1 with 1 being fastest - Slower is stronger
  int dir = (deg > 0)? HIGH:LOW;
  digitalWrite(DIR_PIN,dir);
  int steps = abs(deg)*(1/0.225);
  float usDelay = (1/speed) * 70;
  for(int i=0; i < steps; i++){
    digitalWrite(STEP_PIN, HIGH);
    delayMicroseconds(usDelay);

    digitalWrite(STEP_PIN, LOW);
    delayMicroseconds(usDelay);
  }
}
```

B. Appendix B - Laser Particle Analyser Results

B.1 Pseudo Ash A

Table B1: Laser particle analyser results for Ash A. Analyser produced results for particles >0.011µm. There results have been truncated to only display gain size where corresponding particles were detected. Additional tests using Ash A are in a further table

Grain Size		Testing Chamber					Ash Reduction Measure			
	Bulk	Control	ARM1	ARM2	ARM3	ARM4	ARM 2	ARM 4	ARM 5	ARM 6
0.15	0.019	0.000	0.000	0.000	0.000	0.000	0.000	0.000	0.000	0.000
0.172	0.026	0.000	0.000	0.000	0.000	0.000	0.000	0.000	0.000	0.000
0.197	0.034	0.000	0.000	0.000	0.000	0.000	0.000	0.000	0.000	0.000
0.226	0.041	0.000	0.000	0.000	0.000	0.000	0.000	0.000	0.000	0.000
0.259	0.047	0.000	0.000	0.000	0.000	0.000	0.000	0.000	0.000	0.000
0.296	0.092	0.000	0.000	0.000	0.000	0.000	0.068	0.000	0.000	0.000
0.339	0.124	0.000	0.000	0.000	0.000	0.000	0.193	0.132	0.000	0.000
0.389	0.139	0.000	0.000	0.000	0.000	0.000	0.407	0.305	0.119	0.000
0.445	0.187	0.140	0.000	0.000	0.000	0.000	0.698	0.580	0.253	0.202
0.51	0.205	0.237	0.000	0.000	0.127	0.000	0.907	0.843	0.412	0.328
0.584	0.184	0.304	0.000	0.000	0.182	0.000	0.821	0.868	0.488	0.394
0.669	0.155	0.292	0.000	0.000	0.207	0.000	0.524	0.641	0.428	0.355
0.766	0.098	0.226	0.000	0.000	0.194	0.000	0.261	0.376	0.302	0.257
0.877	0.040	0.156	0.000	0.106	0.161	0.000	0.089	0.205	0.196	0.170
1.005	0.000	0.109	0.111	0.119	0.131	0.000	0.000	0.127	0.135	0.116
1.151	0.019	0.106	0.122	0.133	0.125	0.108	0.000	0.127	0.135	0.106
1.318	0.126	0.127	0.134	0.145	0.139	0.119	0.000	0.171	0.169	0.120
1.51	0.172	0.164	0.145	0.160	0.162	0.129	0.070	0.244	0.223	0.144
1.729	0.219	0.196	0.153	0.171	0.180	0.137	0.122	0.316	0.271	0.161
1.981	0.278	0.237	0.161	0.182	0.202	0.144	0.158	0.416	0.332	0.183
2.269	0.353	0.295	0.168	0.191	0.231	0.148	0.218	0.563	0.416	0.215
2.599	0.443	0.372	0.175	0.201	0.264	0.153	0.308	0.756	0.517	0.254
2.976	0.543	0.458	0.182	0.210	0.297	0.156	0.434	0.986	0.626	0.297
3.409	0.647	0.548	0.189	0.218	0.325	0.158	0.599	1.232	0.733	0.340
3.905	0.751	0.634	0.196	0.226	0.346	0.160	0.810	1.477	0.832	0.384
4.472	0.858	0.713	0.203	0.234	0.361	0.161	1.080	1.716	0.927	0.430
5.122	0.971	0.789	0.211	0.242	0.373	0.162	1.435	1.966	1.030	0.485
5.867	1.096	0.868	0.220	0.253	0.388	0.164	1.913	2.251	1.161	0.559
6.72	1.242	0.962	0.232	0.268	0.412	0.167	2.567	2.600	1.338	0.663
7.697	1.408	1.077	0.248	0.289	0.449	0.174	3.438	3.030	1.580	0.811
8.816	1.591	1.217	0.271	0.317	0.504	0.184	4.526	3.538	1.899	1.018
10.097	1.755	1.377	0.294	0.348	0.576	0.196	5.800	4.095	2.293	1.288
11.565	1.839	1.548	0.303	0.363	0.662	0.198	7.257	4.675	2.767	1.640
13.246	1.883	1.741	0.317	0.384	0.781	0.204	8.559	5.213	3.331	2.099

Grain Size	Bulk	Testing Chamber					Ash Reduction Measure			
		Control	ARM1	ARM2	ARM3	ARM4	ARM 2	ARM 4	ARM 5	ARM 6
15.172	1.879	1.937	0.339	0.415	0.939	0.218	9.204	5.557	3.905	2.639
17.377	1.838	2.110	0.372	0.462	1.135	0.244	8.803	5.578	4.366	3.181
19.904	1.776	2.246	0.426	0.533	1.369	0.288	7.436	5.258	4.602	3.612
22.797	1.706	2.340	0.503	0.639	1.639	0.355	5.640	4.706	4.574	3.843
26.111	1.637	2.404	0.610	0.787	1.942	0.453	4.009	4.087	4.337	3.861
29.907	1.581	2.451	0.760	0.993	2.273	0.594	2.846	3.548	4.015	3.754
34.255	1.553	2.506	0.983	1.285	2.635	0.797	2.163	3.178	3.738	3.653
39.234	1.572	2.609	1.373	1.744	3.084	1.122	1.873	3.044	3.636	3.725
44.938	1.646	2.819	2.106	2.485	3.718	1.692	1.874	3.168	3.797	4.116
51.471	1.724	3.080	3.267	3.484	4.492	2.567	1.967	3.368	4.056	4.682
58.953	1.792	3.343	4.843	4.610	5.297	3.747	2.065	3.533	4.315	5.306
67.523	1.848	3.544	6.567	5.638	5.945	5.074	2.074	3.538	4.446	5.800
77.34	1.831	3.630	8.200	6.330	6.378	6.369	1.995	3.365	4.400	6.096
88.583	1.746	3.518	8.657	6.173	6.253	6.929	1.745	2.913	4.061	5.919
101.46	1.706	3.199	8.142	5.790	5.539	6.800	1.335	2.234	3.436	5.199
116.21	1.792	2.879	8.278	6.251	4.765	7.075	0.905	1.571	2.791	4.352
133.103	1.756	2.855	7.827	5.902	4.594	6.898	0.502	0.993	2.415	3.880
152.453	1.945	3.239	8.169	6.433	5.009	7.537	0.219	0.576	2.309	3.712
174.616	2.436	3.937	8.232	7.451	5.656	8.392	0.085	0.281	2.295	3.502
200	3.103	4.720	7.072	8.133	6.043	8.810	0.000	0.054	2.170	2.959
229.075	3.564	5.021	4.741	7.480	5.417	7.863	0.000	0.000	1.723	1.976
262.376	3.538	4.337	2.422	5.330	3.720	5.481	0.000	0.000	1.051	0.945
300.518	3.270	3.225	1.117	3.127	2.092	3.231	0.000	0.000	0.535	0.265
344.206	3.431	2.605	0.617	1.828	1.227	1.973	0.000	0.000	0.111	0.000
394.244	4.410	2.665	0.343	1.130	0.682	1.335	0.000	0.000	0.000	0.000
451.556	5.400	2.761	0.000	0.576	0.379	0.729	0.000	0.000	0.000	0.000
517.2	5.254	2.257	0.000	0.233	0.000	0.405	0.000	0.000	0.000	0.000
592.387	5.056	1.558	0.000	0.000	0.000	0.000	0.000	0.000	0.000	0.000
678.504	4.585	0.923	0.000	0.000	0.000	0.000	0.000	0.000	0.000	0.000
777.141	3.465	0.388	0.000	0.000	0.000	0.000	0.000	0.000	0.000	0.000
890.116	2.393	0.000	0.000	0.000	0.000	0.000	0.000	0.000	0.000	0.000
1019.515	1.183	0.000	0.000	0.000	0.000	0.000	0.000	0.000	0.000	0.000
1167.725	0.000	0.000	0.000	0.000	0.000	0.000	0.000	0.000	0.000	0.000

B.2 Pseudo Ash B

Table B2: Laser particle analyser results for Ash B. Analyser produced results for particles >0.011µm. There results have been truncated to only display gain size where corresponding particles were detected.

Grain Size		Testing Chamber					Ash Reduction Measure			
	Bulk	Control	ARM1	ARM2	ARM3	ARM4	ARM 2	ARM 4	ARM 5	ARM 6
0.15	0.000	0.000	0.000	0.000	0.000	0.000	0.000	0.000	0.000	0.000
0.172	0.000	0.000	0.000	0.000	0.000	0.000	0.000	0.000	0.000	0.000
0.197	0.000	0.000	0.000	0.000	0.000	0.000	0.000	0.000	0.000	0.000
0.226	0.000	0.000	0.000	0.000	0.000	0.000	0.000	0.000	0.000	0.000
0.259	0.000	0.000	0.000	0.000	0.000	0.000	0.000	0.000	0.000	0.000
0.296	0.000	0.000	0.000	0.000	0.000	0.000	0.000	0.000	0.000	0.000
0.339	0.000	0.139	0.113	0.000	0.000	0.000	0.000	0.000	0.000	0.000
0.389	0.019	0.188	0.154	0.000	0.000	0.000	0.211	0.000	0.000	0.000
0.445	0.166	0.209	0.176	0.000	0.000	0.000	0.464	0.202	0.107	0.149
0.51	0.228	0.194	0.173	0.000	0.000	0.000	0.703	0.321	0.113	0.240
0.584	0.224	0.154	0.147	0.000	0.000	0.000	0.671	0.353	0.103	0.273
0.669	0.157	0.108	0.113	0.000	0.000	0.000	0.394	0.266	0.000	0.219
0.766	0.000	0.000	0.000	0.000	0.000	0.000	0.153	0.147	0.000	0.132
0.877	0.000	0.000	0.000	0.000	0.000	0.000	0.000	0.000	0.000	0.000
1.005	0.000	0.000	0.000	0.000	0.000	0.000	0.000	0.000	0.000	0.000
1.151	0.000	0.000	0.000	0.000	0.000	0.000	0.000	0.000	0.000	0.000
1.318	0.000	0.000	0.000	0.000	0.000	0.000	0.000	0.000	0.000	0.000
1.51	0.000	0.000	0.000	0.000	0.000	0.000	0.000	0.000	0.000	0.000
1.729	0.000	0.070	0.112	0.000	0.000	0.000	0.000	0.000	0.000	0.000
1.981	0.000	0.127	0.128	0.000	0.000	0.000	0.000	0.000	0.000	0.000
2.269	0.01	0.157	0.147	0.000	0.000	0.000	0.000	0.000	0.000	0.000

Grain Size		Testing Chamber					Ash Reduction Measure			
	Bulk	Control	ARM1	ARM2	ARM3	ARM4	ARM 2	ARM 4	ARM 5	ARM 6
	7									
2.599	0.110	0.191	0.166	0.000	0.000	0.000	0.000	0.069	0.104	0.000
2.976	0.180	0.228	0.185	0.000	0.000	0.000	0.000	0.143	0.112	0.105
3.409	0.237	0.266	0.201	0.000	0.000	0.000	0.146	0.196	0.119	0.135
3.905	0.299	0.303	0.217	0.000	0.000	0.000	0.235	0.260	0.127	0.166
4.472	0.360	0.339	0.232	0.000	0.000	0.000	0.359	0.335	0.135	0.199
5.122	0.416	0.377	0.250	0.000	0.000	0.000	0.521	0.423	0.147	0.234
5.867	0.470	0.420	0.271	0.000	0.000	0.000	0.728	0.532	0.163	0.275
6.72	0.522	0.472	0.300	0.000	0.000	0.000	0.988	0.668	0.187	0.326
7.697	0.574	0.535	0.338	0.000	0.000	0.000	1.314	0.837	0.221	0.393
8.816	0.625	0.612	0.388	0.000	0.000	0.000	1.715	1.046	0.269	0.484
10.097	0.675	0.689	0.443	0.000	0.000	0.000	2.196	1.291	0.328	0.604
11.565	0.715	0.734	0.479	0.000	0.000	0.000	2.768	1.576	0.383	0.752
13.246	0.749	0.778	0.523	0.000	0.000	0.000	3.396	1.880	0.457	0.954
15.172	0.775	0.825	0.576	0.000	0.000	0.000	4.012	2.147	0.558	1.217
17.377	0.794	0.882	0.643	0.000	0.000	0.000	4.531	2.319	0.692	1.540
19.904	0.816	0.963	0.737	0.000	0.107	0.000	4.887	2.366	0.873	1.919
22.797	0.848	1.073	0.861	0.000	0.124	0.106	5.056	2.317	1.100	2.331
26.111	0.896	1.209	1.016	0.000	0.145	0.128	5.070	2.248	1.361	2.740
29.907	0.965	1.355	1.202	0.112	0.178	0.159	5.012	2.271	1.643	3.111
34.255	1.057	1.509	1.442	0.150	0.235	0.210	5.002	2.516	1.965	3.433
39.234	1.193	1.721	1.828	0.228	0.370	0.317	5.221	3.192	2.440	3.792
44.938	1.410	2.080	2.528	0.407	0.721	0.571	5.806	4.509	3.259	4.376
51.471	1.70	2.572	3.568	0.766	1.491	1.107	6.472	6.269	4.389	5.169

Grain Size		Testing Chamber					Ash Reduction Measure			
	Bulk	Control	ARM1	ARM2	ARM3	ARM4	ARM 2	ARM 4	ARM 5	ARM 6
	1									
58.953	2.052	3.174	4.912	1.414	2.940	2.128	6.872	7.980	5.684	6.097
67.523	2.422	3.858	6.379	2.408	5.020	3.767	6.573	8.865	6.827	6.946
77.34	2.782	4.448	7.711	3.816	7.679	6.188	5.922	8.999	7.623	7.650
88.583	3.017	4.751	8.127	5.103	8.891	8.411	4.564	7.522	7.403	7.746
101.46	3.034	5.129	8.027	5.719	7.812	9.111	2.808	5.246	6.655	6.918
116.21	2.983	6.309	8.831	6.174	6.797	9.053	1.499	3.543	6.608	5.759
133.103	3.108	6.217	8.206	7.291	6.780	9.237	0.819	2.735	6.033	5.154
152.453	3.603	6.931	8.288	9.285	7.838	10.320	0.594	2.470	6.181	4.976
174.616	4.404	8.242	7.874	11.175	9.029	10.903	0.507	2.471	6.533	4.731
200	5.360	9.109	6.083	12.340	9.733	10.323	0.496	2.560	6.351	4.052
229.075	5.987	8.192	3.483	11.823	8.885	8.085	0.493	2.473	5.124	2.749
262.376	5.681	5.468	1.499	8.849	6.266	4.836	0.463	2.024	3.293	1.342
300.518	4.795	2.956	0.595	5.327	3.686	2.460	0.230	1.290	1.919	0.508
344.206	4.361	1.661	0.331	3.177	2.250	1.384	0.128	0.716	1.293	0.105
394.244	4.880	1.113	0.000	2.144	1.565	0.769	0.000	0.301	0.719	0.000
451.556	5.489	0.618	0.000	1.327	0.976	0.427	0.000	0.106	0.399	0.000
517.2	5.036	0.344	0.000	0.621	0.482	0.000	0.000	0.000	0.000	0.000
592.387	4.583	0.000	0.000	0.345	0.000	0.000	0.000	0.000	0.000	0.000
678.504	4.022	0.000	0.000	0.000	0.000	0.000	0.000	0.000	0.000	0.000
777.141	2.779	0.000	0.000	0.000	0.000	0.000	0.000	0.000	0.000	0.000
890.116	1.646	0.000	0.000	0.000	0.000	0.000	0.000	0.000	0.000	0.000
1019.515	0.778	0.000	0.000	0.000	0.000	0.000	0.000	0.000	0.000	0.000
1167.72	0.00	0.000	0.000	0.000	0.000	0.000	0.000	0.000	0.000	0.000

Grain Size		Testing Chamber					Ash Reduction Measure			
	Bulk	Control	ARM1	ARM2	ARM3	ARM4	ARM 2	ARM 4	ARM 5	ARM 6
5	0									

B.3 Pseudo Ash C

Table B3: Laser particle analyser results for Ash C. Analyser produced results for particles >0.011µm. There results have been truncated to only display gain size where corresponding particles were detected.

Grain Size	Bulk	Testing Chamber						Ash Reduction Measure			
		Control	ARM 1	ARM 2	ARM3	ARM 4	ARM 5	ARM 2	ARM 4	ARM5	ARM 6
0.15	0.000	0.000	0.000	0.000	0.000	0.000	0.000	0.000	0.000	0.000	0.000
0.172	0.000	0.000	0.000	0.000	0.000	0.000	0.000	0.000	0.000	0.000	0.000
0.197	0.000	0.000	0.000	0.000	0.000	0.000	0.000	0.000	0.000	0.000	0.000
0.226	0.000	0.000	0.000	0.000	0.000	0.000	0.000	0.000	0.000	0.000	0.000
0.259	0.000	0.000	0.000	0.000	0.000	0.000	0.000	0.000	0.000	0.000	0.000
0.296	0.000	0.000	0.000	0.000	0.000	0.000	0.000	0.000	0.000	0.000	0.000
0.339	0.000	0.000	0.000	0.000	0.000	0.000	0.000	0.000	0.000	0.000	0.000
0.389	0.000	0.000	0.000	0.000	0.000	0.000	0.000	0.159	0.000	0.000	0.000
0.445	0.000	0.000	0.000	0.000	0.000	0.000	0.000	0.227	0.000	0.000	0.000
0.51	0.000	0.000	0.000	0.000	0.000	0.000	0.000	0.214	0.000	0.000	0.000
0.584	0.000	0.000	0.000	0.000	0.000	0.000	0.000	0.130	0.000	0.000	0.000
0.669	0.000	0.000	0.000	0.000	0.000	0.000	0.000	0.000	0.000	0.000	0.000
0.766	0.000	0.000	0.000	0.000	0.000	0.000	0.000	0.000	0.000	0.000	0.000
0.877	0.000	0.000	0.000	0.000	0.000	0.000	0.000	0.000	0.000	0.000	0.000
1.005	0.000	0.000	0.000	0.000	0.000	0.000	0.000	0.000	0.000	0.000	0.000
1.151	0.000	0.000	0.000	0.000	0.000	0.000	0.000	0.000	0.000	0.000	0.000
1.318	0.000	0.000	0.000	0.000	0.000	0.000	0.000	0.000	0.000	0.000	0.000
1.51	0.000	0.000	0.000	0.000	0.000	0.000	0.000	0.000	0.000	0.000	0.000
1.729	0.000	0.000	0.000	0.000	0.000	0.000	0.000	0.000	0.000	0.000	0.000
1.981	0.000	0.000	0.000	0.039	0.000	0.000	0.000	0.000	0.000	0.120	0.000
2.269	0.000	0.000	0.00	0.14	0.000	0.06	0.11	0.11	0.00	0.146	0.10

Grain Size	Bulk	Testing Chamber						Ash Reduction Measure			
		Control	ARM 1	ARM 2	ARM3	ARM 4	ARM 5	ARM 2	ARM 4	ARM5	ARM 6
			0	7		9	3	7	0		9
2.599	0.148	0.175	0.000	0.182	0.000	0.107	0.138	0.208	0.000	0.168	0.159
2.976	0.233	0.201	0.000	0.206	0.000	0.106	0.158	0.347	0.151	0.180	0.205
3.409	0.307	0.215	0.000	0.218	0.000	0.035	0.171	0.536	0.357	0.186	0.242
3.905	0.360	0.219	0.000	0.222	0.000	0.000	0.179	0.778	0.690	0.182	0.267
4.472	0.396	0.217	0.000	0.220	0.000	0.000	0.184	1.076	1.154	0.177	0.285
5.122	0.427	0.211	0.000	0.217	0.000	0.000	0.187	1.452	1.768	0.172	0.298
5.867	0.462	0.206	0.000	0.215	0.000	0.000	0.191	1.935	2.551	0.168	0.310
6.72	0.506	0.202	0.000	0.215	0.000	0.000	0.193	2.555	3.487	0.167	0.321
7.697	0.556	0.200	0.000	0.217	0.000	0.000	0.195	3.326	4.468	0.171	0.328
8.816	0.606	0.197	0.000	0.221	0.000	0.000	0.194	4.206	5.281	0.177	0.331
10.097	0.651	0.194	0.000	0.222	0.000	0.000	0.188	5.140	5.792	0.185	0.324
11.565	0.682	0.188	0.000	0.212	0.000	0.000	0.170	6.122	5.990	0.190	0.293
13.246	0.687	0.179	0.000	0.202	0.000	0.000	0.150	6.818	5.435	0.198	0.257
15.172	0.661	0.171	0.034	0.195	0.000	0.107	0.132	6.954	4.338	0.204	0.223
17.377	0.621	0.110	0.125	0.192	0.000	0.126	0.118	6.464	3.197	0.208	0.198
19.904	0.591	0.000	0.169	0.203	0.000	0.158	0.108	5.565	2.365	0.214	0.185
22.797	0.596	0.000	0.241	0.228	0.125	0.212	0.104	4.589	1.911	0.226	0.189
26.111	0.648	0.174	0.356	0.279	0.160	0.298	0.108	3.793	1.778	0.257	0.215
29.907	0.758	0.213	0.534	0.370	0.210	0.432	0.124	3.297	1.903	0.329	0.281
34.255	0.929	0.296	0.807	0.531	0.288	0.649	0.164	3.134	2.240	0.499	0.422
39.234	1.173	0.479	1.247	0.851	0.442	1.023	0.268	3.313	2.731	0.935	0.746
44.938	1.515	0.891	1.986	1.494	0.776	1.676	0.543	3.755	3.261	2.031	1.487
51.471	1.954	1.706	3.09	2.60	1.414	2.66	1.17	4.14	3.70	4.253	2.87

Grain Size	Bulk	Testing Chamber						Ash Reduction Measure			
		Control	ARM 1	ARM 2	ARM3	ARM 4	ARM 5	ARM 2	ARM 4	ARM5	ARM 6
			6	3		2	4	4	3		9
58.953	2.472	3.095	4.546	4.189	2.481	3.917	2.444	4.247	3.972	7.632	4.974
67.523	3.009	4.967	6.098	5.936	3.953	5.187	4.491	3.922	4.027	10.903	7.253
77.34	3.537	7.421	7.545	7.548	5.758	6.258	7.505	3.332	3.871	13.576	9.347
88.583	3.865	8.895	8.095	7.768	6.940	6.470	9.753	2.449	3.496	12.269	9.384
101.46	3.810	8.186	7.723	6.811	6.917	6.049	9.601	1.578	2.995	8.509	7.847
116.21	3.546	6.848	7.459	6.378	6.707	5.969	8.794	0.997	2.506	5.949	6.891
133.103	3.720	6.698	7.468	6.308	7.022	6.333	8.595	0.670	2.357	5.241	6.532
152.453	4.367	7.380	8.130	7.182	8.160	7.395	9.417	0.534	2.389	5.271	6.796
174.616	5.277	8.195	8.657	8.476	9.327	8.571	9.892	0.492	2.437	5.350	7.012
200	6.275	9.019	8.467	9.419	10.057	9.419	9.267	0.497	2.391	5.113	6.784
229.075	6.894	8.880	6.987	8.675	9.480	9.033	7.032	0.491	2.073	4.067	5.794
262.376	6.549	6.876	4.573	5.898	7.206	6.960	4.044	0.438	1.507	2.431	4.143
300.518	5.668	4.038	2.621	3.050	4.682	4.530	1.970	0.000	0.916	1.161	2.695
344.206	5.389	1.989	1.628	1.474	3.137	2.952	1.041	0.000	0.509	0.569	1.876
394.244	6.133	0.871	0.905	0.670	2.313	1.987	0.578	0.000	0.000	0.217	1.236
451.556	6.289	0.000	0.503	0.203	1.472	1.049	0.321	0.000	0.000	0.000	0.664
517.2	4.292	0.000	0.000	0.113	0.684	0.260	0.000	0.000	0.000	0.000	0.218
592.387	2.251	0.000	0.000	0.000	0.288	0.000	0.000	0.000	0.000	0.000	0.000
678.504	0.943	0.000	0.000	0.000	0.000	0.000	0.000	0.000	0.000	0.000	0.000
777.141	0.188	0.000	0.000	0.000	0.000	0.000	0.000	0.000	0.000	0.000	0.000
890.116	0.058	0.000	0.000	0.000	0.000	0.000	0.000	0.000	0.000	0.000	0.000
1019.515	0.000	0.000	0.000	0.000	0.000	0.000	0.000	0.000	0.000	0.000	0.000
1167.72	0.000	0.000	0.00	0.00	0.000	0.00	0.00	0.00	0.00	0.000	0.00

Grain Size	Bulk	Testing Chamber						Ash Reduction Measure			
		Control	ARM 1	ARM 2	ARM3	ARM 4	ARM 5	ARM 2	ARM 4	ARM5	ARM 6
5			0	0		0	0	0	0		0

B.4 Pseudo Ash A – Additional Testing

Table B4: Laser particle analyser results for additional tests with Ash A. Analyser produced results for particles >0.011µm. There results have been truncated to only display gain size where corresponding particles were detected.

Grain Size		Testing Chamber			ARM		
	Bulk	ARM 1 & 4	1000g	2000g	ARM 1 & 4	1000g	2000g
0.15	0.019	0.000	0.000	0.000	0.000	0.000	0.000
0.172	0.026	0.000	0.000	0.000	0.000	0.000	0.000
0.197	0.034	0.000	0.000	0.000	0.000	0.000	0.000
0.226	0.041	0.000	0.000	0.000	0.000	0.000	0.000
0.259	0.047	0.000	0.000	0.000	0.000	0.000	0.000
0.296	0.092	0.000	0.000	0.000	0.000	0.000	0.140
0.339	0.124	0.000	0.000	0.000	0.000	0.052	0.235
0.389	0.139	0.000	0.000	0.000	0.207	0.234	0.424
0.445	0.187	0.000	0.000	0.000	0.441	0.462	0.679
0.51	0.205	0.000	0.000	0.000	0.690	0.680	0.897
0.584	0.184	0.000	0.000	0.000	0.757	0.699	0.892
0.669	0.155	0.130	0.000	0.000	0.594	0.510	0.660
0.766	0.098	0.155	0.000	0.000	0.367	0.293	0.396
0.877	0.040	0.158	0.000	0.000	0.207	0.156	0.225
1.005	0.000	0.147	0.000	0.000	0.125	0.036	0.146
1.151	0.019	0.133	0.106	0.000	0.115	0.038	0.153
1.318	0.126	0.129	0.117	0.118	0.142	0.096	0.214
1.51	0.172	0.132	0.125	0.135	0.187	0.191	0.315
1.729	0.219	0.134	0.133	0.151	0.229	0.252	0.424
1.981	0.278	0.138	0.138	0.166	0.286	0.339	0.579
2.269	0.353	0.145	0.143	0.181	0.369	0.470	0.808
2.599	0.443	0.154	0.147	0.194	0.479	0.651	1.120
2.976	0.543	0.162	0.150	0.207	0.608	0.872	1.502
3.409	0.647	0.169	0.153	0.216	0.747	1.119	1.927
3.905	0.751	0.173	0.156	0.222	0.890	1.374	2.359
4.472	0.858	0.173	0.157	0.225	1.036	1.629	2.782
5.122	0.971	0.170	0.160	0.226	1.198	1.894	3.199
5.867	1.096	0.169	0.162	0.228	1.399	2.186	3.634
6.72	1.242	0.169	0.166	0.231	1.662	2.524	4.110
7.697	1.408	0.173	0.174	0.238	2.012	2.911	4.634
8.816	1.591	0.184	0.186	0.249	2.463	3.331	5.183
10.097	1.755	0.199	0.199	0.262	3.016	3.749	5.700
11.565	1.839	0.217	0.202	0.263	3.683	4.148	6.103
13.246	1.883	0.245	0.211	0.269	4.447	4.442	6.333
15.172	1.879	0.287	0.227	0.287	5.172	4.515	6.288
17.377	1.838	0.346	0.256	0.324	5.671	4.298	5.936
19.904	1.776	0.429	0.304	0.389	5.798	3.831	5.363

Grain Size		Testing Chamber			ARM		
	Bulk	ARM 1 & 4	1000g	2000g	ARM 1 & 4	1000g	2000g
22.797	1.706	0.551	0.375	0.494	5.549	3.235	4.708
26.111	1.637	0.736	0.477	0.646	5.061	2.647	4.082
29.907	1.581	1.024	0.616	0.855	4.547	2.158	3.526
34.255	1.553	1.491	0.812	1.128	4.191	1.808	3.028
39.234	1.572	2.276	1.120	1.526	4.163	1.614	2.549
44.938	1.646	3.584	1.654	2.177	4.554	1.595	2.044
51.471	1.724	5.482	2.469	3.126	5.060	1.670	1.549
58.953	1.792	7.753	3.574	4.332	5.376	1.824	1.120
67.523	1.848	9.731	4.845	5.600	5.117	2.037	0.789
77.34	1.831	11.341	6.125	6.726	4.570	2.242	0.525
88.583	1.746	11.052	6.797	7.016	3.435	2.433	0.336
101.46	1.706	8.882	6.882	6.673	1.980	2.543	0.242
116.21	1.792	6.705	7.357	6.910	0.911	2.580	0.236
133.103	1.756	5.703	7.276	6.670	0.365	2.656	0.261
152.453	1.945	5.241	8.064	7.225	0.123	2.887	0.325
174.616	2.436	4.702	8.989	8.043	0.000	3.209	0.426
200	3.103	3.865	9.220	8.259	0.000	3.371	0.470
229.075	3.564	2.662	7.891	7.050	0.000	3.012	0.331
262.376	3.538	1.415	5.215	4.710	0.000	2.144	-0.200
300.518	3.270	0.633	2.916	2.749	0.000	1.341	0.293
344.206	3.431	0.351	1.716	1.772	0.000	0.763	0.000
394.244	4.410	0.000	1.071	0.985	0.000	0.780	0.000
451.556	5.400	0.000	0.616	0.547	0.000	0.900	0.000
517.2	5.254	0.000	0.152	0.000	0.000	1.014	0.000
592.387	5.056	0.000	0.000	0.000	0.000	0.907	0.000
678.504	4.585	0.000	0.000	0.000	0.000	0.511	0.000
777.141	3.465	0.000	0.000	0.000	0.000	0.133	0.000
890.116	2.393	0.000	0.000	0.000	0.000	0.000	0.000
1019.515	1.183	0.000	0.000	0.000	0.000	0.000	0.000
1167.725	0.000	0.000	0.000	0.000	0.000	0.000	0.000

C. Appendix C - Testing Document

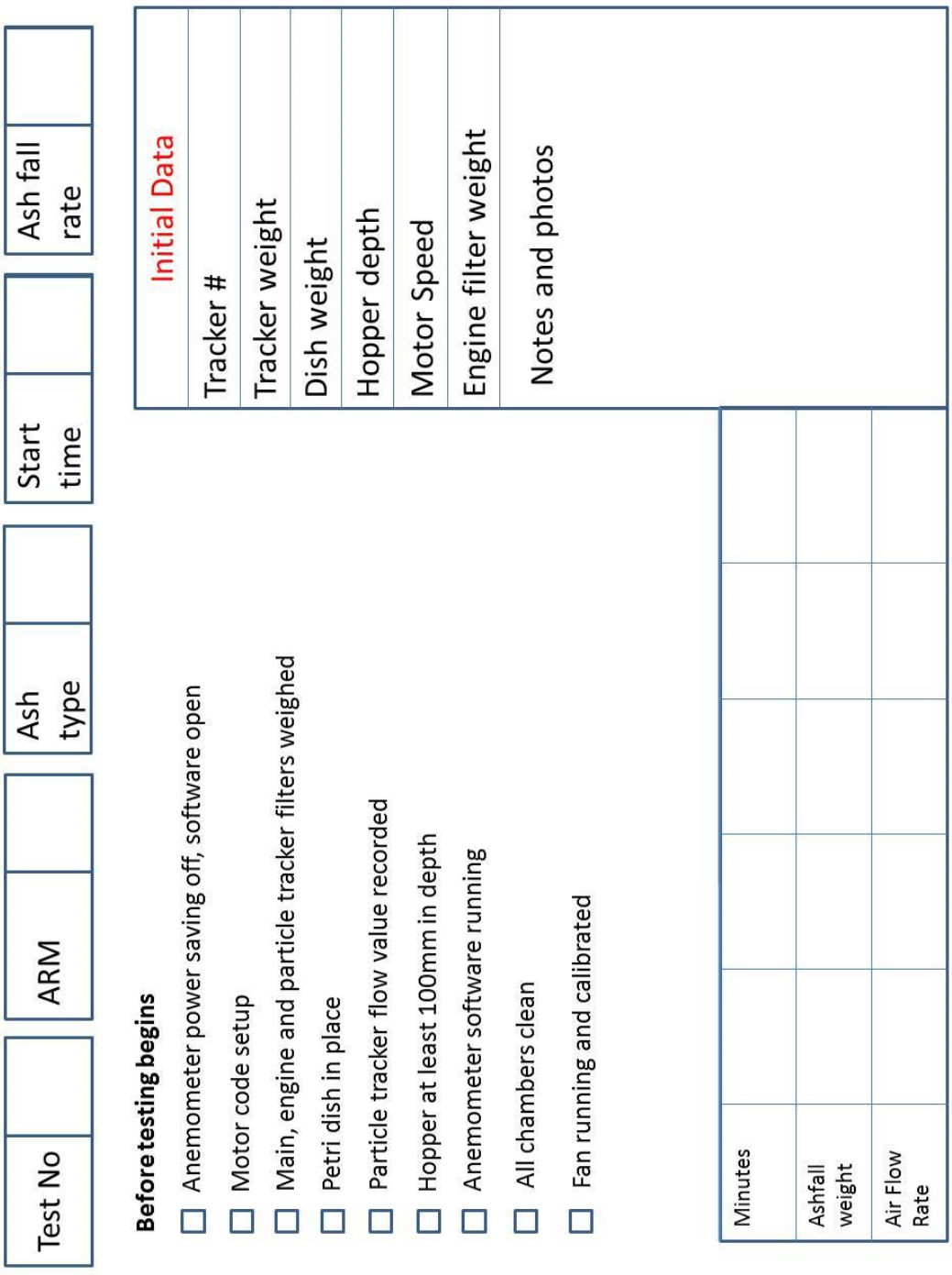

Figure C1: Testing Document - page 1

Minutes									
Ashfall weight									
Air Flow Rate									

Final Data	Notes
Tracker weight	
Dish weight	
Engine filter weight	
Tracker #	
Hopper depth	
End Time	
End of test checklist ☐ Particle tracker weighed ☐ Engine filter and dish weighed ☐ Particle tracker flow recorded ☐ Anemometer file saved ☐ Hopper Depth recorded ☐ Time Recorded	

Figure C2: Testing document - page 2